Specific PET-ligands for Selected 5-HT and $GABA_A$-Receptor Subtypes

PET-Liganden mit Spezifität für definierte 5-HT und $GABA_A$-Rezeptor-Subtypen

Dissertation

zur Erlangung des Grades

„Doktor der Naturwissenschaften“

am Fachbereich Biologie der

Fabian Debus

geb. am 19.09.1976 in Frankfurt am Main

Mainz, im März 2008

Erklärung

Hiermit versichere ich, dass ich die vorliegende Dissertation eigenständig verfasst und keine anderen als die angegebenen Hilfsmittel verwendet habe.

Die Dissertation habe ich weder als Arbeit für eine staatliche oder andere wissenschaftliche Prüfung eingereicht noch ist sie oder ein Teil dieser als Dissertation bei einer anderen Fakultät oder einem anderem Fachbereich eingereicht worden.

Mainz, im März 2008

Dekan:

1. Berichterstatter:

2. Berichterstatter:

Tag der mündlichen Prüfung: 28.05.2008

Danksagung

Eine solche Schrift kann niemals als Ergebnis der Arbeit eines Einzelnen, sondern sollte immer als Resultat der Arbeit einer großen Anzahl von fleißigen Menschen betrachtet werden, die dabei mitgeholfen haben, dass aus einer Idee ein gelungenes Projekt wurde.

Bei meinen beiden Betreuern, Prof. Dr. H. L. und Prof. Dr. F. R., möchte ich mich für das spannende und abwechslungsreiche Thema bedanken. Außerdem für Ihr Vertrauen und Ihre Diskussionsbereitschaft. Insbesondere Herrn Prof. Dr. H. L. möchte ich für seine Unterstützung und seine vorbildliche Betreuung danken. Ich hätte mir keinen besseren Doktorvater wünschen können und bin sehr dankbar für alles, was ich in diesen drei Jahren in seiner Arbeitsgruppe lernen durfte.

Besonderer Dank gebührt der gesamten Arbeitsgruppe für Ihre herzliche Gemeinschaft und das produktive Miteinander. Im Einzelnen gebührt Frau R. Dank für das Licht im Dunkel der Bürokratie. Frau B. D. danke ich für ihre hervorragende Arbeit und Unterstützung im Umgang mit den Versuchstieren bei den *in vivo* Bindungsversuchen sowie den PET-Untersuchungen sowie allgemein für ihre ständige Hilfsbereitschaft, Dr. I. B. für seine kompetente Hilfe bei molekularbiologischen Fragen und seine Diskussionsbereitschaft sowie Dr. H. R. für seine hervorragende Unterstützung bei allen elektrophysiologischen Themen und sein stets offenes Ohr.

Ich möchte mich bei Prof. Dr. C. H. und allen Mitarbeitern seiner Arbeitsgruppe für ihre Diskussionsbereitschaft und Hilfsbereitschaft bedanken. Insbesondere Dr. U. S. möchte ich für seine Unterstützung und wertvollen Tipps im Bereich Versuchstiere danken.

Von unschätzbarem Wert war die exzellente Arbeit von Dipl. Chemiker M. H. und Dipl. Chemikerin T. C., beide Mitarbeiter der Arbeitsgruppe von Prof. Dr. F. R., ohne die diese Arbeit nicht durchführbar gewesen wäre. Ein ebenso großes Dankeschön geht jedoch an die gesamte Arbeitsgruppe R., insbesondere an Dr. M. P., der nicht Müde wurde mit Rat und Tat dabei zu sein, wann immer Not am Mann war.

Ich bedanke mich ganz herzlich bei Prof. Dr. H. L. für die Verleihung des Stipendiums sowie die hervorragende und engagierte Leitung des DFG-Graduiertenkollegs „Entwicklungsabhängige und krankheitsinduzierte Modifikationen im Nervensystem“ der Universität Mainz, seine Diskussionsbereitschaft, sein Vertrauen und seine Unterstützung.

Eine große Bereicherung und Hilfe waren auch alle Kooperationspartner, insbesondere mein Aufenthalt bei der Arbeitsgruppe von Prof. Dr. E.K., sowie der Arbeitsgruppe von Prof. Dr. G. K., und dort besonders M. P.. Allen danke ich für die schöne Zeit und die Gastfreundschaft während der Aufenthalte sowie für die anregenden Diskussionen und Tipps im Bereich Autoradiographie und PET.

Last but not least ein herzliches Dankeschön an alle Lektoren, die es auf sich genommen haben die Arbeit zu lesen und zu korrigieren.

1 TABLE OF CONTENTS

1.1 Table Index:

1.2 Figure Index

$5HT_{1A}$/-$5HT_{2A}$Rs	5-hydroxytryptamine 1/2-receptors
ach	acetyl choline
AD	Alzheimer's disease
bp	base pairs
BSA	bovine serum albumin
BZ	benzodiazepine(s)
CNS	central nervous system
cpm	counts per minute
C-terminal	carboxyterminal
DNA	deoxy ribonucleic acid
dpm	disintegration per minute
E. coli	Escherichia coli
eGFP	enhanced green fluorescent protein
ethbr	ethidium bromide
fcs	fetal calf serum
fig.	figure
GABA	γ-aminobutyric acid
$GABA_AR$	γ-aminobutyric acid A receptor
h	hour
HEK 293	human embryonic kidney cells 293
µ	micro
M	molar
MΩ	mega ohm
MEM	minimal essential medium
mV	milli volt
min.	minutes
N-terminal	aminoterminal
OD	optical density
PBS	phosphate buffered saline
PET	positron emission tomography
mPET	micro positron emission tomography

rpm	roundings per minute
RT	room temperature
SDS	sodium dodecyl sulfate
sec.	seconds
tab.	table
TLC	thin layer chromatography
tris	tris(hydroxymethyl)aminomethane
UV	ultra violet
ON	over night
w/v	weight per volume

2 INTRODUCTION

Over the last three decades scientific progress in neuroscience has made obvious the biological basis of the diversity and multitude of neurological and psychiatric diseases. Illnesses of the nervous system are particularly severe as they usually affect the whole system of the human body if not the individual's personality. In most cases essential functions of our system are impaired which can cause frustration, depression or at least unhappiness. To be able to manage everyday life in society there are several indispensable cognitive performances our central nervous system has to provide. Alertness, the ability to judge or discriminate, to organize and structure due tasks and available time as well as the ability to concentrate and focus are as important functions as the ability to learn and subsequently incorporate and memorize newly learned abilities, processes and contents. In many psychiatric disorders and degenerative diseases of the central nervous system one or more of these abilities are impaired, which is true for example for Alzheimer's disease and schizophrenia. Also these impairments are likely to start on a molecular level at a time when the individual has not yet become fully aware of them or does not yet greatly suffer from them. One possibility of early diagnosis in such cases is the use of positron emission tomography.

2.1 Positron Emission Tomography

Positron Emission Tomography (PET) is a nuclear imaging technique which can be used to non-invasively monitor the location of a radionuclide in a living organism. In contrast to, e.g. CT or MRT, PET is a functional imaging technique. Its strength lies in the imaging of physiological processes like receptor binding or metabolism. The technique makes use of the unique decay characteristics of a number of positron emitting radionuclides.

After its emission from the atom nucleus the positron travels a short distance, the distance being dependent on its energy and the tissue, and finally combines with an electron to form a positronium. This state lasts about 10^{-10} seconds, after which annihilation of the positronium occurs and two high-energy γ-photons are emitted in opposite directions. Molecules of interest can be labeled with these positron emitting radionuclides and then be used as a radiotracer (or radiopharmacon). In a PET-scanner the γ-photons can be detected with detectors arranged in a circular fashion with always two detectors in exact opposite position or at least two detectors in opposite position.

The electrical signals originating from the photons are fed into a computer for further processing by mathematical algorithms. For one PETscan usually 10^6 - 10^9 decays are detected. After the correction and reconstruction process a PETscan can be converted into a 3D tomographic image volume, which consists of voxels, equivalent to pixels of a 2D-image. The signal intensity in each of the image voxels is proportionate to the amount of radiotracer in that voxel and thus can be used to perform quantitative analyses in living organisms.

By measuring the tissue concentration of radiotracers in a time sequence the rate of biological processes can be determined and mathematical modeling thereof can be applied. In recent years the physical improvements of the technique as well as improvements of the mathematical reconstruction algorithms resulted in smaller PET scanners which can be used to scan as small animals as mice and rats.

2.1.1 Small Animal Positron Emission Tomography

Improvements of the PET technique in the early nineties made possible the manufacturing of small animal PET scanners. Various scintillator crystals were tested over the years to improve spatial resolution and scanner sensitivity, two characteristics which unfortunately are usually improved with a loss of performance of the other. One of the earliest prototypes was the RATPET, developed in cooperation of the MRC Cyclotron Unit, London and the University of California Los Angeles together with CTI Microsystems, Knoxville, TN, USA (Bloomfield, Rajeswaran et al. 1995). This project finally led to the most widely used microPET Focus 120 scanner, distributed by Siemens (Tai, Ruangma et al. 2005). Over the years limitations such as software problems and complicated handling of scanners were overcome and small animal positron tomography is to-date an ever increasingly used, highly valuable tool for molecular imaging and preclinical studies (Myers 2001; Nanni, Rubello et al. 2007). Moreover, it has been shown by Atack et al. (Atack, Scott-Stevens et al. 2007) that in vivo binding studies, with bound ligand being detected *ex vivo* by filtration and scintillation counting, and in vivo PET-studies are equally valid approaches to the measuring of the occupancy of drug binding sites of e.g. the $GABA_A$ receptor (Phelps 2004).

2.1.2 PET - Ligands

As mentioned above, many kinds of molecules can be labeled with, e.g. ^{11}C, ^{13}N, ^{15}O and ^{18}F, which are all radioisotopes usable for positron emission tomography. Which labeling route is chosen depends on the nature of the molecule. In order to keep the chemical and especially the biochemical characteristics of the unlabeled molecule a fluorine atom in the structure needs to be part of it when a labeling with ^{18}F is desired.

The design and synthesis of PET-ligands can aim at three biological processes; they may detect enzyme-mediated transformations, they may detect stoichiometric binding interactions or they determine perfusion. For this project all ligands were designed to quantitate stoichiometric binding interactions.

While pharmacological drugs and PET-ligands have some characteristics in common, PET-ligands, especially if they target molecules in the brain, are required to meet additional demands. Any drug needs high specificity, high affinity and most often high efficacy for the target molecule. A PET-ligand targeting the brain additionally needs to pass the blood brain barrier. One of the major demands is a very low non-specific binding and a high specific radioactivity, so that even at low concentrations a large number of disintegrations can be counted by the camera. This leads to the further result that the final drug concentration is usually too low to produce any pharmacological or even toxicological effect. Additionally PET-ligands need to have a long biological half-life and ideally no or few active metabolites. The blood pool clearance is another factor which plays a role in visualization techniques as a slow clearance would lessen the contrast of the image as a result of a bad target-to-background ratio and is therefore to be avoided (Phelps 2004).

2.1.3 PET Modeling

Mathematical modeling of PET measurements is needed to relate the observed radioactivity to properties of the biological parameters under investigation. Studies in this thesis involve measurements of receptor binding. Therefore the following description focuses on models that are used to obtain information on receptor characteristics and the interaction of the receptor with the radioligand. One of the most used outcome parameters in PET receptor binding studies is the so called binding potential (*BP*). The *BP* corresponds to the ratio of B_{max} (total receptor concentration) over K_D (the equilibrium dissociation constant) and can be derived from the Michaelis-Menten equilibrium equation, which is functionally identical to the law of mass action. At equilibrium, the association and dissociation of the ligand from the receptor are equal, which implies:

$$k_{on}*L*R = k_{off}*LR,$$

where k_{on} is the association rate constant, k_{off} the dissociation rate from the receptor and *L, R* and *LR* the free concentration of the radioligand, available receptors and ligand receptor complex respectively. In a more pharmacologic notation *LR* is denoted as *B,* the total receptor concentration as B_{max}, k_{off}/k_{on} as K_D and *R* as B_{max} - *B.* Substitution and rearrangement leads to the equation:

$$B = \frac{B_{\max} * L}{K_D + L}$$

At tracer doses, *L* is much smaller than *KD* and the equation simplifies to:

$$B = \frac{B_{\max} * L}{K_D}$$

or:

$$\frac{B}{L} = \frac{B_{\max}}{K_D} = BP$$

Thus, at equilibrium and at tracer doses, the *BP* is equal to the ratio of specifically bound ligand to free ligand. In experiments where ligand binding achieves equilibrium during scanning, the *BP* can be derived directly from the PET measurements.

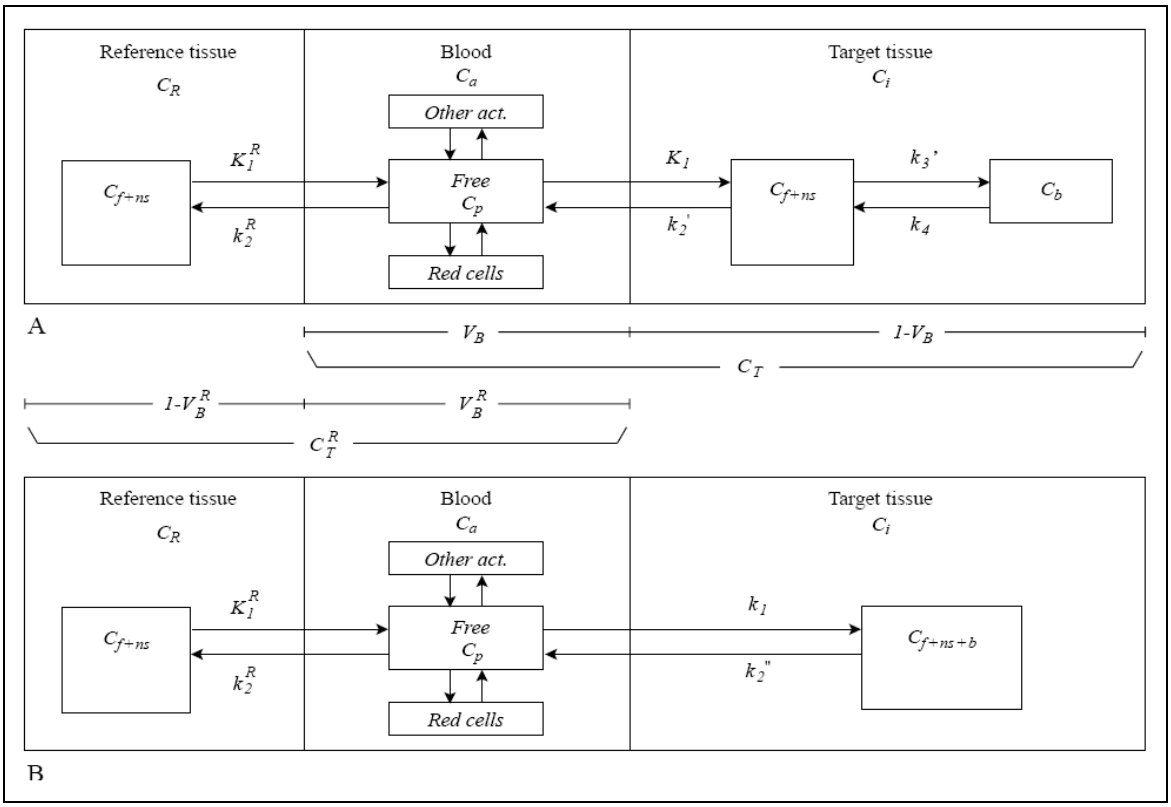

Figure 1: Reference tissue models. A region devoid of specific receptors is used as an indirect input function to the target region containing the specific receptors of interest. **A** The model takes into account differences in delivery and free ligand concentration between target and reference tissue, but assumes the same volume of distribution of the free + nonspecifically bound tracer in the two tissues. The binding potential of the ligand is given by the ratio k3'/k4. **B** Simplified reference tissue model in which the kinetics of the free and specifically bound ligand are not kinetically distinguishable (Schmidt and Turkheimer 2002).

In these experiments, the activity in a reference region (**Figure 1**) is used to measure free radioligand binding. The reference region does not contain significant specific binding and it is assumed that the nonspecifically bound and free ligand concentrations are identical to those in the receptor containing region. Nonspecific binding is usually in rapid equilibrium with the free compartment and is therefore assumed not to be distinguishable from the free radioligand concentration (Lammertsma, Bench et al. 1996; Lammertsma and Hume 1996; Logan, Fowler et al. 1996; Gunn, Lammertsma et al. 1997; Gunn, Gunn et al. 2001; Meyer and Ichise 2001; Lingford-Hughes, Hume et al. 2002; Schmidt and Turkheimer 2002; Udo de Haes 2005).

2.2 The GABAergic System

About one third of the CNS synapses have GABA as their main inhibitory transmitter. The hyperpolarization of a neuron caused by anion influx through the channel pore of GABA's main receptor, the $GABA_A$ receptor, provides the main counterpart to excitatory action in a neuron. Enhancement of GABA action causes anxiolysis, muscle relaxation and sleep up to unconsciousness. Blocking of the receptor causes anxiety and seizures with all intermediate states between those extremes, depending on the drug and its dose. As shown in **Figure 2** L-glutamic acid decarboxylase (GAD) catalyzes the conversion of L-glutamate to GABA via decarboxylation resulting in the accumulation and storage of GABA within vesicles of inhibitory neurons. Upon arrival of an action potential at the nerve terminal, the presynaptic membrane depolarizes inducing the opening of voltage-gated Ca^{2+} channels. Influx of Ca^{2+} ions through these channels increases its intracellular concentration and triggers the fusion of the synaptic GABA-containing vesicles with the presynaptic membrane. When released into the synaptic cleft GABA freely diffuses within the 20 nm synaptic cleft and binds to both post- and presynaptic receptors. Termination of synaptic transmission is achieved by clearing the neurotransmitter by a combination of diffusion out of the cleft and active transport into contiguous neuronal and/or glial cells (Berezhnoy, Nyfeler et al. 2004).

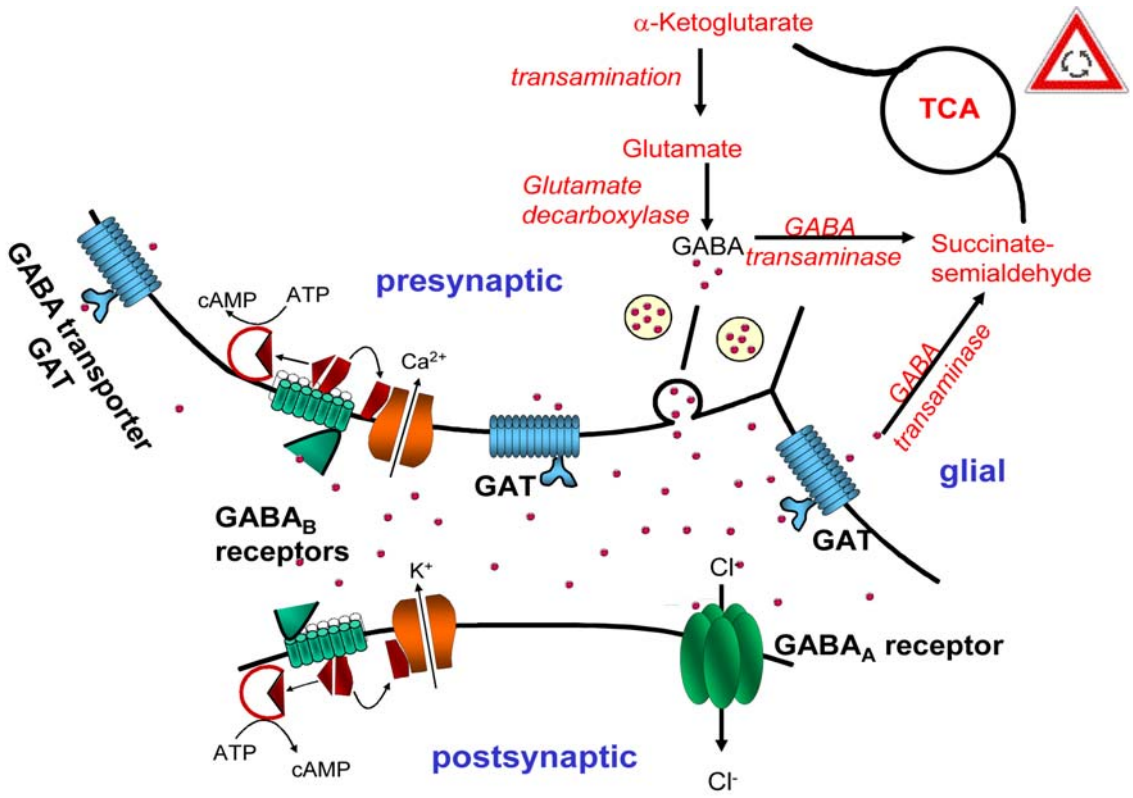

Figure 2: The GABAergic system, modified from (Bohme, Rabe et al. 2004). **GAT** GABA transporter, **TCA** tri carbonic acid cycle, **ATP** adenosine tri phosphate, **cAMP** cyclic adenosine mono phosphate.

2.2.1 The $GABA_A$ Receptor

GABA acts via three classes of receptors in the vertebrate CNS, $GABA_A$, $GABA_B$ and $GABA_C$ receptors, that differ in their structure, function and pharmacology. $GABA_A$ and $GABA_C$ receptors belong to the group of the Cys loop ligand-gated ion channel superfamily while $GABA_B$ receptors are members of the group of G-protein coupled receptors (Barnard, Skolnick et al. 1998). Nineteen related $GABA_A$ receptor subunit genes have been identified in the vertebrate nervous system so far: α 1-6, β 1-3, γ 1-3, δ, ε, π, θ, ρ 1-3. Thus, a vast number of theoretically possible combinations exist, as $GABA_A$ receptors are hetero-pentameric ion channels composed of five subunit proteins (**Figure 3**). However, McKernan et al. could show for the rat brain, that only a limited number of combinations occur in the brain in appreciable numbers (Quirk, Blurton et al. 1996). A detailed description of the distribution of the most abundant $GABA_A$ receptor mRNAs was published by Wisden et al. in 1992 (Campos, de Cabo et al. 2001). Their data were supplemented by the $GABA_A$ receptor protein distribution as measured by immunocytochemistry methods by Sperk et al. and Pirker et al. (Sperk, Schwarzer et al. 1997; Pirker, Schwarzer et al. 2000).

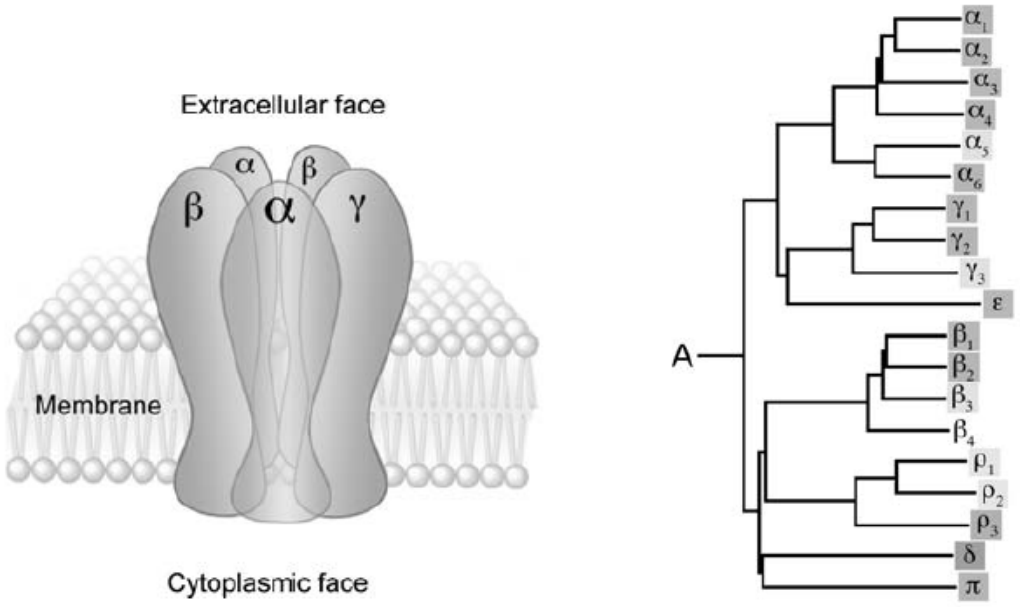

Figure 3: The diversity of the $GABA_A$ receptor, modified from (Berezhnoy, Nyfeler et al. 2004)

According to their data, the α1 subunit is the most widely distributed subunit. It is present in practically all brain regions with the striatum, the reticular thalamic nucleus or the internal granular layer of the olfactory bulb being areas of the brain with slightly lower expression of α1. α2 subunit expression was determined to be highest in the accessory olfactory bulb, dentate molecular layer, hippocampal area CA3, central and lateral amygdaloid nuclei, septum, striatum, accumbens and hypothalamus while α3 subunit expression is most prominent in the external plexiform and glomerular layers of the olfactory bulb, in the inner layers of the cerebral cortex, the endopiriform nucleus, in the amygdala, the lateral septum, the claustrum and in the superior colliculus. The distribution of the α4 subunit is densest in the thalamus, the striatum and nucleus accumbens, the tuberculum olfactorium and the molecular layer of the dentate gyrus. The α6 subunit displays a unique distribution as it is present almost exclusively in the granule cell layer of the cerebellum. Minor signals of both labeled mRNA and immunoreactivity was found in the granular layer of the cochlear nuclei and in processes traversing between the dorsal cochlear nucleus and ventral posterior cochlear nucleus. The particular distribution and other characteristic parameters of the α5 subunit are explained below. The majority of $GABA_A$ receptors in the brain contain α-, β- and γ-subunits and those containing α1, α2, α3 and α5 in conjunction with a β- and γ2-subunit (around 80 % of the total $GABA_A$ receptor population) contain a BZ binding site which allosterically modulates the functional effects of GABA (Pritchett and Seeburg 1990; Seeburg, Wisden et al. 1990). Using genetically modified (knock-in) mice it has been demonstrated

that $GABA_A$ receptors containing an α1-subunit mediate the sedative/muscle relaxant effects of benzodiazepines (McKernan, Rosahl et al. 2000), whereas α2- and/or α3-subunit-containing receptors mediate the anxiolytic and anticonvulsant effects (Rudolph, Crestani et al. 1999; Bohme, Rabe et al. 2004). Chambers et al. proposed that a selective α5 inverse agonist may have therapeutic utility as a cognition-enhancing agent that may lack the unwanted side effects associated with activity at other $GABA_A$ receptor subtypes (Chambers, Atack et al. 2003)

2.2.2 The α5 Subunit

According to Pirker et al. the distribution of the α5-subunit in the rat brain is quite different from that of other α-subunits. They observed particularly high concentrations of α5-subunit immunoreactivity in the olfactory bulb, inner layers of the cerebral cortex, endopiriform nucleus, subiculum, Ammon's horn (especially in the CA1 region) and in the ventromedial hypothalamic nucleus. The authors find it worth pointing out that the distribution is in almost complete agreement with the regional distribution of [^{3}H]L-655,708, a ligand suggested to selectively label α5-subunit containing $GABA_A$ receptors (Quirk, Blurton et al. 1996; Sur, Fresu et al. 1999; Pirker, Schwarzer et al. 2000). In 2000 Wainwright et al. could obtain an antibody that labels human α5 subunit containing $GABA_A$ receptors and also found a very high density of this subunit in pyramidal neurons of the hippocampal formation. As the authors point out, excitatory input reaches the hippocampus mainly via glutamate-containing, perforant pathway projections originating from layer II of the entorhinal cortex, synapsing onto dentate gyrus granule cells. GABA, being the primary inhibitory input on CA1, CA2 and CA3 pyramidal neurons, exerts inhibitory influence on this excitatory pathway. Therefore, antagonism of GABA-ergic activity at this level in the hippocampus is predicted to enhance hippocampal and therefore, potentially, cognitive function (Wainwright, Sirinathsinghji et al. 2000). Although α5 receptors account for less than 5 % of the total $GABA_A$ receptor population in the brain, in the hippocampus they represent 20 % of all $GABA_A$ receptors (Sieghart 1995; Quirk, Blurton et al. 1996; Sur, Quirk et al. 1998), thereby also implicating this $GABA_A$ receptor subtype in learning and memory processes (Chambers, Atack et al. 2003). In 2003 Chambers et al. found a selective $GABA_A$ α5 receptor inverse agonist which enhanced cognition in a hippocampal-dependent memory task, whithout the convulsant or proconvulsant liabilities associated with nonselective $GABA_A$ inverse agonists, thereby adding proof to the long anticipated role of α5 containing receptors in memory and cognition processes. More supportive data was collected over the next few years (Chambers, Atack et al. 2004; Sternfeld, Carling et al.

2004; Collinson, Atack et al. 2006; Dawson, Maubach et al. 2006). In addition to the potentially clinically relevant role of the α5 subunit in memory and cognition processes, the α5 subunit was connected to areas as diverse as epilepsy (Sander, Kretz et al. 1997; Poulter, Brown et al. 1999; Houser and Esclapez 2003), bipolar affective disorder (Papadimitriou, Dikeos et al. 1998; Papadimitriou, Dikeos et al. 2001; Otani, Ujike et al. 2005), Alzheimer's disease (Howell, Atack et al. 2000), ethanol action (McKay, Foster et al. 2004; Cook, Foster et al. 2005; Stephens, Pistovcakova et al. 2005) and autism (Delong 2007).

2.3 The Serotonergic System

The pharmacological effects of 5-hydroxytryptamin (serotonin, 5-HT) were first described during the 1930s by Vittorio Erspamer. He extensively studied the subject and published more detailed findings in a Nature article in 1952, after M. Rapport established the structure of 5-HT in 1949 (Rapport 1949; Erspamer and Asero 1952).

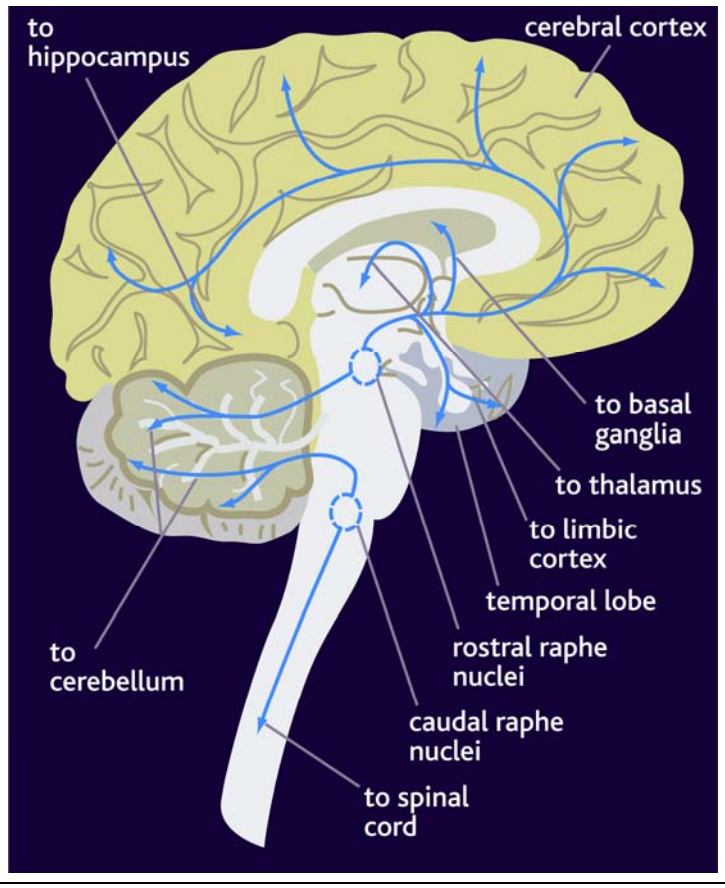

Figure 4: Diagram of the serotonergic pathways in the human brain originating in the raphe nuclei (http://www.cnsforum.com/imagebank/item/Neuro_path_SN_DA/default.aspx).

Later, 5-HT was found to be present in different regions of the mammalian brain which led to the proposal of 5-HT as a neurotransmitter (Jacobs and Azmitia 1992). The ma-

jority of serotonergic cell bodies that innervate the brain are located in the raphe nuclei in the brainstem: the dorsal raphe (DRN) and median raphe (MRN) (**Figure 4**). The serotonergic neurons project to large parts of the brain. The DRN projects preferentially to the cortex and striatum, whereas the MRN innervates structures such as the septum, hypothalamus and dorsal hippocampus. Several brain structures like the amygdala and ventral hippocampus are innervated by the DRN as well as the MRN (Jacobs and Azmitia 1992; Pineyro and Blier 1999).

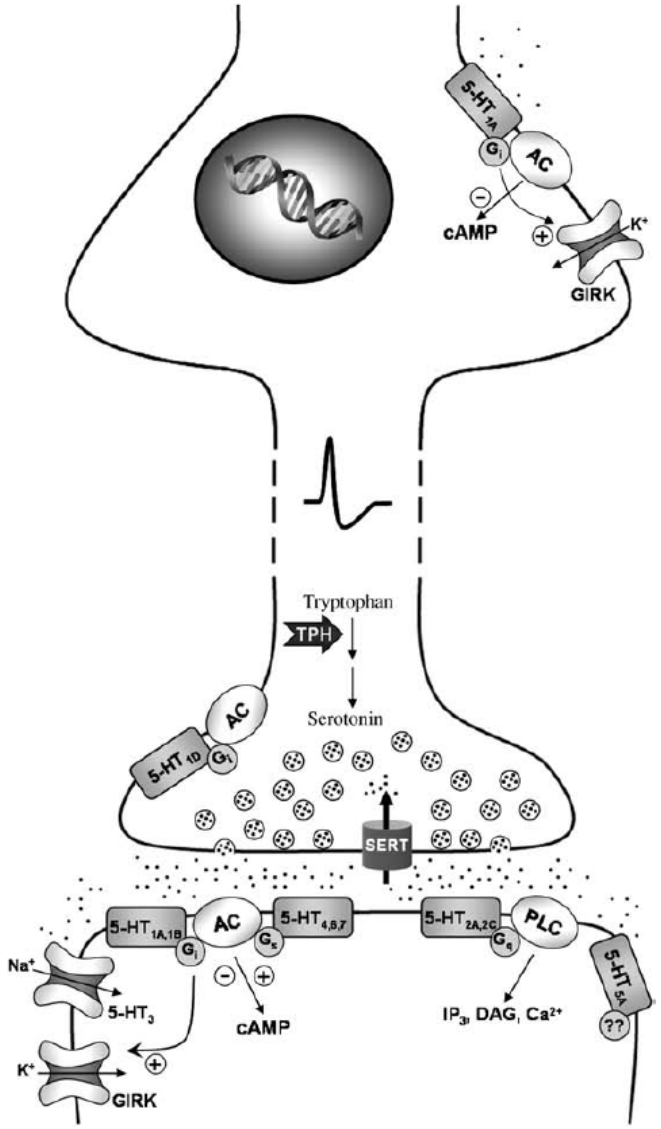

Figure 5: Model of a serotonergic neuron and synapse. Diagram of a serotonergic neuron originating from the brain stem raphe nuclei (Gray and Roth 2007). **AC**, adenylyl cyclase; **PLC**, phospholipase C; **SERT**, serotonin transporter; **GIRK**, G-protein-coupled inwardly rectifying potassium channels; **TPH**, tryptophan hydroxylase; **IP3**, inositol trisphosphate; **DAG**, diacylglycerol.

5-HT is formed by the hydroxylation and decarboxylation of the essential amino acid tryptophan (Wurtman, Hefti et al. 1980). It is predominantly synthesized in the cytoplasm of the nerve terminals and thereafter accumulated into a secretory compartment for regulated exocytotic release. After release, the action of the neurotransmitter is terminated by an efficient transporter (SERT). The SERT is mainly located on serotonergic axons and, possibly, a small proportion is present on glia cells (**Figure 5**). After reuptake in the neuron, 5-HT is degraded by monoamine oxidases or stored in the synaptic vesicles for future use (Zhou, Tao-Cheng et al. 1998; Pineyro and Blier 1999; Shih, Chen et al. 1999). Most serotonergic neurons fire with a spontaneous, slow, regular discharge pattern. The activity is at its highest during active waking and low during sleep. More recent, a subpopulation of serotonergic neurons was found that displays repetitive burst firing activity which may result in facilitation of synaptic 5-HT release (Gartside, Hajos-Korcsok et al. 2000).

The serotonergic system is involved in the control of mood and numerous behavioral, cognitive and physiological processes. It is also implicated in psychiatric disorders such as depression and anxiety. Several studies also report the possible involvement of this receptor in psychiatric and neurodegenerative disorders (Barnes and Sharp 1999; Hjorth, Bengtsson et al. 2000; Bantick, Deakin et al. 2001; Udo de Haes 2005).

2.3.1 5-HT Receptors

Over the last 20 years, serotonergic receptors have been classified into seven receptor families on the basis of their structural and functional properties: 5-HT_1 - 5-HT_7. These receptor types comprise a large number of different subtypes. For an overview see **Table 2**. Except from the 5-HT_3 receptors, which belong to the super family of cys-loop receptors, all other 5-HT receptors are G-protein coupled receptors. All 5-HT receptor (sub)types are distributed in highly distinct brain areas, such that individual brain regions express their own patterns of serotonergic receptor subtypes (Saxena, De Vries et al. 1998; Barnes and Sharp 1999).

Table 2: The Serotonin Sytem (Gray and Roth 2007)

Receptor	Prototypical Agonist	Prototypical Antagonist	Therapeutic Indications	Commonly Prescribed Medications and Drugs of Abuse
5-HT_{1A}	8-OH-DPAT	WAY100635	Anxiety, depression, neuroprotection	Buspirone (agonist); clozapine (partial agonist)
5-HT_{1B}	Sumatriptan	SB 224289	Anxiety, depression, migraine headache	Sumatriptan
5-HT_{1D}	Sumatriptan	BRL 15572	Migraine headache, depression	Sumatriptan
5-HT_{1E}	5-HT	None	Unknown	None
5-HT_{1F}	LY334370	None	Migraine headache	Sumatriptan
5-HT_{2A}	DOB	M100907	Schizophrenia, depression, anxiety, sleep disorders	LSD (agonist); atypical antipsychotic drugs and many antidepressants (antagonists)
5-HT_{2B}	BW 723C86	SB 204741	None	Pergolide, fenfluramine, and MDMA (agonists); clozapine (antagonist)
5-HT_{2C}	WAY-629	SB 206553	Appetite suppression	LSD (agonist); tricyclic antidepressants (antagonists)
5-HT_3	None	Odansetron	Emesis	Odansetron
5-HT_4	BIMU 8	SB 204070	Cognition enhancement, gastrointestinal motility	Cisapride
5-HT_5	None	None	Unknown	LSD (agonist)
5-HT_6	2-Ethyl-5-methoxy-N,Ndimethyltryptamine	MRS-245	Cognition enhancement	Many antidepressants and atypical antipsychotic drugs (antagonists)
5-HT_7	None	SB 258719	Insomnia, depression	Antidepressants and many atypical antipsychotic drugs

2.3.2 The 5-HT_{2A} Receptor

The subfamily of 5-HT_2 receptors consists of the three members 5-HT_{2A-C}The distribution of 5-HT_{2A} receptors in the CNS has been extensively characterized by autoradiography, in situ hybridization and immunohistochemistry. Receptor autoradiography studies using [^{3}H]spiperone, [^{3}H]ketanserin, [^{125}I]DOI and [^{3}H]MDL 100907 as radioligands have demonstrated high levels of 5-HT_{2A} receptor binding sites in many forebrain regions, with lower levels in the basal ganglia and hippocampus (Fazakes de St.

Groth 1963; Pazos, Cortes et al. 1985; Pazos and Palacios 1985; Pazos, Probst et al. 1987; Lopez-Gimenez, Mengod et al. 1997) The 5-HT_{2A} receptors are particularly abundant in the pyramidal neurons primarily from cortical layers IV and V (Willins, Deutch et al. 1997). The 5-HT_{2A} receptors are essential for mediating a large number of physiological processes in the periphery and in the CNS, including platelet aggregation, smooth muscle contraction and modulation of mood and perception. Most, but not all hallucinogens, including LSD, function as agonists at 5-HT_{2A} receptors, while all clinically approved atypical antipsychotic drugs are potent 5-HT_{2A} receptor antagonists (Meltzer, Matsubara et al. 1989).

2.4 PET and Pharmacology of the $GABA_A$ and 5-HT_{2A} Receptors

2.4.1 Receptor Binding Studies

Using a specific radioligand, the regional distribution of a receptor can be measured as well as disease or medication related changes in receptor density can be monitored. These data may provide information on the involvement of a receptor in the pathogenesis and treatment of, e.g. psychiatric disorders.

First PET experiments with a ligand binding to the benzodiazepine binding site of the $GABA_A$ receptor were conducted in 1985. Persson et al. succeeded with their [^{11}C] labeled flumazenil and were able to gather valuable imformation on the feasibility of PET experiments with benzodiazepine ligands in humans (Persson, Ehrin et al. 1985). Opacka-Juffry et al. evaluated two α5-subunit specific ligands as putative PET ligands in 1999. Their conclusion is, however, that neither [^{3}H]L655,708 nor [^{3}H]RY80 are suitable candidates for further development as PET ligands (Opacka-Juffry, Hirani et al. 1999). Gründer et al. came to the conclusion that, although [^{11}C]flumazenil has some advantages over their [^{18}F]FEF (higher affinity, slower metabolism, slower kinetics), [^{18}F]FEF could be a suitable PET ligand for quantitative assessment of central benzodiazepine receptors in the human brain, whith the major advantage that it can be used independently of an on-site cyclotron (Grunder, Siessmeier et al. 2001). In 2004, Mitterhauser et al. evaluated 2'-[^{18}F]fluoroflumazenil ([^{18}F]FFMZ) as potential benzodiazepine site PET ligand. They conclude that [^{18}F]FFMZ has the same affinity to the GABA receptor as FMZ. The biodistribution of [^{18}F]FFMZ in rats showed uptake in the brain and together with autoradiographic findings the presented data confirmed the potential of [^{18}F]FFMZ for PET imaging of the GABA-ergic system (Mitterhauser, Wadsak et al. 2004).

Lingford-Hughes et al. characterized a fully quantitative PET method for labeling the α5 subtype of the $GABA_A$ benzodiazepine receptors *in vivo* in humans in 2002, using [^{11}C]Ro15-4513. Such a development was timely given the rapidly expanding knowledge at the time about which subtypes mediate specific effects of benzodiazepines in rodents. The finding that humans have a different distribution of these receptors than rodents is clearly important when applying results of experiments using rat models to humans. Moreover, because α5-containing $GABA_A$-benzodiazepine receptors are predominantly located in the limbic system, the authors conclude once more that this suggests they might play a role in emotional states, memory, and in disease processes such as dementia (Lingford-Hughes, Hume et al. 2002). Maeda et al. (2003) report that their results obtained with [^{11}C]Ro15-4513 in combination with zolpidem, an α1-, α2- and α3-selective benzodiazepine binding site ligand, indicate that the BP of [^{11}C]Ro15-4513 with high specific radioactivity can reflect a relatively high signal of the α5 subunit. For quantification of [^{11}C]Ro15-4513 binding, the authors continue, its specific radioactivity needs to be controlled at a high level, because the binding site of [^{11}C]Ro15-4513 was easily blocked by its cold mass due to low density. Although the role of the α5 subunit was then and is still not as clear as compared with other α subunits, [^{11}C]Ro15-4513 binding is abundant in the anterior cingulate and insular cortices and these distributions suggest a possible role in emotion and memory (Suhara, Yasuno et al. 2001; Suhara, Okubo et al. 2002). From Maeda et al. and Lingford-Hughes et al.'s studies, one can conclude that Ro15-4513 will be useful for studying the function of the α5 subunit in the $GABA_A$/*BZ* receptor complex and that subtype selective PET ligands for this subunit are of great interest (Maeda, Suhara et al. 2003).

For the 5-HT_{2A} receptor [^{11}C]MDL 100907 is available since 1996, when Lundkvist et al. performed their first PET experiments with it (Lundkvist, Halldin et al. 1996). A few years later Kakiuchi et al. showed an age-related reduction of tracer binding in monkeys (Kakiuchi, Nishiyama et al. 2000). The role of the serotonergic system in depression is indicated by studies that showed differences in 5-HT_{1A}, 5-H_{T2} and SERT density in untreated and treated patients (Biver, Wikler et al. 1997; Massou, Trichard et al. 1997; Meyer, Kapur et al. 2001; Yatham, Liddle et al. 2001; Messa, Colombo et al. 2003; Bhagwagar, Hinz et al. 2006). Numerous 5-HT_{2A} receptor binding studies using [^{18}F]altanserin have been published. (Biver, Lotstra et al. 1997; Meltzer, Smith et al. 1998; Smith, Price et al. 1998; Rudolph, Crestani et al. 1999; van Dyck, Soares et al. 2000; Staley, Van Dyck et al. 2001; Pinborg, Adams et al. 2003; Adams, Pinborg et al. 2004; Pinborg, Adams et al. 2004; Sheline, Mintun et al. 2004; Kristiansen, Elfving et al. 2005; Haugbol, Pinborg et al. 2007). Their experiments ranging from tracer validation to sophisticated research on diseases like dementia and schizophrenia.

2.4.2 Drug Occupancy

The relationship of pharmacokinetic and pharmacodynamic parameters of a drug with behavioral and therapeutic efficacy can be evaluated in PET occupancy studies. The pharmacokinetics of the drug can directly be measured using radiotracers that are positron emitting analogues of the drug itself. The procedure of labeling drugs however, is complex and time consuming, and may have other disadvantages (Fowler et al. 1999). Therefore, in most cases, established PET radioligands are used that occupy the same receptor as the drug of interest. The drug induced change in ligand binding is obtained as a measure of drug occupancy. Specifically, this method may be used to relate the receptor occupancy of the drug to dose, plasma drug levels and treatment response, thereby providing information on therapeutic doses and frequency of administration (Gefvert et al. 1998; Grunder et al. 1997; Learned-Coughlin et al. 2003; Nordstrom et al. 1992; Rabiner et al. 2002a,b). Data have shown that antidepressants also occupy 5-HT_2 receptors (Meyer et al. 1999) and interaction with this receptor may be involved in the therapeutic activity of these drugs (Loo et al. 2003; Meyer et al. 2003).

When Persson et al. did their experiments with [^{11}C]Flumazenil in 1985 they already suggested that the ligand might also be used for the research on drug occupancy of the benzodiazepine binding site. Given an a5-subunit selective compound drug occupancy PET studies might help to further broaden our knowledge of this subunit's involvement in the action of benzodiazepines *in vivo*.

2.4.3 Measurement of Changes in Neurotransmitter Release

In order to study the (dys)function of neurotransmitter systems, it is important to quantify changes in the levels of these neurotransmitters in the living brain. The combined use of radiolabeled ligands with a serotonergic or GABAergic challenge may provide information on neurotransmitter release in specific regions of the brain. The approach is based on the assumption that an injected radiolabeled ligand competes for the same receptor as the endogenous transmitter. So, increases in neurotransmitter release result in a decreased binding of the radioligand and decreased neurotransmitter release induces an increase in ligand binding. The changes in ligand binding are used as a measure of the change in neurotransmitter levels. For this study this would only be relevant with potential 5-HT_{2A} receptor ligands as the compounds for the $GABA_A$ receptor are supposed to bind to its benzodiazepine binding site.

2.4.4 Drug Interaction with a Task Assignment

The effect of a decrease in 5-HT levels on cognitive function in depressed patients was studied by Smith et al. (1999). They reported an attenuation of the task (verbal fluency) related activation in the anterior cingulate after this challenge, which was correlated to an increase in depressive symptoms. These examples illustrate the possibilities of PET in psychiatric research and drug development. The different findings have provided useful knowledge on the involvement of the serotonergic systems in the pathogenesis and treatment of psychiatric disorders. The use of PET is still expanding and a large amount of research is directed to the development of new radiotracers and methods which may provide further insight in these processes (Udo de Haes 2005).

2.5 $GABA_A$ Receptor α5-Subunit and 5-HT_{2A} Receptor and their Role in Learning and Memory

First $GABA_AR$ α5-subunit specific inverse agonists were discovered by Chambers et al. in 2002, of which 6,6-dimethyl-3-(2-hydroxyethyl)thio-1-(thiazol-2-yl)-6,7-dihydro-2-benzothiophen-4(5*H*)-one has been identified as the one with the best binding properties. Functionally it is a selective inverse agonist for $GABA_ARs$ containing the α5-subunit. A little later the same group reported that this compound enhances cognitive performance in rats in the delayed 'matching-to-place' Morris water maze test - a hippocampus-dependent memory task - without the convulsant or proconvulsant activity associated with nonselective, $GABA_A$ receptor inverse agonists. In 2004, again the same group published the discovery of yet another α5-subunit selective inverse agonist with cognition enhancing properties which was selected for clinical evaluation (Chambers, Atack et al. 2002; Chambers, Atack et al. 2003; Chambers, Atack et al. 2004). Further similarly structured compounds were found subsequently (Sternfeld, Carling et al. 2004) which displayed comparable properties at α5-containing $GABA_A$ receptors (Street, Sternfeld et al. 2004; Dawson, Maubach et al. 2006). In 2002, Collinson et al. discovered enhanced learning and memory and altered GABAergic synaptic transmission in mice lacking the α5 subunit of the $GABA_A$ receptor (Collinson, Kuenzi et al. 2002). Four years later Glykys and Mody reported hippocampal network hyperactivity after selective reduction of tonic inhibition in $GABA_A$ receptor α5-subunit deficient mice. These authors suggested that there might be an evolutionary pressure to diminish the levels of this subunit, especially because the α5 distribution in the adult brain is spatially restricted. One possible reason for the enduring presence of α5 subunits in hippocampal pyramidal cells PCs could be that the advantages in learning/memory stemming from its loss may be counterbalanced by a hyperexcitable epi-

leptic phenotype. The α5 subunit has also been found in the human hippocampus with a distinct localization to the CA1 and CA3 regions (Wainwright, Sirinathsinghji et al. 2000). The authors concluded that the ability to modulate tonic inhibition mediated by these receptors may balance the needs for increased excitation required for better learning with those for controlling the hyperexcitability. More compounds with inverse agonistic efficacy on α5-subunit containing GABAA receptors have been found in the meantime with comparable results (Collinson, Atack et al. 2006; Guerrini, Ciciani et al. 2007) but so far, none of them were suitable as PET ligands, nor have they yet been turned into clinically used drugs.

Serotonin 5-HT_{2A} receptors in frontal cortex and hippocampus modulate local circuitry. Both of these brain areas are known to be involved in associative learning across a number of species and learning paradigms (Weible, McEchron et al. 2000). Starting in the nineties numerous publications led to the assumption that 5-HT_{2A} agonists can enhance associative learning, while antagonists like ritanserin and cyproheptadine impaired it (Titov, Shamakina et al. 1983; Hensman, Guimaraes et al. 1991; Alhaider, Ageel et al. 1993; Ma and Yu 1993; Kobayashi, Ohno et al. 1995; Vitiello, Martin et al. 1997; Williams, Rao et al. 2002; Harvey 2003). Deficits in associative learning are symptoms of a number of clinical states, including schizophrenia and Alzheimer's disease. Harvey (2000) comes concluded that the 5-HT_{2A} receptor is critically involved in learning, and that alterations in this receptor can lead to abnormalities in cognitive functions in both humans and experimental animals (Harvey 2003).

2.6 $GABA_A$ Receptor α5-Subunit and 5-HT_{2A} Receptor and their Role in Schizophrenia and Alzheimer's Disease

Alzheimer's disease (AD) is the most common neurodegenerative disease and is one of the most costly disorders to developed societies, ranking third after cancer and heart disease. The prevalence of AD in Western societies appears to double every ten years for people older than 65, with estimates ranging from 16 – 29 % for people aged over 85 (Maubach 2003). An alternative effort to the now most widely used pharmacological treatment, e.g. the cholinesterase inhibitors, should be to enhance cognition through the negative modulation of the $GABA_A$ receptor ion channel activity by BZ inverse agonists. Non-selective inverse agonists of the BZ site do enhance cognitive performance but cannot be used therapeutically because of profound anxiogenic and convulsant side-effects. However, selective inverse agonists of the α5 receptor subtype may offer an improved safety window. Pre-clinical results are encouraging, with the α5-selective inverse agonists enhancing memory with little side effects. In addition to that the

$GABA_A$ receptors in brain areas most affected by AD ameliorate cognitive function under conditions comparable to AD. If the efficacy and safety profiles of α5 inverse agonists in humans are similar to those seen in preclinical studies, it is anticipated that these compounds would have significantly better tolerability compared to currently marketed cholinergic therapies (Maubach 2003).

As mentioned before, several subtypes of serotonin receptors have been characterized. Later on, postmortem studies found 5-HT_{2A} receptor losses in AD. These were substantiated by the use of [^{18}F]altanserin which provided *in vivo* evidence of a robust age-related decline, primarily before age 60, in many brain regions, with the cingulate showing the steepest decline and the hippocampus the shallowest decline. In a study of nine AD patients and ten age matched healthy controls, a 40 % reduction in 5-HT_{2A} BP in AD was found in the amygdalohippocampal complex, anterior cingulate, prefrontal cortex, lateral temporal cortex and sensorimotor cortex (Meltzer, Smith et al. 1998; Meltzer, Price et al. 1999; Sheline, Mintun et al. 2002; Cohen 2007)

Compared to its envolvement in AD, the importance of 5-HT_{2A} receptors in schizophrenia was recognized a lot earlier, namely as early as 1954, with further support coming with the discovery that reserpine, a drug with some efficacy in treating schizophrenia, depletes 5-HT and the demonstration of a serotonergic component of antipsychotic drug binding in 1978 (Gaddum and Hameed 1954; Gray and Roth 2007). The discovery that clozapine, a drug highly effective in treating schizophrenia, is a 5-HT_{2A} receptor antagonist that downregulates 5-HT_{2A} receptors further reinforced the hypothesis that 5-HT_{2A} receptor blockade may be beneficial in schizophrenia (Gray and Roth 2007). Selective 5-HT_{2A} receptor antagonists (especially MDL 100907 and SR46349B) have shown promise in animal models and humans to be predictive of atypical antipsychotic action and have demonstrated efficacy in treating schizophrenia. Most recent data published by Hurlemann et al. state that 5-HT_{2A} receptor density is decreased in the at risk mental state of potentially schizophrenic patients, a study performed using the 5-HT_{2A} receptor antagonist [^{18}F]altanserin and PET imaging (Hurlemann, Matusch et al. 2007).

2.7 Aims of this Work

This work aimed at developing ligands useful in the diagnosis of memory loss and learning malfunctions associated with various psychiatric diseases, like AD, depression and schizophrenia. A $GABA_A$ receptor line and a 5-HT_{2A} receptor line were followed.

Although [^{18}F]Altanserin, a tolerably good radio tracer for the use in PET imaging, even for humans, is already available and used for research and diagnosis of processes or illnesses where the 5-HT_{2A} receptor is involved, there is still a need for better 5-HT_{2A} receptor selective tracers. It was the aim of this work to evaluate a MDL 100907 analog, [^{18}F]MHMZ, for its potential use in PET imaging, thereby combining the better selectivity of MDL 100907 over altanserin with the superior properties of ^{18}F as compared to ^{11}C, when it comes to longer dynamic PET studies (> 60 min.) or transportation of the injectable tracer to other facilities.

To-date no $GABA_A$ receptor α5-subunit specific radio tracer is available that could be used for PET imaging. Therefore, this work aimed for the evaluation of six novel potential $GABA_A$ receptor α5-subunit specific ligands, all containing a fluorine atom, which might enable radio-labeling with ^{18}F and subsequent PET experiments to extend the understanding of the above mentioned processes and diseases in which the α5-subunit appears to play a role.

3 MATERIALS AND METHODS

3.1 Materials, Buffers, Media, Software and Hardware

Please refer to the appendix for a list of all materials, buffers, media, software and harware used for this work.

3.1.1 Chemicals

If not indicated otherwise, all chemicals and standard laboratory equipment were bought from one of the following companies in analytical grade purity: CARL ROTH GmbH + CO. KG, Karlsruhe, Germany; Sigma-Aldrich Chemie GmbH, Steinheim, Germany; Merck KG, Darmstadt, Germany; VWR, Darmstadt, Germany

3.1.2 Animals

If not indicated otherwise, for all experiments where rats or rat brains were needed, like receptor autoradiography, filtration binding assays or micro positron emission tomography, only adult, fully-grown, male Wistar or Sprague-Dawley rats were used which were either from in-house breed or purchased from the European branch of Charles-River Laboratories, Inc., Wilmington, MA, USA.

3.2 Chemistry

3.2.1 [^{18}F]MHMZ

The potential PET-ligand for the 5-HT_{2A} receptor line of this work is [^{18}F]MHMZ. It was synthetised as published by (Herth, Debus et al. 2008). The structures of [^{11}C]MDL 100907, [^{18}F]MHMZ and the precursor MDL 105725 are displayed in **Figure 6**.

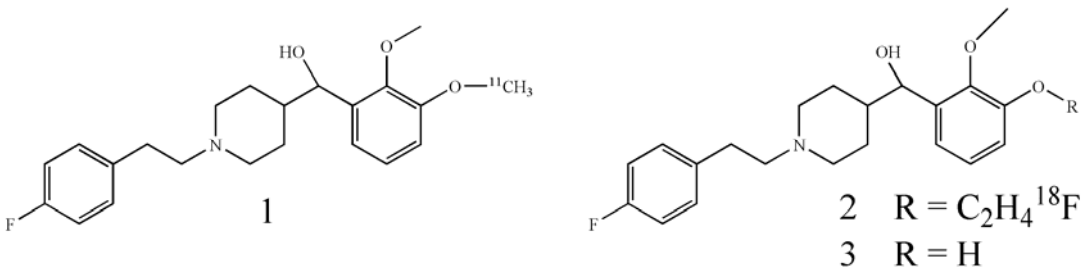

Figure 6: Structures of [^{11}C]MDL 100907 **(1)**, [^{18}F]MHMZ **(2)** and MDL 105725 **(3)**

In **Table 3** K_i values of MHMZ, altanserin and MDL 100907 are displayed as determined by Mikael Palner (research group of Prof. Gitte Knudsen, Rigshospitalet, Copenhagen, Denmark).

Table 3: K_i values of three different 5-HT_{2A} receptor ligands

Compound	K_i [nM]
MHMZ	9.00 ± 0.10
altanserin	0.74 ± 0.88
MDL 100907	2.10 ± 0.13

3.2.2 TC Compounds

The potential PET-ligands for the $GABA_AR$ line of this work are new compounds, synthetised on the basis of substitutions at 6-(6-Fluor-pyridine-2-yl)methyloxy-7,8,9,10-tetrahydro-(7,10-ethano)-1,2,4-triazolo [3,4-a]phthalazines. Synthesis was performed by Tanja Capito, Department of Radiochemistry, University of Mainz. It was conducted similar to data published by (Street, Sternfeld et al. 2004). Six non-radioactive „cold" compounds were synthetised which show differences in the substitution of a residue at position three of the 7,8,9,10-tetrahydro-(7,10-ethano)-1,2,4-triazolo[3,4-a]phthalazine-basis. Synthesis details are part of Tanja Capito's PhD thesis and will be published elsewere.

Table 4: Structures of the six benzodiazepine derivatives tested for the $GABA_A$ receptor line of this work.

	R/Name	**R/Name**
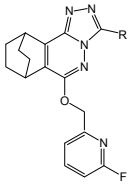	 **TC07**	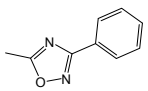 **TC10**
	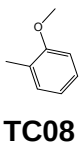 **TC08**	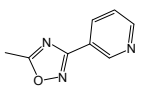 **TC11**
	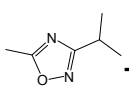 **TC09**	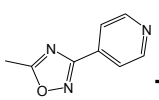 **TC12**

3.3 Bacteria

3.3.1 Cloning Vector

Cloning vectors used were either pRK5 or pRK7. A representative cloning vector is displayed in **Figure 7** below containing the sequence for the α5 subunit of the $GABA_A$ R. (A list of all used cloning vectors is given in the appendix).

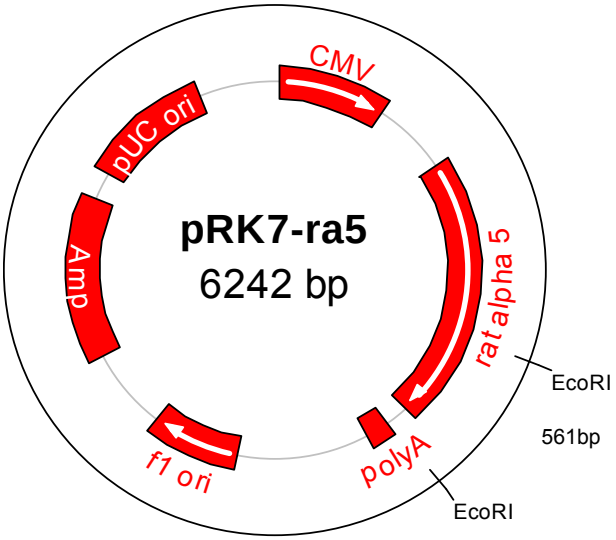

Figure 7: Representative cloning vector containing the sequence of the α5 subunit of the $GABA_A$ R and an ampicillin resistance **(Amp)**. The size of the fragment resulting from an EcoRI digest is also shown. The vector is a pUC 18 based vector for expression in eukaryotic cells controlled by a cytomegalovirus promotor and enhancer. **Poly A** = poly A polimerase, **pUC ori** = bacteria origin of replication, **CMV** = viral promotor, **f1 ori** = bacteriophage origin of replication.

3.3.2 Competent Bacteria

Competent DH5α-cells were obtained according to a rubidium chloride protocol. 500 mL LB medium were inoculated with 1 mL of an over-night bacteria culture and incubated at 37 °C at 200 - 300 rpm in an incubater shaker. Bacteria were pelleted at a density of OD_{595nm} of 0.4 - 0.7. Pellets were resuspended in 150 mL TFB I and put on ice for 15 min., before centrifuging again and resuspension in 20 mL TFB II. Bacteria were either used immediately or stored at -80 °C.

3.3.3 Bacteria Transformation

Bacteria transformation was done according to the protocol by Inoue et al. (Inoue, Nojima et al. 1990). Competent cells were slowly warmed up and 50 - 200 µL were placed into pre-cooled sterile 15 mL tubes. 3.4 µL mercaptoethanol 1:10 diluted by dH_2O were added and incubated for 10 min on ice. After that ~ 3 - 5 µL ligation solution was added

and incubated for 30 min on ice. 800 µL of SOC medium were pre-warmed to 42 °C. After incubation cells were heat-shocked in pre-warmed water for 40 sec. and incubated for another two minutes. Subsequently cells were mixed with 800µl SOC medium and incubated for one hour at 37 °C and 240 rpm in an incubator shaker. Preselection of clones was done by ampicillin. 100 µL of each preparation was transferred to an LB-plate with ampicillin and incubated over night at 37 °C in an incubator.

3.4 Plasmid Maxi Preparation

3.4.1 Culture for Plasmid Maxi Purification

For CsCl density gradient purification bacteria were grown in a 10 – 50 mL preculture for ~ 6 h at 37 °C in an incubator shaker at 240 rpm. Precultures were then added to 200 mL of TB medium and then incubated over night or up to 24 h total. Afterwards bacteria were pelleted at 3000 g at 4 °C. Bacteria pellets were either processed immediately or stored at -20 °C for a few days until further plasmid purification steps.

For Qiagen and Promega plasmid purification kits bacteria were grown as precultures in LB medium for ~ 6 - 8h and afterwards put in a total volume of 200mL and were then incubated over night for up to 16 h total. For these kits bacteria cultures were supposed to still be in the logarithmic growth phase. After incubation bacteria were pelleted at 6000 g and 4 °C for 15 min. Pellets were either processed immediately or stored at -20 °C until further use.

3.4.2 CsCl density gradient method

Bacteria pellets were completely resuspended in 30 mL of solution I by repeated pipetting with a pipette. The bacteria suspension was transferred to a fresh 250 mL bucket and 60 mL of solution II was added. After cautious mixing by inverting the vessel several times it was incubated for 10 min on ice. After incubation, 50 mL of ice-cold solution III was added and content was mixed by inverting several times. Incubation of 5 min on ice followed this step. Buckets were then centrifuged at 27.000 g for 15 min and supernatants filtered through a paper tissue into a fresh bucket. DNA was precipitated with 100mL isopropanol at RT which made the total solution volume ~250 mL. The solution was immediately centrifuged at 27.000 g at 4 °C for 20 min. Supernatants were carefully decanted or aspirated with a pipette. Pellets were resuspended in 25 mL 1 X TE buffer. After complete resuspension 25 g CsCl were added and the solution was poured into a 50 mL disposable centrifugation tube. 2 mL ethidium bromide were added (10 mg/mL in H_2O). Samples were centrifuged at 3000 g

for 15 min (Heraeus Megafuge, see table). The supernatant was poured into thin walled Beckman ultra centrifuge tubes. Tubes were balanced, capped and inserted into a Beckman VTi50 vertical rotor. Samples were centrifuged for ~ 36 h at 25 °C and 200.000 g. Afterwards the tubes were uncapped and a hole was pierced into the tube 0.5 cm below the lower of the two bands. In cases of low yield an ultraviolet light lamp was used to make visible the bands. With needle and syringe the lower band was extracted which led to 2 - 4 mL sample volume. 200 µL ethidium bromide were added and filled into fresh Beckman ultra centrifuge tubes which fit the Beckman VTi65.2 rotor. After balancing with CsCl solution and capping, samples were centrifuged in a Beckman VTi65.2 rotor at 25 °C and 400.000g for ~ 4 h. After centrifugation band was extracted as described above. Out of the ~ 1 – 2 mL sample the remaining ethidium bromide was extracted with saltwater saturated isopropanol until supernatant was completely clear. The DNA containing sample was then dialyzed against a more than 100-fold excess of 1 X TE. TE buffer was changed at least once.

3.4.3 Quiagen HiSpeed® Plasmid Purification Maxi Kit

Alternatively to the described CsCl method the plasmid purification maxi kit by Qiagen was used. The yield is usually not as high as with the CsCl density gradient method but a lot faster and the DNA concentration is sufficient for transfection with most of the used $GABA_A$ receptor subunit clones. The purification is based on an anion-exchange resin method with columns binding supercoiled DNA, while, at low salt conditions, RNA, proteins, dyes and low-molecular-weight impurities are removed by washing steps. Plasmid DNA is eluted in a high-salt buffer and afterwards concentrated and desalted by isopropanol precipitation.

Purification Steps

Bacteria pellets were resuspended in 10 mL buffer P1. After complete resuspension 10 mL buffer P2 were added and the samples mixed thoroughly by vigorously inverting the sealed tube 4-6 times. Samples were then incubated for 5 min at RT. 10 mL prechilled buffer P3 was added and the samples were mixed immediately and thoroughly by inverting them. The lysates were then poured into the QIAfilter cartridges and incubated at RT for 10 min. In the meantime the HiSpeed Maxi tips were equilibrated by applying 10 mL buffer QBT to them and allowing them to empty by gravity flow. The lysate was then filtered into the HiSpeed Maxi tips, which were allowed to empty by gravity flow and were washed by applying 60 mL buffer QC. Afterwards DNA was eluted into a 50 mL plastic tube by applying 15 mL buffer QF. DNA was precipitated by adding 0.7 volumes of room temperated isopropanol to the eluted DNA solution. Samples were incubated for 5 min and then pressed through the

QIAprecipitator Maxi Module. The DNA bound to the precipitator was then washed at least twice with 70 % ethanol and after drying eluted into an 1.5 mL collection tube with 1 mL TE buffer.

3.4.4 Promega PureYield™ Plasmid Maxiprep System

Bacteria pellets were resuspended in 12 mL of cell resuspension solution. After completion 12 mL lysis solution was added and samples were mixed gently but thoroughly and incubated for 3 min. 12 mL of neutralization solution were added and samples were mixed thoroughly. The lysate was centrifuged at 14 000 g for 20 min at RT in a fixed-angle rotor. A column stack was prepared which consisted of a blue PureYield™ Clearing Column on the top of a white PureYield™ Maxi Binding Column. The stack was placed on the vacuum manifold and the lysate was poured into it. Vacuum was applied until all lysate had passed through the columns. The clearing column was removed and the maxi binding column washed with 5 mL of endotoxin removal wash buffer, 20 mL of column wash buffer and then dried under vacuum for 5 min. Remaining ethanol was removed with paper towel and the column was placed into a fresh 50 mL centrifugation tube. 1.5 mL of nuclease-free water was added to the column and the column was then centrifuged in a swinging bucket rotor at room temperature at 2000 x g for 5 min. Eluate was collected into a 1.5 mL tube and kept at 4/-20 °C until further processing.

3.5 Restriction Analysis of Bacteria Plasmid DNA

3.5.1 Determination of DNA Concentration

DNA concentrations after maxi plasmid preparations were determined by a nano drop photometer. OD_{260} and OD_{280} values were measured at a wavelength of 260 nm and 280 nm respectively. DNA solutions were diluted 1:10 in TE buffer or nuclease free dH_2O. An OD_{260} of 1 is equivalent to a DNA concentration of ca. 50 µg/mL. The OD_{260}/OD_{280} quotient should be at around 1.8 ± 0.2 for optimal transfection efficiencies.

3.5.2 Restriction Enzyme Digest

For diagnostic restriction enzyme digests a total volume of 20 µL was chosen. Always between 1 and 2 µg DNA were used and 2 µL of the adequate 10 x buffer concentrate. 1 µL of enzymes was used which was equivalent to 5 - 20 units of the respective enzymes. For enzymes that needed BSA, 1 µL 100 x BSA was added and mixture was

topped up with sterile deionized water to 20 µL. Details are given in Table 5 below. Incubation was always 60 min. at 37 °C.

Table 5: Restriction Enzyme Digest

subunit	bp fraction	enzyme	10 x buffer	BSA	DNA µg/µL	DNA	H_2O
α1	1559	EcoRI 1µL	P1 2µL		0.88	2 µL	15 µL
α2	16 + 1263	EcoRI 1µL	P1 2µL		0.63	2 µL	15 µL
α3	646	KpnI 1µL	P1 2µL	1 µL	0.72	2 µL	14 µL
α4	621 + 1238	KpnI 1µL	P1 2µL	1 µL	0.66	2 µL	14 µL
α5	561	EcoRI 1µL	P1 2µL		0.6	2 µL	15 µL
α6	1558	EcoRV/HindIII 1µL	P2 2µL	1 µL	0.49	3 µL	13 µL
β2	959	PstI 1µL	P3 2µL	1 µL	0.42	3 µL	13 µL
β3	1062	HindIII 1µL	P2 2µL		0.43	3 µL	14 µL
γ2	1857	XhoI 1µL	P2 2 µL	1 µL	1.5	1 µL	15 µL

3.5.3 Agarose Gel Electrophoresis

DNA fractions of different lengths can be separated by agarose gel electrophoresis. Agarose (0.75 - 1.5 % w/v) was boiled in TAE buffer in a microwave oven and the solution was poured into a horizontal electrophoresis chamber. Ethidium bromide was added at a concentration of 0.6 µg/mL to the slightly cooled agarose gel solution just before the gel was poured into the chamber. Gels were run at 5 V/cm distance between electrodes. Before loading, DNA solutions were mixed with loading dye. As a length marker DNA sizer V from Peqlab was used. It consists of λ phage DNA digested with BstE II restriction enzyme.

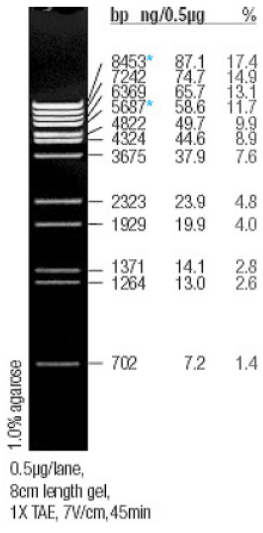

Figure 8: DNA sizer V from Peqlab. Image from Peqlab catalog. Gel conditions differ slightly from conditions used in the experiments performed for this work.

3.6 Cell Culture

3.6.1 Maintenance Culture

HEK cell (HEK293 cells) maintenance cultures were grown in 20 mL MEM medium per culture flask. Every Friday at least two fresh culture flasks were taken and 15 or 18 mL of fresh medium were added. Afterwards one flask with confluently grown cells was taken, medium was removed, cells were washed twice with DPBS and 3 mL of cell culture salt solution were added. The flask was vigorously shaken to dislodge the cells. After a maximum of two minutes ~125 ml of fresh pre-warmed MEM medium were added and flasks were gently shaken and turned upside down to singularize the cells. Finally 5 and 2 mL of this cell suspension was added to the fresh bottles containing 15 and 18 ml medium respectively. Contents were gently mixed and flasks were kept in an incubator at 37 °C and 5 % CO_2 until further use.

3.6.2 Plating Out of Cells for Binding Assays

Once a week cells were plated out for binding assays. The desired amount of large (145/20 mm) Greiner Cellstar cell culture dishes were prepared with 14.4 mL of pre-warmed fresh MEM medium. Then flasks with confluently grown cells were taken, medium was removed, cells were washed twice with DPBS and 3 mL of cell culture salt solution were added. The flask was vigorously shaken to dislodge the cells. After a maximum of two minutes ~ 125 mL of fresh pre-warmed MEM medium were added and flasks were gently shaken and turned upside down to singularize the cells. Cell suspensions were joined in one 600 mL Nunc cell culture bottle, gently mixed and then 5 mL suspension were added to each of the culture dishes. Culture dishes were kept in an incubator at 37 °C and 5 % CO_2 until further use.

3.6.3 Plating Out of Cells for Electrophysiology

Plating out of cells for electrophysiology was carried out as described above, only using small (94/16 mm) Greiner cell culture dishes with five round cover slips each. The culture dishes were placed opened under UV light for sterilization and to roughen them up so cells stick better to the glass. Usually four dishes were prepared with always two in the same way. Cell culture dishes were prepared with 8,5 mL of pre-warmed fresh

MEM medium for Tuesday transfection, the other pair with 7.2 mL for Monday transfection. Finally 2.8 mL suspension were added to latter dish, 1.5 mL to the former.

3.6.4 Transfection for Binding Assay

The 2 x BBS, the $CaCl_2$ and the water were brought to room temperature. A transfection plan (**Figure 9**) was prepared according to the amounts DNA per plate per desired subunit and the concentrations achieved after DNA maxi preparation for each subunit and eGFP. A representative transfection plan for all used alpha subunits in combination with β3 and γ2 is given below. The said amount of water, the DNA and the $CaCl_2$ were pipetted in this order. 1 mL 2 x BBS per plate were added to the respective Greiner tube and mixed by aspirating up and down with an automatic pipette for 30 seconds. 2 mL of transfection suspension per plate were dropped onto the cells. Each plate was gently shaken after application of the transfection suspension. All five dishes were stored in an incubator with 3 % CO_2 and 37 °C. Medium was exchanged after 24 hours and dishes were further incubated at 5 % CO_2 and 37 °C. Cells were harvested 48 hours after transfection.

Transfection Date												
		subunit I		subunit II		subunit III		additional		H2O	CaCl2	BBS
		concentration µg/µl		"		"		"				
number of plates	*X*	amount DNA per plate µg	*µl*	"	*µl*	"	*µl*	"	*µl*	*ml*	*ml*	*ml*
		α1pRK5		β3.pRK5		γ2.pRK5		egfp		H2O	CaCl2	BBS
		2,625		0,432		1,5		0,85				
	5	5	9,5	1	11,6	0,75	2,5	2,5	14,7	4,35	0,625	5
		α2pRK7		β3.pRK5		γ2.pRK5		egfp		H2O	CaCl2	BBS
		0,7		0,432		1,5		0,85				
	5	12	85,7	1	11,6	0,75	2,5	2,5	14,7	4,28	0,625	5
		α3pRK5		β3.pRK5		γ2.pRK5		egfp		H2O	CaCl2	BBS
		3,2		0,432		1,5		0,85				
	5	3	4,7	1	11,6	0,75	2,5	2,5	14,7	4,36	0,625	5
		rα4.pRK7		β3.pRK5		rγ2S.pRK5		egfp		H2O	CaCl2	BBS
		1,78		0,432		1,5		0,85				
	5	25	70,2	1	11,6	0,75	2,5	2,5	14,7	4,29	0,625	5
		rα5.pRK7		β3.pRK5		rγ2S.pRK5		egfp		H2O	CaCl2	BBS
		0,46		0,432		1,5		0,85				
	5	2	21,7	1	11,6	0,75	2,5	2,5	14,7	4,34	0,625	5
		rα6.pRK7		β3.pRK5		rγ2S.pRK5		egfp		H_2O	$CaCl_2$	BBS
		1,8		0,432		1,5		0,85				
	5	5	13,9	1	11,6	0,75	2,5	2,5	14,7	4,35	0,625	5

Figure 9: Representative example of a transfection plan for binding assays. All alpha subunits are displayed in combination with beta 3 and gamma 2 short, usually co-transfected with eGFP for control of transfection effiency.

3.6.5 Transfection for Electrophysiology

Transfection for electrophysiology was carried out as described above, except that the CaCl2 and 2 x BBS volumes were halfed and the DNA amount was 0.4-fold. Radioligand Binding Assay

3.6.6 Cell Harvesting

Culture medium was discarded and cells were washed twice with pre-warmed PBS. Then 8 mL ice cold PBS were added to each dish and subsequently cells were dislodged from the dishes by pipetting back and forth with a 5 mL pipette tip and a 5 mL pipette (Gilson). Cell suspensions from each dish were transferred to 50 mL Greiner centrifugation tubes and stored on ice until further processing. A sample from each transfection was taken onto glas slides and covered with cover slips. The tubes were capped and cells were spun down in a centrifuge at 300 x g and 4 °C for 10 min. During centrifugation transfection efficiency was checked with an Olympus fluorescence microscope.

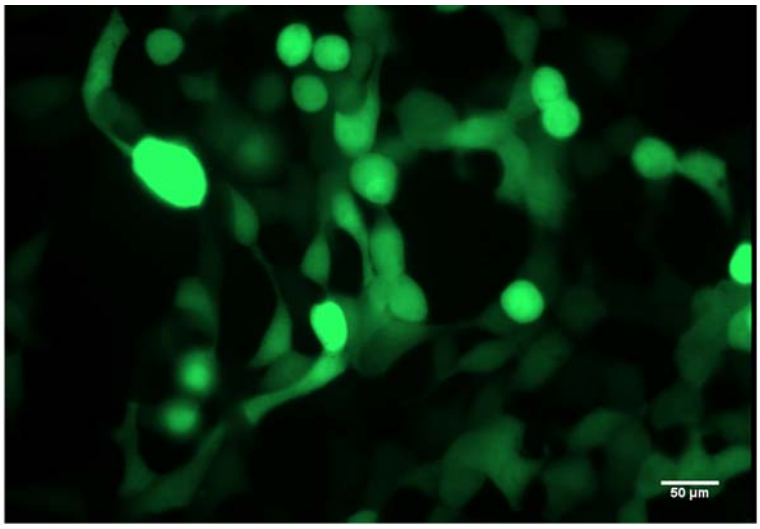

Figure 10: Transfection control HEK293 cells.

eGFP has an excitation maximum at ~ 488 nm and an emission maximum at ~ 510 nm, so a 485/515 filter was used. Cells were used when more than 10 % of the cells were transfected. After centrifugation the supernatant was discarded and 30 mL of ice cold 50 mM Tris/Citrate pH 7.4 was added to each tube. Cells were homogenized with ultra-turrax and poured into sorvall centrifugation tubes. Suspensions were centrifuged at 27.000 x g at 4 °C for 20 min with a Sorvall SS34 rotor. Then supernatant was discarded and pellets either used immediately or frozen at -20 °C and stored until further use.

3.6.7 Transfection Control

A vector containing the sequence for eGFP was always co-transfected along with the DNA of the three $GABA_AR$ subunits contained in the pentamer. During the first centrifugation step of cell harvesting a small aliquot was transferred onto glass slides, covered with a cover-slip and examined with a fluorescence microscope.

3.6.8 Membrane Preparation

The cell pellet was resuspended in as much of 50 mM Tris/Citrate pH 7.4 buffer as needed for the experiment but at a protein concentration lower than 150 µg per reaction tube.

3.6.9 Proteine Quantification with Bradford Assay

Protein quantification was done with a BIO-RAD kit. The Bio-Rad Protein Assay is a dye-binding assay in which a graded color change of the dye occurs in response to various concentrations of protein (Bradford 1976). The absorbance maximum for an acidic solution of Coomassie® Brilliant Blue G-250 shifts from 465 nm to 595 nm when binding to protein occurs (Fazakes de St. Groth 1963; Reisner, Nemes et al. 1975; Sedmack and Grossberg 1977). The dye binds to primarily basic and aromatic amino acid residues, especially arginine (Compton and Jones 1985). Spector (Spector 1978) found that the extinction coefficient of a dye-albumin complex solution was constant over a 10-fold concentration range. Thus, Beer's law may be applied for accurate quantitation of protein by selecting an appropriate ratio of dye volume to sample concentration. A standard curve was done by a dilution series of BSA dissolved in dH_2O and subsequently protein contents were determined by calculating the amount of protein by the following equation:

$$x = \frac{y - 0{,}051}{0{,}0511} \text{ µg protein; } r^2 = 0{,}9966$$

The equation gives µg of protein per measured sample and has to be corrected for the applied dilution. With each protein assay a BSA standard with the concentration of 1.4 mg/mL was measured as a control.

3.6.10 Binding Assay

Racks with reaction tubes were kept on ice. Membrane pellets were resuspended in adequate amount of 50 mM Tris/Citrate pH 7,4 buffer and samples were taken for protein content determination. Subsequently all solutions and membranes were pipetted according to experiment plan in the sequence buffer for total binding, competitor for

non-specific binding, dilution series of test compound, radio tracer and finally membrane preparations. After addition of the membranes the incubation lasted for 60 min. Racks with reaction tubes were covered with parafilm for the whole incubation period. After the incubation reaction tube contents were filtered trough glasfiber filter paper with 5 mL of 10 mM Tris/HCl pH 7.5 and then washed with another 5 mL of same buffer on a Brandel cell harvester. Filter papers of each reaction tube were transferred to liquid scintillation vials and topped with 4 mL of scintillation fluid. Filter papers were incubated for >30 min and transferred to a Beckman LS 6000 SC liquid scintillation counter.

3.6.11 Detection of Signal

The scintillation fluid added to the samples contains fluorophores, which convert the γ-rays, which are emitted after contact with the high energy particle first to UV light and, after contact with a second fluorophore, to visible light pulses. Each decay event therefore causes a shower of light pulses which can be detected and enhanced with photomultiplier tubes of a liquid scintillation counter. The size of the shower is determined by the energy of the particle. True events are only counted when events are detected from two PMTs at the same time. Due to interferences with certain colored contents and other interfering agents in a sample, so-called “quench” occur. The term describes the fact that not all decays can be counted by the PMTs in the end. A correction curve has to be made and the data subsequently corrected for quench losses in count number to obtain the decays.

3.6.12 Data Evaluation

Binding data was first entered into Microsoft Excel data sheets, normalized as % of total binding and then transferred into GraphPad Prism 4.0 data tables as % of total binding, plotted against the logarithm of the competitor concentration. Data were fitted with non-linear regression according to the sigmoidal function for one site competition binding experiments (A_1 = bottom, A_2 = top):

$$y = A_1 + \left(\frac{A_2 - A_1}{1 + 10^{(x - \log IC_{50})}}\right)$$

For the calculation of K_i values from the IC_{50} the equation from Y. Cheng and W. H. Prusoff (Cheng and Prusoff 1973) was used (K_i = inhibition constant, L = concentration of free ligand, K_d = affinity of the tracer):

$$K_i = \frac{IC_{50}}{1 + \frac{[L]}{K_d}}$$

3.7 Autoradiography

3.7.1 Preparation of Rat Brain Sections

Rats were narcotisised with CO_2 and subsequently decapitated by a rodent guillotine. Brains were carefully removed from the skull, shortly rinsed in ice cold 50 mM Tris/Citrate pH 7.4 buffer to remove hairs and blood. The brains were then frozen on a pre-cooled -80 °C cold steel plate. Brains were either stored in parafilm and aluminum foil at -80 °C or transferred to a Leica cryostate and kept in parafilm at -24 °C for 30 min. After warming up to -24 °C brains were frozen onto object carrier with tissue tack freezing medium in the desired orientiation for either sagittal, coronal or transversal sectioning. Sections were cut at 14 µm thickness, knife angle of 5° and an object temperature of -13 °C. Sections were melted onto super frosted glas slides (Menzel), air dried and were either used immediately or stored at -80 °C until further use.

3.7.2 Autoradiography Assay

Receptor autradiographies were carried out on ice for [^{3}H]Ro15-4513 and [^{3}H]Ro15-1788 experiments. Sections were circled with water repellent pap-pen to make sure that the whole reaction solution remains above the section. Sections were kept in steam saturated culture dishes during the whole incubation period. All solutions were prepared and sections were covered with an adequate mixture. At the end of the incubation period sections were washed 3 x 10 sec with ice cold buffer, shortly dipped into ice cold dH_2O, to remove salts, and quickly dried in a stream of cold air. Sections were then exposed to a tritium sensitive Fujifilm imaging plate and read-out after 3 - 5 days exposure.

Receptor autradiographies were carried out at room temperature for [^{18}F]MHMZ. Sections were circled with water repellent pap-pen to make sure that the whole reaction solution remains above the section. Sections were kept in steam saturated culture dishes during the whole incubation period. All solutions were prepared and sections were covered with adequate mixture. After incubation period sections were washed with ice cold buffer (see Table 10) 3 x 2 min, 2 x 2 min in buffer containing 0,01 % triton x-100, 1 x 2 min in pure buffer. Then they were dipped into ice cold dH_2O shortly, to get rid of salts, and quickly dried in a stream of cold air. After sections had dried they were exposed to Fujifilm imaging plates for 3 hours. The exposure time was varied according to specific activities and amount of tracer used.

3.7.3 Detection

3.7.3.1 Tritium Sensitive X-Ray Film

Standard Amersham Hyperfilm-^{3}H was used for “classical” detection of autoradiographic signals. X-ray films are poly-ethylene screens coated with a thin layer of a photo emulsion which contains grains of silver halides like silver-bromide and silver-iodide. When hit by γ-rays or light a latent image is created by an ion transfer. After exposure the film is processed in a developer solution which produces metallic silver which appears black where the invisible latent image had been before. Tritium sensitive x-ray film is not coated with a protective layer which stops the silver halide emulsion from being scratched off the film’s core plastic. In addition to the non-linearity of x-ray film post-processing scratches across the signal represent another drawback of this method.

3.7.3.2 Microimager

The second detection or read-out method used was by the use of a µ-imager, manufactured by Biospace, France. The live-imaging device works with a scintillation sheet, which is brought into close contact with the planar sample, absorbes the energy emitted by the radioactive isotope and fluoresces photons of a characteristic wavelength which in turn are read-out by a charge-coupled device camera (CCD-camera) and converted into a digital image. The µ-imager produces a resolution of 15 micron at best performance conditions.

3.7.3.3 Storage Phosphor Fuji FLA-7000

The third method tested fort the detection of autoradiographic signals is called storage phosphor technique. In storage phosphor screens, a substantial amount of the absorbed energy is captured after exposure by electrons that are trapped in a metastable energy level. The absorbed x-ray relief is stored as a ‘latent image’ until it is released by exposure to light of a longer wavelength than the characteristic emission of the phosphor (read-out process). When released from their meta-stable energy level, electrons emit light (photostimulated luminescence) that can be collected by a photomultiplier tube. For the read-out process, a fine laser beam with a spot size of 50 – 200 mm is used. The photostimulated luminescence is proportional to the absorbed x-ray intensity. The output of the photomultiplier is logarithmically amplified and subsequently digitised by an analogue/digital converter with 8 to 14 bit resolution. With the used Fujifilm FLA-7000 scanner a pixel size of 25 micron was achieved (Schaefer-Prokop and Prokop 1997).

3.8 In Vivo Binding

In vivo binding experiments were performed with in-house bred adult Sprague-Dawley rats, usually 8 - 10 weeks old with a body weight of 250 g – 310 g. Rats were given i.p. either vehicle (DMSO), 5 mg/kg flumazenil for the determination of non-specific binding/baseline or 5 mg/kg TC07 30 min before decapitation. 3 min before decapitation rats received 8 µCi/kg [^{3}H]Ro15-1788 i.v. into the tail vein. The radio tracer was diluted from a 1 mCi/mL solution with 0.9 % isotonic NaCl solution finally containing 0.8 % ethanol. After decapitation, brains were quickly removed from the skull, forebrain and cerebellum separated, weighed and homogenized in ice cold 50 mM Tris/Citrate pH 7.4 buffer: Cerebella weighed ~ 0,5 g and forebrains ~ 1.5 g. They were homogenized in 15 and 25 mL buffer respectively. Always 6 x 200 µL of each homogenate were pipetted into six glass tubes and immediately filtered through glass fiber filters (Schleicher & Schüll #5) with a Brandel cell harvester. Filter papers were transferred to scintillation vials and mixed with 4 mL Zinsser Analytics Aquasafe 300 Plus scintillation fluid. After incubation of 30 min vials were read out in Beckman liquid scintillation counter. Protein content of each homogenate was determined with Bradford assay (BIO-RAD). Dpm were normalized for protein content and corrected for dilution factor and non-specific binding and finally given as specifically bound dpm/mg protein. For the displacement studies means were taken from the vehicle animals and taken as total binding. The mean of the results of TC07 treated animals is given as percentage of total.

3.9 Electrophysiology

Electrophysiological experiments were carried out in the whole cell patch clamp mode (Neher, Sakmann et al. 1978) on transiently transfected HEK293 cells 48 hours after transfection. During the recordings cells were voltage clamped at a potential of -40 mV while the electrical resistance of the micro pipettes, filled with intracellular solution, was between 4.5 and 9 MΩ. GABA dose-response curves were recorded upon giga seal (electrical resistance of more than one giga ohm) and subsequent opening of the cell by a slight negative pressure with a GABA dilution series starting at 0.1 µM Gaba, continuing with 0.3, 1, 3, 10, 30, 100, 300 µM and finally 1 mM Gaba. GABA and test compounds were applicated with an SF77B fast step perfusion system applicator by Warner Intruments. Currents were recorded by HEKA PULSE, a recording software supplied with the HEKA EPC-9 amplifier used for amplification of the signal. Results are given as peak currents (I) divided by maximum current (I_{max}) and fitted with Graphpad Prism 4.0 software with the following function:

$$y = A_1 + (\frac{A_2 - A_1}{1+10^{(\log x_0 - x)\,p}})$$

Figure 11: Function for the fit of a sigmoidal dose-response curve. $\mathbf{A_1}$ bottom, $\mathbf{A_2}$ top, $\mathbf{x_0}$ EC_{50}, **p** hillslope

The EC_{20} was determined to be 3 µM GABA for $\alpha5\beta3\gamma2$ receptors. This concentration was used as a baseline current for competition measurements with TC07 and TC12. TC07 and TC12 were dissolved in bath solution containing 3 µM GABA at 1 nM, 3 nM, 10 nM, 30 nM, 100 nM, 300 nM and 1 µM concentrations. After normalization of the current peaks as described above results are given as % of 3 µM GABA current (EC_{20} current).

pull	heat	velocity	time
1	495	22	150
2	485	20	150
3	480	18	100
4	475	18	100

Table 6: Parameters for Sutter Instruments pipette puller for the pulling of electrophysiology micro pipettes out of raw boro-silicate glass tubes.

The pulse generator protocol and application protocol of GABA solutions as well as test compounds was a 10.5 sec protocol with 1 sec initiation baseline recording, 4 sec application and 5.5 sec post application recording.

3.10 Positron Emission Tomography

Micro positron emission tomography (microPET) scans were done with a Siemens/Concorde Microsystems microPET Focus 120 small animal PET (saPET) camera. Animals were eight week old Sprague-Dawley rats (~ 250 g) bought with catheters in the femoral artery and vein from Charles River Laboratories, France. Animals were anesthetized with isoflurane at a concentration of 1.8 %. Application of radiotracer was done i.v. into the femoral vein catheter, blood samples were collected via the femoral artery catheter. After application of substances or collection of blood samples catheters were flushed with heparinized isotonic 0.9 % NaCl solution. Volumes of blood collected were given back as isotonic 0.9 % NaCl solution. Results are given as standardized uptake values (SUV) which is defined by: (activity concentration in Bq/mL) * body

weight in g / (injected dose in Bq). Scans were carried out as dynamic scans over 60 min.

Figure 12: Positron emission tomography equipment. PET camera was a Siemens/Concord Microsystems Focus 120. Anesthetic was isoflurane at a concentration of 1.8 %. Animals were anesthetised and catheterised. The head was tape-fixed to minimize image blurring trough head motion.

Kinetic modeling and image quantification was done using the PMOD software package (version 2.95) and a 4-parameter reference tissue model. Details are described in the legend of **Figure 1** on page 15 and in the chapter Micro Positron Emission Tomography Experiments.

3.11 Metabolite Study

Blood samples of ~ 200 µL were collected during micro positron emission tomography scan at 5 min, 10 min, 30 min and 60 min/end of scan. Blood was collected in 1.5 mL heparinized Eppendorff tubes and gently mixed with heparin. After the last sample was collected blood was centrifuged at 3000 x g for 5 min, 50 µL plasma were taken and mixed with 200 µL acetonitrile to denature the proteins. Plasma proteins were spun down by centrifugation at 3000 x g for 5 min and 5 µL of supernatant were dropped onto thin layer chromatography (TLC) plates. TLC plates were developed with HCL_3/MeOH (5 : 2, v/v) for ~ 10 min and read out with Packard Bell β+-imager. Percentages of original tracer are given relative to the amount of active metabolite.

4 RESULTS

4.1 Binding Assays Rat Brain Membranes TC Compounds

Street et al. (Street, Sternfeld et al. 2004) found many of their tested compounds, which were used as a basis for the development of the compounds tested in this study, to be $GABA_A$ R subunit α5 specific to a large extent. Although not very likely, structure modifications can cause total loss of affinity for the benzodiazepine binding site or at least loss of selectivity among α-subunits.

In a first step the characteristics of the potential $GABA_A$ receptor specific compounds were tested on crude rat brain membrane preparations of the cortex, the cerebellum and the hippocampus in radio ligand binding assays. Four different conditions were employed: A low and a high concentration of [^{3}H]Ro15-4513, at the K_D of α5-containing $GABA_A$ Rs and of the remaining α-subunit containing receptors, and 1 nM [^{3}H]Ro15-1788 (flumazenil) on its own and together with 10 µM zolpidem. The latter three conditions were only used for the four most promising potential PET-ligands.

[^{3}H]Ro15-4513 is a ligand which binds with more or less the same affinity to all alpha subunit containing $GABA_A$ Rs except the α5 subunit, were it has a ten-fold higher affinity (Seeburg, Wisden et al. 1990; Carter, Thomsen et al. 1992; Hadingham, Wingrove et al. 1993; Sieghart 1995; Campos, de Cabo et al. 2001). On the other hand [^{3}H]Ro15-1788 (flumazenil) is a ligand which only recognizes receptors containing the subunits α1-3 and α5 (Seeburg, Wisden et al. 1990; Carter, Thomsen et al. 1992; Hadingham, Wingrove et al. 1993; Campos, de Cabo et al. 2001) with an affinity in the low nanomolar range and has a much lower affinity for α4 and α6 subunits.

Together with data of the distribution of the α-subunits (Laurie, Seeburg et al. 1992; Campos, de Cabo et al. 2001), which claim that the rat cerebellum contains mainly α1 and α6 subunits, data obtained with this radio tracer could shed further light on whether the difference between the tracer displacement in different brain regions seen with [^{3}H]Ro15-4513 hints on a subtype selectivity of the four remaining test compounds, especially a major difference between the affinity for α1- as compared to α5-subunit containing $GABA_A$ receptors. An additional ligand, zolpidem, is supposed to help with this approach. Pritchett and Seeburg first reported that $GABA_A$ receptors consisting of an α1 subunit in combination with β3 and γ2 subunits showed high affinity for zolpidem, whereas receptors with α2 or α3 subunits showed much lower affinity, and receptors

containing α5 subunits showed no affinity at all (Pritchett and Seeburg 1990). Using zolpidem together with flumazenil should leave almost exclusively flumazenil binding at α5-containing $GABA_A$Rs. Displacement by one of the TC compounds would be better detectable in such conditions.

4.1.1 [^{3}H]Ro15-4513

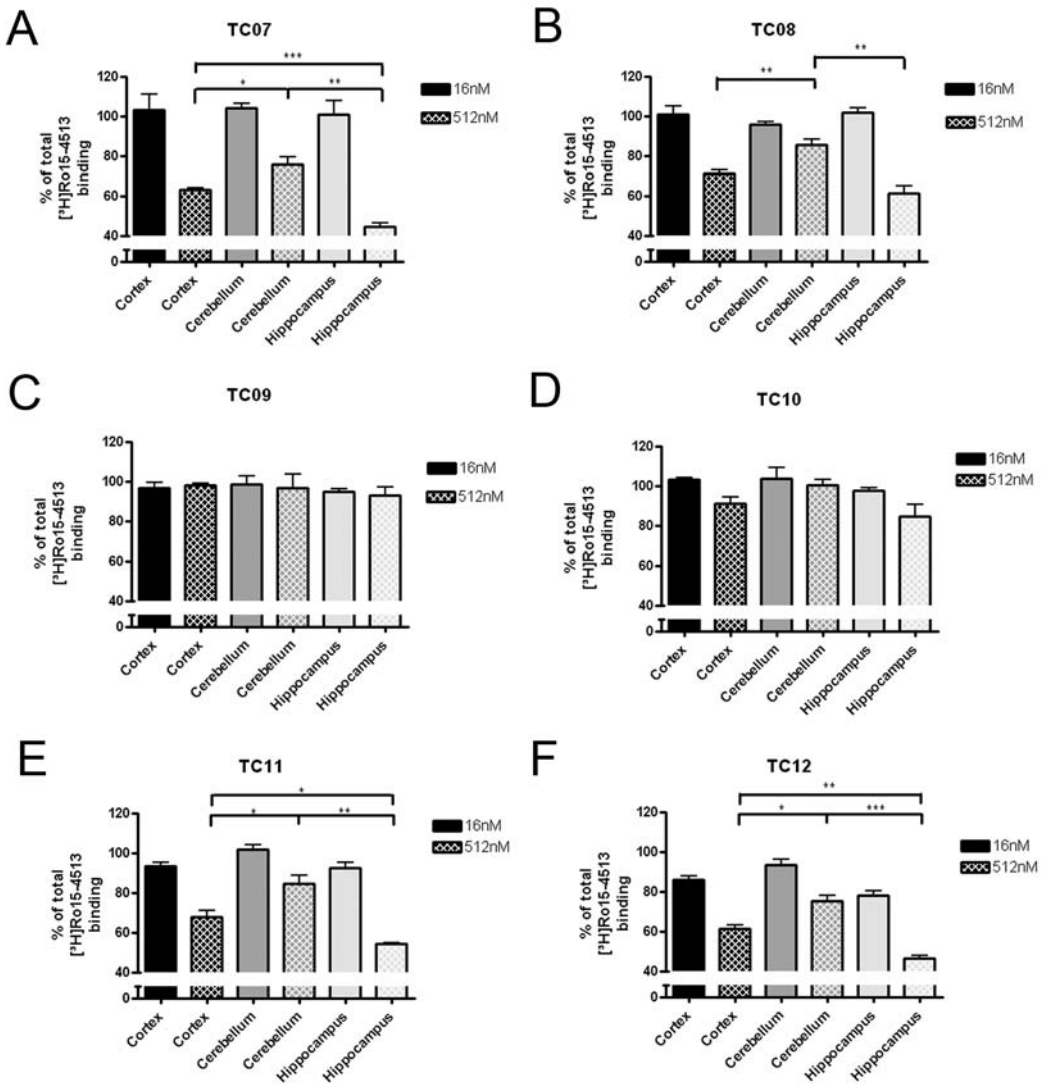

Figure 13: Competition binding assay with crude membrane preparations of rat brain homogenates of the cerebellum, cortex and hippocampus. Binding of 1 nM [^{3}H]Ro15-4513 was challenged by six different potential competitors. The data implicate displacement of radiotracer with compounds **A**, TC07, **B**, TC08, **E**, TC11 and **F**, TC12 at 512nM. At this concentration these compounds also appeared to have statistically significant differences in their effect on the binding of the tracer in the three different brain regions studied. Experiments were repeated at least 3 times. Shown are means ± SD. (* $p \leq 0,05$; ** $p \leq 0,01$; *** $p \leq 0,001$)

Binding of 1 nM [^{3}H]Ro15-4513 was challenged by the six different potential competitors, TC07, TC08, TC09, TC10, TC11 and TC12 (structures shown in **Table 4**, page 32). The data displayed in **Figure 13** demonstrate displacement of radiotracer with compounds TC07, TC08, TC11 and TC12 at 512 nM. At this concentration these compounds also displayed statistically significant different effects on the binding of the tracer between the three different brain regions studied. The most pronounced effect was observed in the hippocampus and the largest difference was calculated between cerebellum and hippocampus.

As TC09 and TC10 had little or no affinity to the benzodiazepine binding site, subsequent tests were performed only with TC07, TC08, TC11 and TC12.

Displacement of 6 nM [^{3}H]Ro15-4513 was lower in all tested brain areas as compared to experiments with 1 nM of the tracer. Like the data for 1 nM [^{3}H]Ro15-4513 the differences between brain areas suggest highest displacement in the hippocampus and the biggest difference between hippocampus and cerebellum (**Figure 14**).

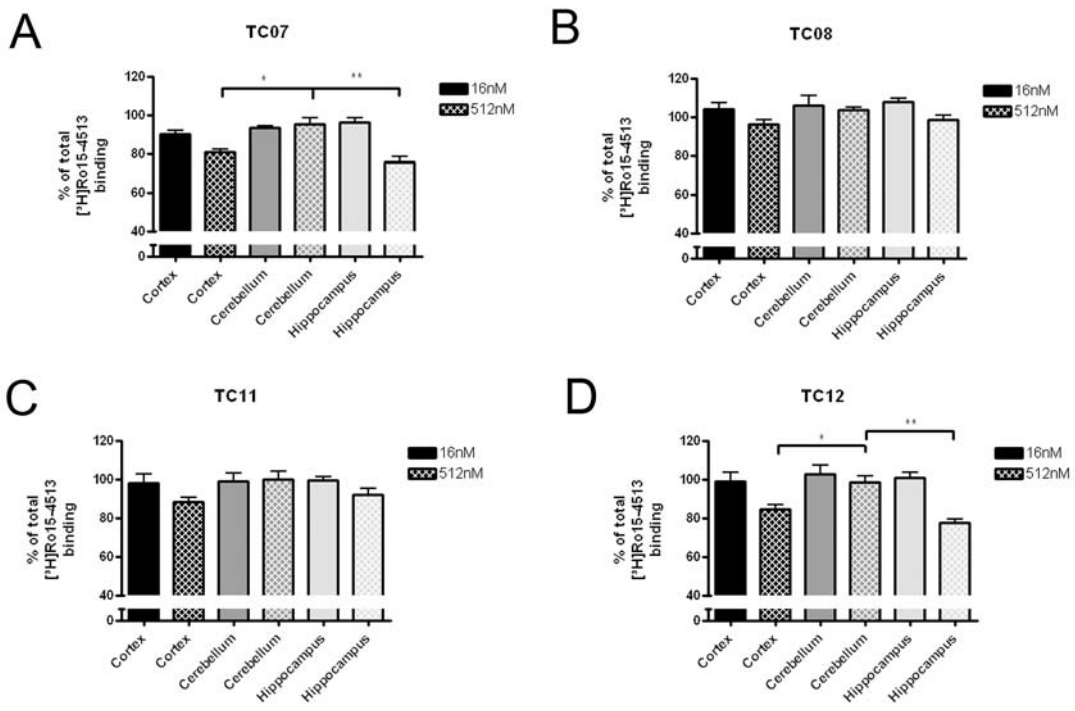

Figure 14: Competition binding assay with crude membrane preparations of rat brain homogenates of the cerebellum, cortex and hippocampus. Binding of 6nM [^{3}H]Ro15-4513 was challenged by four different competitors. The data implicate displacement of radiotracer with compounds **A**, TC07, **B**, TC08, **C**, TC11 and **D**, TC12 at 512nM. At this concentration compounds **A**, TC07 and **D**, TC12 also appeared to have statistically significant differences in their effect on the binding of the tracer in the three different brain regions studied. Experiments were repeated at least 3 times. Shown are means ± SD. (* $p \leq 0,05$; ** $p \leq 0,01$)

4.1.2 [^{3}H]Ro15-1788 (Flumazenil)

Displacement of [^{3}H]Ro15-1788 could be detected with all four tested compounds at a concentration of 512 nM with most effective displacement in the hippocampus and significant difference between the displacement in the hippocampus and the cerebellum (**Figure 15**). TC08 and TC11 seemed to have a slightly lower affinity to the benzodiazepine binding site as measured against [^{3}H]Ro15-4513 and along with that a lower subtype selectivity. This tendency had also been prominent in experiments with [^{3}H]Ro15-4513 binding. Neither TC08 nor TC11 produced significant differences in the displacement of [^{3}H]Ro15-1788 in any of the three tested brain regions.

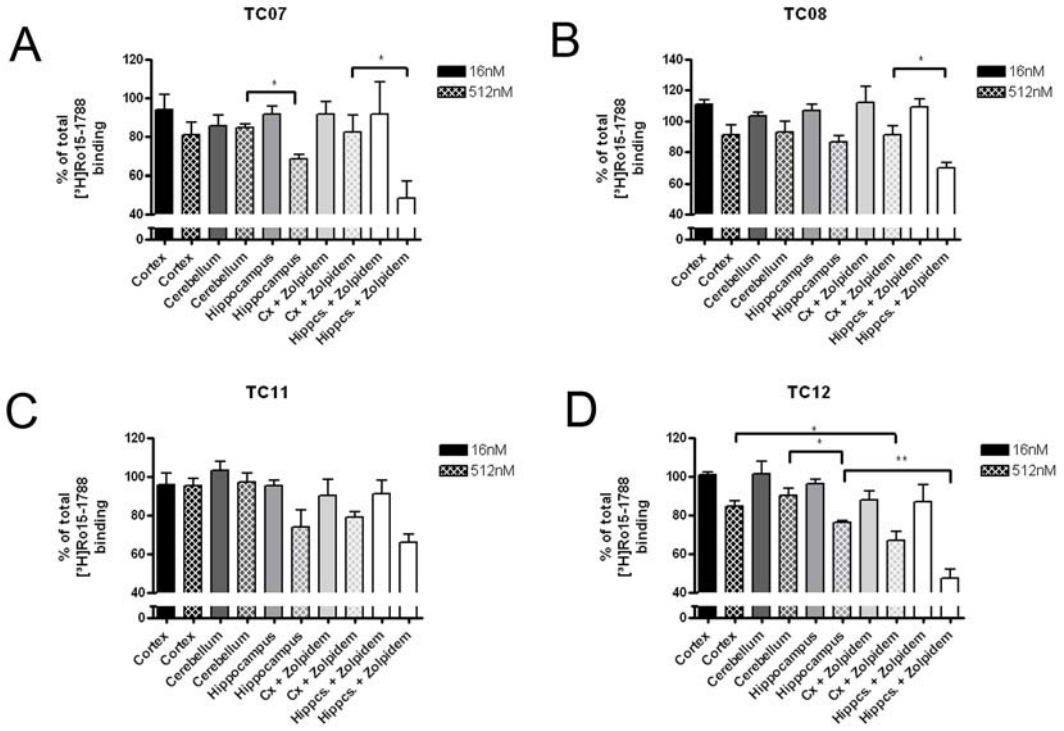

Figure 15: Competition binding assay with crude membrane preparations of rat brain homogenates of the cerebellum, cortex and hippocampus. Binding of 1nM [^{3}H]Ro15-1788 was challenged by four different competitors. In addition, cortex and hippocampus membranes were incubated with 10µM zolpidem present. The data implicate displacement of radiotracer with compounds **A**, TC07, **B**, TC08, **C**, TC11 and **D**, TC12 at 512nM. At this concentration compounds **A**, TC07 and **D**, TC12 also appeared to have statistically significant differences in their effect on the binding of the tracer in the cerebellum and hippocampus. In the presence of zolpidem compound **D**, TC12 displays a significantly higher inhibition of radiotracer binding in the cortex and hippocampus. Experiments were repeated at least 3 times. (* $p \leq 0,05$; ** $p \leq 0,01$)

The promising results of the crude brain membrane binding assays justified a deeper look into the characteristics proper of the four potentially $GABA_AR$ α5 subunit selective

compounds and made necessary the transient transfection of HEK293 cells and expression of recombinant $GABA_A$Rs in that cultured tumor cell line.

4.2 Plasmid Maxi Preparation

All plasmid maxi preparations, which were therefore necessary, independent from the employed methods, produced very pure DNA in very good yields which was usable for large scale HEK293 cell transfection. For DNA concentrations used see Figure 9 in chapter 3 Materials and Methods. Results of restriction analysis of plasmid maxi preparations are shown in **Figure 16**.

4.2.1 Restriction Analysis

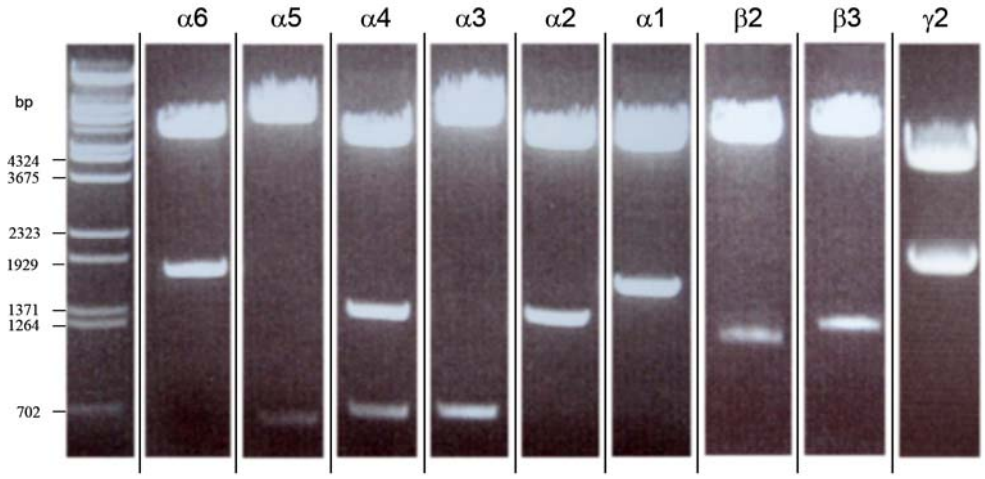

Figure 16: Restriction enzyme analysis of bacteria plasmid maxi preparations of $GABA_A$ R subunits α1-6, β2/3 and γ2. A Sizer V DNA ladder (λ-DNA BstE II digested) from Peqlab was used. Lengths of DNA fragments were for α1=1559bp; α2=1263+16bp; α3=646bp; α4=621+1238bp; α5=561bp; α6=1558bp; β2=959bp; β3=1062bp and γ2=1857bp

All subunits could be obtained in ultra-pure quality and produced excellent transfection efficiencies of at least 20 %. As can be seen in Figure 10 page 40, control of transfection efficiencies was performed. The displayed result is representative for most transfections and when achieved led to very good binding assay results represented by high specific binding of the employed radio tracer.

4.3 Effect of β Subunit on TC Compound Binding

As explained above for a functional benzodiazepine binding site two α, two β and a γ subunit have to assemble. Thus, it is a very large number of possible combinations but only few really occur in the mammalian brain in appreciable amount (Quirk, Blurton et al. 1996). For example the α1 subunit predominantly occurs together with the β2 subunit, wereas the α5 subunit predominantly occurs together with the β3 subunit. For unclear reasons, a much larger amount of DNA is needed to suffiently transfect HEK293 cells with the β2 subunit than with the β3. In addition, transfection with β3 leads to a better signal to noise ratio.

It would therefore be beneficial and economic to use the β3 subunit for all experiments but as the α1 subunit preferentially occurs together with the β2 subunit and α1-containing receptors amount to ~ 70 % of all $GABA_A$Rs in the mammalian brain (Hevers and Luddens 1998) it had to be shown that there is no significant difference in the binding of the used compounds to the benzodiazepine binding site whether β2 or β3 were used. Results of these control experiments are shown in **Figure 17**. No significant difference could be detected between the use of either β2 or β3. In addition to that information the data justified the assumption that at least compounds TC07 and TC12 might be α5 selective ligands as there was 50 % displacement detectable with 512 nM of TC07 and 40 % with TC12 at α5-containing receptors.

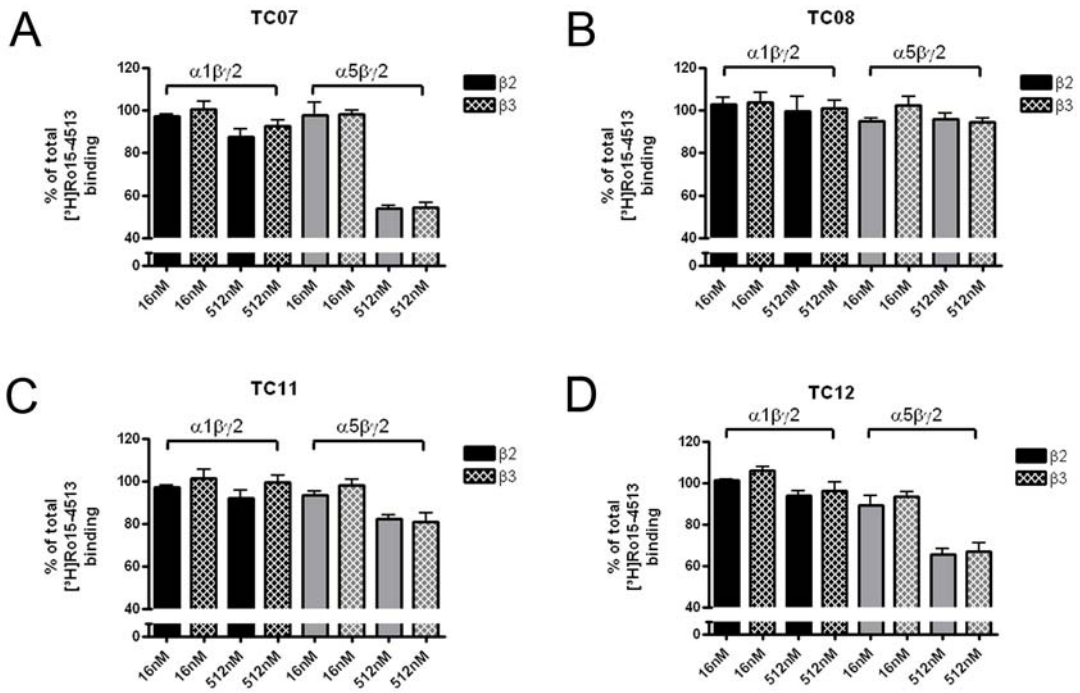

Figure 17: Competition binding assay with crude membrane preparations of transiently transfected HEK 293 cells. Recombinant $GABA_A$ Rs were expressed with α1 or α5, two different β subunits and the γ2 subunit and tested on the β subunit's potential influence on the inhibitory effect of four novel compounds. Binding of 6 nM [^{3}H]Ro15-4513 was challenged by four competitors. No significant difference in tracer binding or its displacement by the competitors could be seen whether β2 or β3 was transfected. Compounds in **A** and **D** show greater displacement of radiotracer at membranes with α5 containing $GABA_A$Rs at 512 nM as compared to **B** and **C**. Also at this concentration compounds **A**, **C** and **D** show significantly greater displacement of radiotracer at $GABA_A$Rs containing α5 subunits as compared to those containing α1. Experiments were repeated at least four times. Shown are means ± SD.

In comparison there was only a displacement of about 10 % of total binding on α1-containing receptors for both of these compounds. TC08 led to no relevant displacement neither at 16 nor at 512 nM and in like manner on both, α1 and α5 containing receptors. A concentration of 512 nM of TC 11 on the other hand caused a displacement of [^{3}H]Ro15-4513 of about 20 % which was α5 specific.

4.4 $GABA_A$ Receptor Subtype Specificity of TC Compounds in Transiently Transfected HEK293 Cells

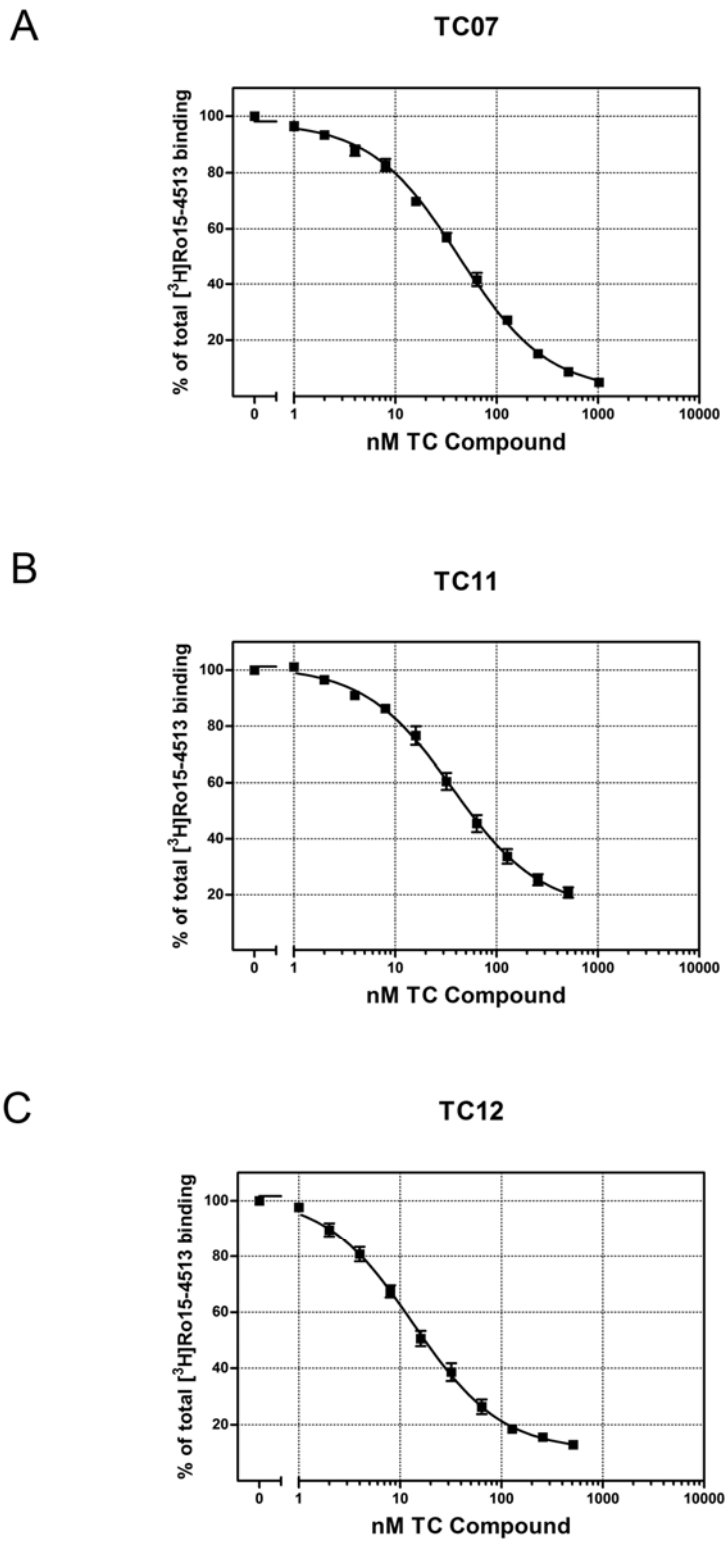

Figure 18: Inhibition of [^{3}H]Ro15-4513 binding to membranes from HEK293 cells transiently transfected with $\alpha5\beta3\gamma2$ $GABA_A$ receptors. **A**, TC07, at a concentration of 1 µM almost com-

pletely displaces the radiotracer from its binding site whereas **B**, TC11 and **C**, TC12 at similar concentrations do not. Experiments were repeated at least 4 times. Shown are means ± SD.

All six, α1 through α6 $\alpha\beta3\gamma2$ receptors were transiently transfected in HEK293 cells. Binding assays were performed with at least seven concentrations of each compound. Data acquisition and evaluation was performed as stated above. Mean dose-response curves for $\alpha5\beta3\gamma2$ containing receptors and compounds TC07, TC11 and TC12 are displayed in **Figure 18**. TC07, at a concentration of 1 µM almost completely displaced the radiotracer from its binding site whereas TC11 and TC12 at similar concentrations did not.

A summary of all results obtained with the six TC compounds with the six $GABA_A$ receptor subtypes expressed in HEK293 cells is given in **Table 7**.

Table 7: K_i and IC_{50} values of six potential $GABA_A$ α5 subunit specific PET ligands. Shown are means ± SD.

	K_i[nM]	**K_i[nM]**	**K_i[nM]**	**K_i[nM]**	**K_i[nM]**	**K_i[nM]**
	TC07	TC08	TC09	TC10	TC11	TC12
$\alpha1\beta3\gamma2$	>1000	>1000	>1000	>1000	>1000	>1000
$\alpha2\beta3\gamma2$	223 ± 28	>1000	>1000	>1000	106 ± 18	22 ± 5
$\alpha3\beta3\gamma2$	142 ± 6	>1000	>1000	>1000	>1000	54 ± 29
$\alpha4\beta3\gamma2$	408.2	>1000	>1000	>1000	>1000	>1000
$\alpha5\beta3\gamma2$	**12** ± 1.2	>1000	>1000	>1000	**10.4** ± 1	**4** ± 0.4
$\alpha6\beta3\gamma2$	>1000	>1000	>1000	>1000	>1000	>1000

	IC_{50}[nM]	**IC_{50}[nM]**	**IC_{50}[nM]**	**IC_{50}[nM]**	**IC_{50}[nM]**	**IC_{50}[nM]**
	TC07	TC08	TC09	TC10	TC11	TC12
$\alpha1\beta3\gamma2$	>1000	>1000	>1000	>1000	>1000	>1000
$\alpha2\beta3\gamma2$	417	>1000	>1000	>1000	252	41
$\alpha3\beta3\gamma2$	281	>1000	>1000	>1000	>1000	80
$\alpha4\beta3\gamma2$	681.9	>1000	>1000	>1000	>1000	>1000
$\alpha5\beta3\gamma2$	42.6	>1000	>1000	>1000	36.8	13.9
$\alpha6\beta3\gamma2$	>1000	>1000	>1000	>1000	>1000	>1000

TC07, TC11 and TC12 show good affinities and specificity for the α5-subtype while the IC_{50} of TC08, TC09 and TC10 for $\alpha i\beta3\gamma2$ is much larger than 1 µM.

4.5 Autoradiography

The results from the binding assays on rat brain membranes and recombinant $GABA_A$ Rs expressed in HEK293 cells justified further *in vitro* experiments yielding quantifiable data in a "natural setting" more closely resembling future PET experiments, e.g., autoradiographic imaging on rat brain sections.

For optimal autoradiographic results high sensitivity for the low energy β-emission of ^3H is necessary. Three different methods were available that provided the needed sensitivity but each of which had advantages and disadvantages. Therefore, an assessment was performed previous to the autoradiographic experiments proper (**Figure 19**).

4.5.1 Methodological Evaluation

14 µm rat brain sections from similar regions of the brain were incubated with the same concentration of [^{3}H]Ro15-4513 and subsequently exposed to either traditional tritium sensitive x-ray film (GE Healthcare/Amersham), a life-imaging β-counter (µ-imager, Biospace, France) or a Fujifilm tritium sensitive imaging plate/phosphor screen. Exposure time was 5 weeks, 48 hours and 72 hours respectively.

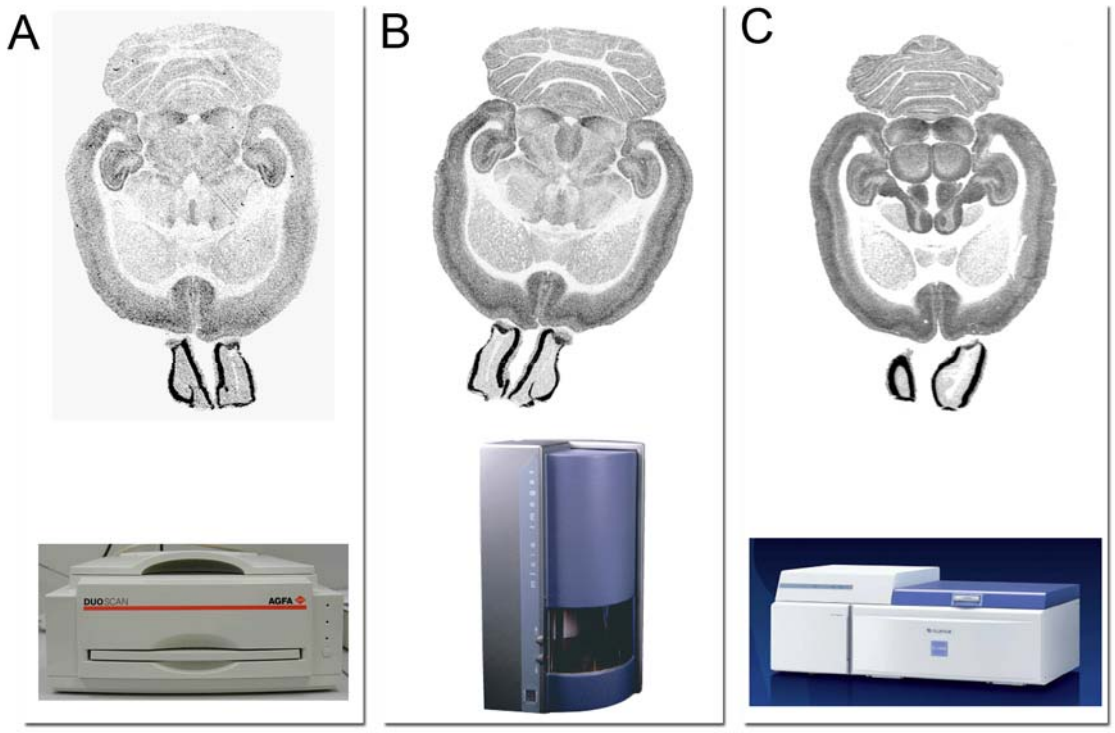

Figure 19: Three different autoradiography detection systems, **A**, ^{3}H-sensitive x-ray film, scanned with a high quality flat bed scanner, AGFA, **B**, real-time β+ Microimager, Biospace and **C**, Fuji FLA7000 scanner for phosphor imaging plates were evaluated for four main qualities: time of exposure, resolution, image quality and costs. Experimental conditions were identical for all three detection methods. While the resolution in **A** was very good and the costs relatively low, the major drawbacks were ≥ 5 weeks exposure, nearly unavoidable scratches in the film

emulsion and non-linear emission signal curve at very low and very high disintegration rates. The image displayed in **B** was obtained after 24 h exposure. Major drawbacks were high costs for apparatus and imaging foil and the fact that only one sample of a maximum size of 4 x 4 cm could be detected. The image displayed in **C** has an as good resolution as the one in **B**, exposure was 72 hours. Up to 100 samples can be scanned at a time (biggest imaging plate 20 x 40 cm) and costs are lower than in **B**. Moreover the apparatus in **B** is more expensive than in **C**.

While results from exposure to x-ray film (**Figure 19**, A) led to high resolution images at relatively low costs, major drawbacks of this method were the extremely long exposure time as compared to the other two methods and the scratches in the film emulsion which were almost unavoidable even with increasing routine. The signal of the results from detection with the Biospace µ-imager (**Figure 19**, B) was more intense than the one obtained after a five week exposure to x-ray film at an almost identical resolution. Major drawbacks of the µ-imager were relatively high costs and the fact that only one sample at a time could be read out (field of view = 4 x 4 cm). For the later applied protocols at least 20 sections/samples were expected at a time. The exposure to Fujifilm phosphor screens and the subsequent read-out with the Fujifilm scanner FLA-7000 produced high-resolution images (**Figure 19**, C) which were comparable to those obtained with the µ-imager after a 72-hour exposure time.

4.5.2 Transversal Autoradiographies TC Compounds

Thus, exposure to Fujifilm phosphor screens was chosen as the method of signal detection for autoradiographic experiments. First experiments were performed on 14 µm rat brain sections. **Figure 20** shows the results of a competitive binding experiment with 6 nM [^{3}H]Ro15-4513 challenged by 512 nM TC07, TC08, TC11 and TC12. Images are displayed false colour coded with dark blue representing background level and dark red representing maximum signal intensity. TC07, TC11 and TC12 displaced a higher amount of radiotracer in the hippocampus as compared to displacement in cortical regions. Incubation with TC08 did not lead to visually recognisable displacement neither in hippocampus nor in cortex regions. Results from image quantification are summarized in **Figure 21**. For TC07, TC11 and TC12 a significant difference between cerebellum and hippocampus binding could be detected. Displacement with TC12 also caused significant differences in displacement between cortex and hippocampus and between striatum and hippocampus. TC08 on the other hand did not cause any significant displacement at all.

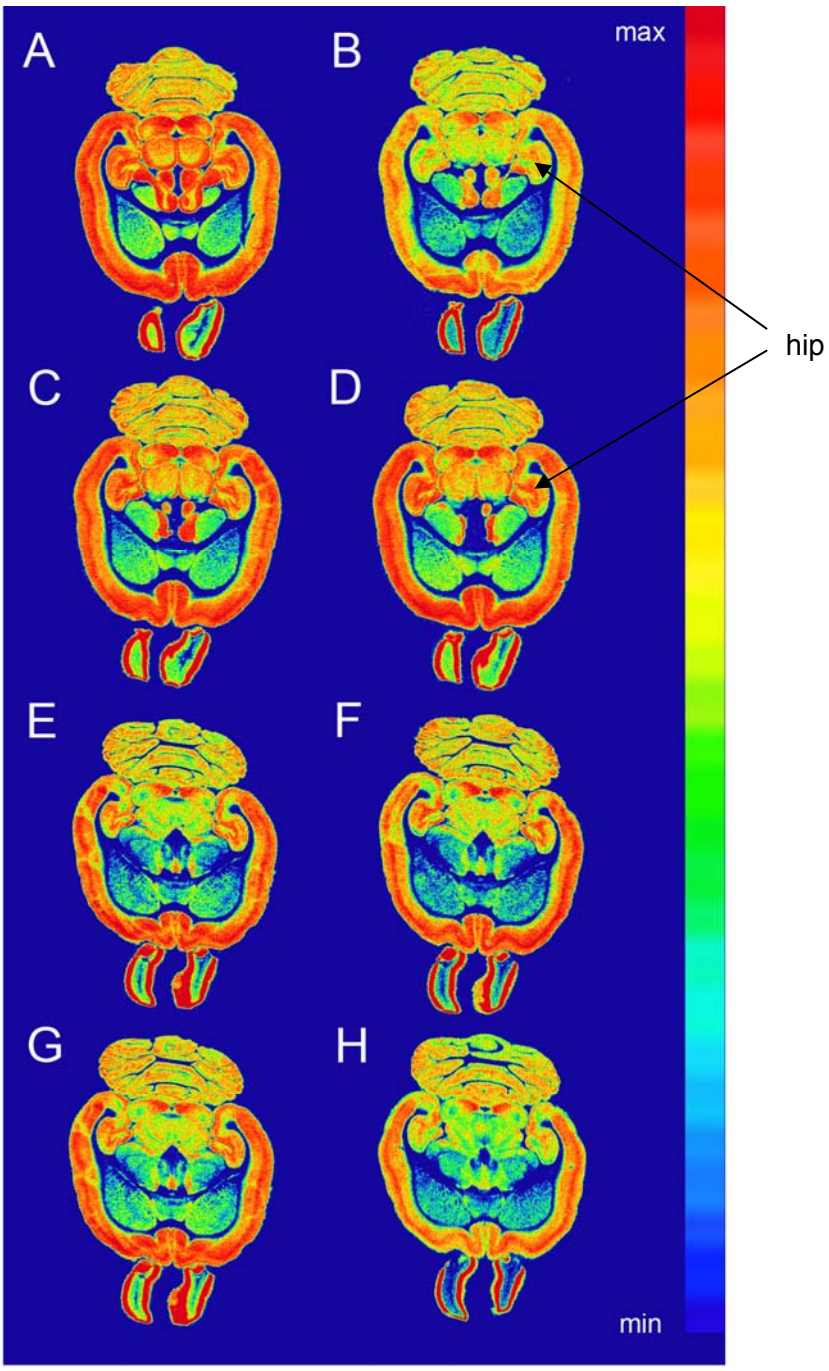

Figure 20: Transversal autoradiographic assay with 6nM [^{3}H]Ro15-4513 on 14 µm rat brain sections. **A**, **C**, **E** and **G** are total binding, **B**, **D**, **F**, and **H** are in the presence of 512 nM of **B**, TC07, **D**, TC08, **F**, TC11 and **H**, TC12. Images are displayed false colour coded with dark blue representing background level and dark red representing maximum signal intensity. TC07, TC11 and TC12 displaced a higher amount of radiotracer in the hippocampus (**hip**) as compared to displacement in cortical regions. Fujifilm photo-stimulated luminescence imaging plates and a Fujifilm FLA-7000 scanner were used for detection.

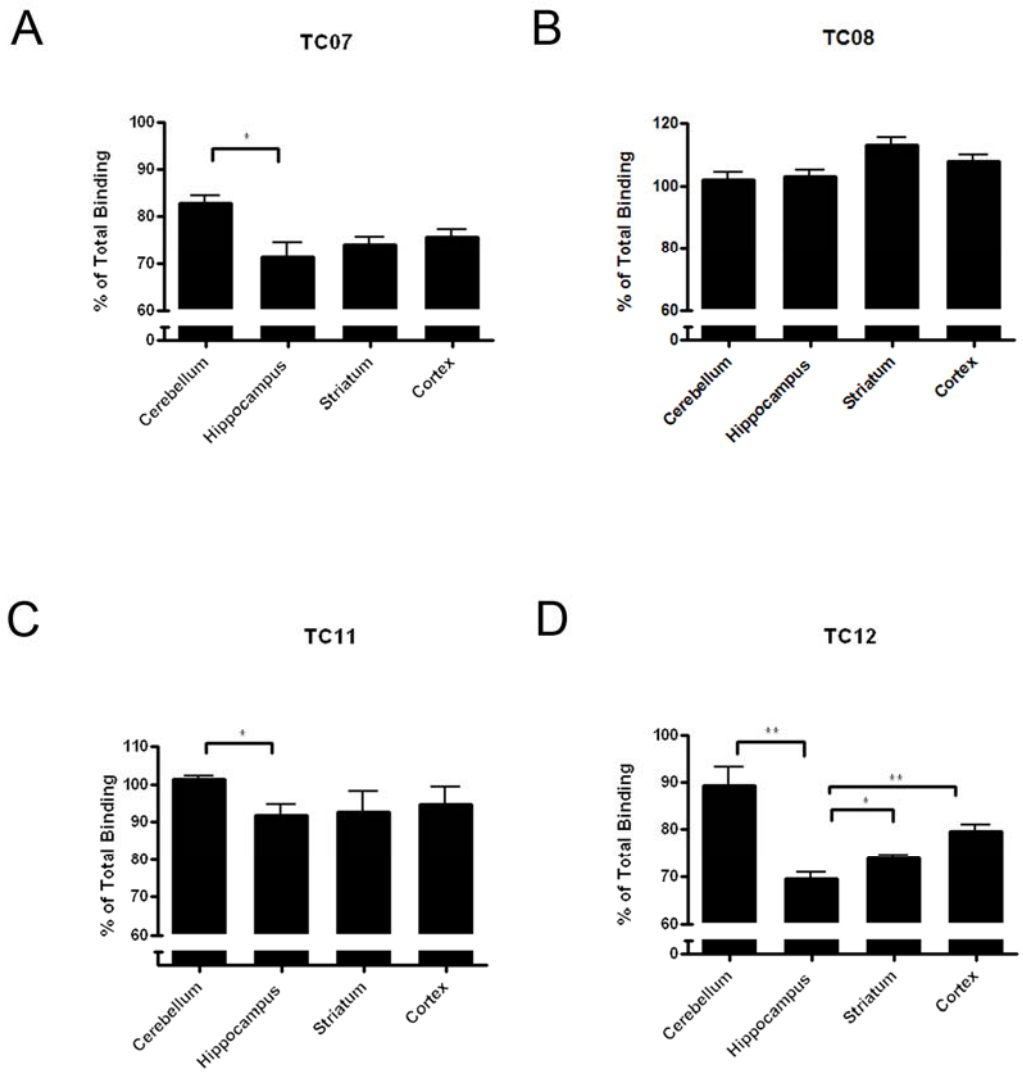

Figure 21: Numerical results from autoradiographies displayed in Figure 20. 6 nM [^{3}H]Ro15-4513 binding to 14 µm rat brain sections challenged by 512 nM of four different potential benzodiazepine binding site PET ligands, **A**, TC07, **B**, TC08, **C**, TC11 and **D**, TC12. Incubation with TC07, TC11 and TC12 leads to a greater displacement of radiotracer in the hippocampus than in the cerebellum. Incubation with TC12 leads to highly significant differences in the amount of displacement between all four tested brain regions. Incubation with TC08 does not cause any detectable displacement. Shown are means ± SD. (* $p \leq 0,05$; ** $p \leq 0,01$)

4.5.3 Coronal Autoradiographies TC Compounds

Rat brain sections were cut as well in coronal orientation to visualize the hippocampus from this perspective and with [^{3}H]Ro15-1788 (flumazenil) having a different receptor subtype selectivity.

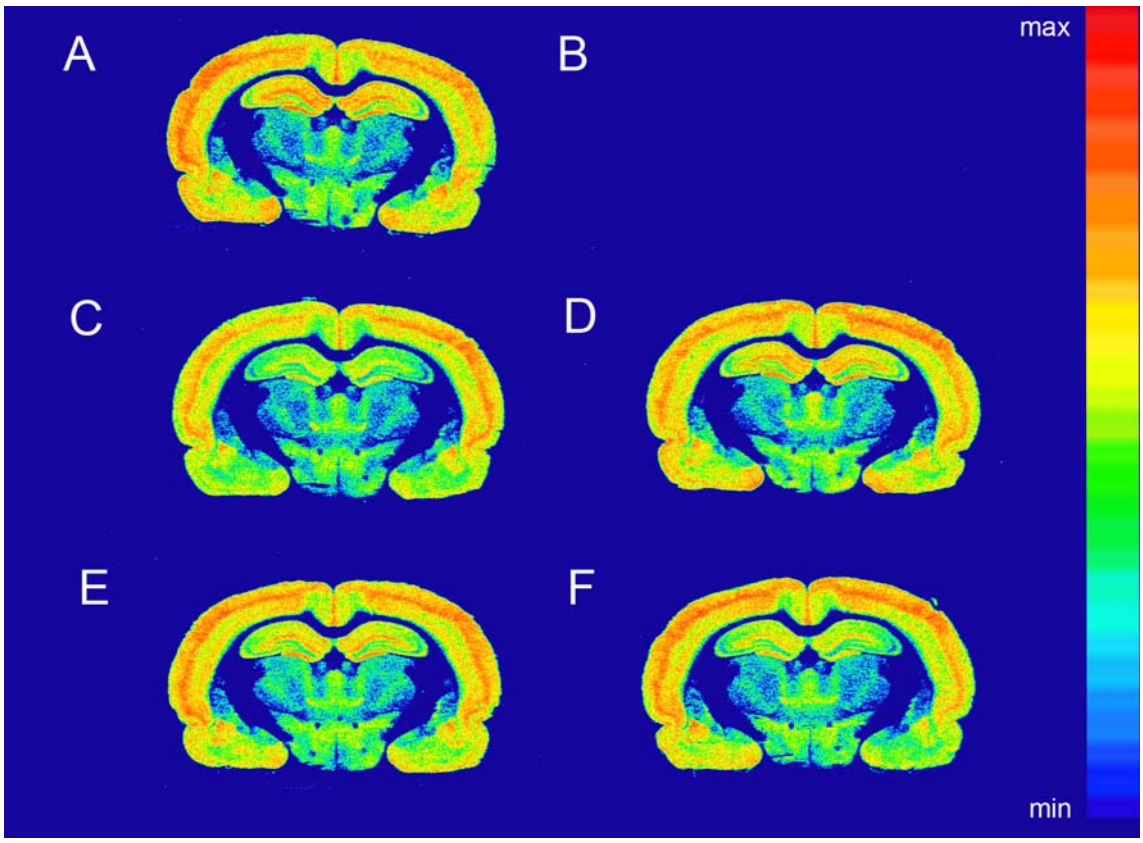

Figure 22: Competitive coronal 14 µm rat brain sections autoradiographic assay with 1 nM [^{3}H]Ro15-1788. **A** total binding; **B** non-specific binding; **C** TC07; **D** TC08; **E** TC11; **F** TC12. Competitors were prepared at a concentration of 512 nM. Images are displayed in false colour coding with dark blue representing background level and dark red representing maximum signal intensity. TC07 and TC12 caused a higher displacement of radiotracer in the hippocampus than in the cortex. Incubation with TC08 and TC11 does not lead to any visually detectable displacement of [^{3}H]Ro15-1788. Nonspecific binding was determined in the presence of an excess concentration of Ro15-4513 and was at background level.

Results of these experiments are given as representative images of at least three replicates for each tested compound (**Figure 22**). Images are displayed in false colour coding with dark blue representing background level and dark red representing maximum signal intensity. TC07 and TC12 caused a higher displacement of radiotracer in the hippocampus than in the cortex. TC07 caused a greater displacement in the cortex than does TC12. Incubation with TC08 and TC11 did not lead to displacement of [^{3}H]Ro15-1788. Nonspecific binding was determined in the presence of an excess concentration of Ro15-4513 and was at background level. Quantification of the autoradiographs led to data shown in **Figure 23**. Results were similar to those obtained with [^{3}H]Ro15-4513 binding.

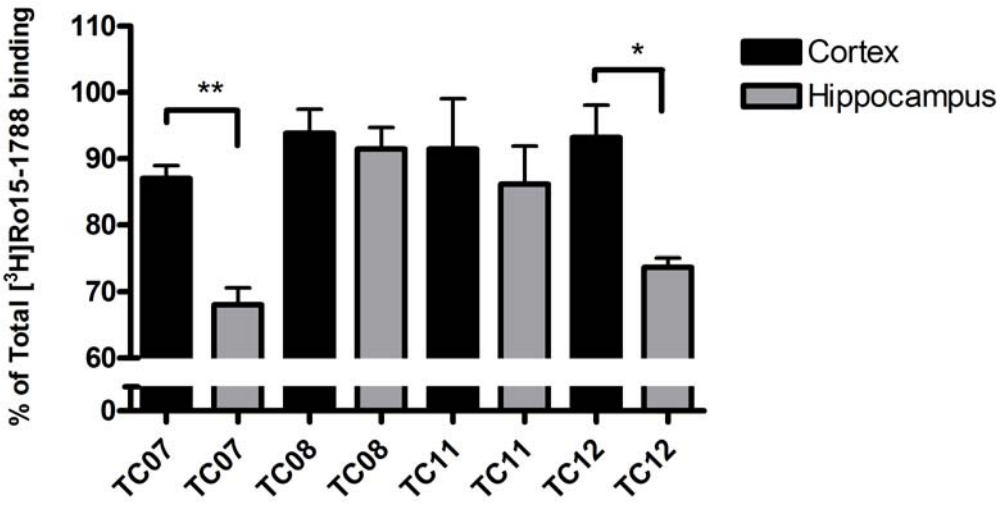

Figure 23: Results of the autoradiographic assay displayed in Figure 22. 1 nM [^{3}H]Ro15-1788 binding to coronal 14 µm rat brain sections challenged by compounds TC07, TC08, TC11 and TC12. Only incubation with 512 nM TC07 and TC12 causes a significant displacement of radiotracer. Also only for TC07 and TC12 a significant difference between hippocampus and cortex displacement can be seen. Shown are means ± SD. (* $p \leq 0,05$; ** $p \leq 0,01$)

Significant displacement could only be detected for TC07 and TC12 and it was also with these compounds that a significant difference was measured between cortex and hippocampus displacement. Although the mean data of hippocampus displacement caused by co-incubation with TC11 hints on a difference between cortex and hippocampus binding, the deviation was too large to make this difference statistically significant.

To get an idea how much of the total binding was binding to α5 containing receptors, an experiment was performed employing 10 µM zolpidem in addition to TC compounds and radiotracer. 1 nM [^{3}H]Ro15-1788 was incubated with 10 µM zolpidem and 512 nM of TC07, TC08, TC11 and TC12 and the results of the subsequent quantification were given as % of the total [^{3}H]Ro15-1788 binding in the presence of zolpidem. **Figure 24** shows the images obtained by the mentioned experiment and it can be seen that non-specific binding was at background level. **A** shows total binding, **B** is non-specific binding, **C** represents total binding in the presence of zolpidem and **D** through **G** are from left to right TC07, TC08, TC11 and TC12. The data obtained with displacing [^{3}H]Ro15-1788 on its own without zolpidem, shown in Figure 23, is here visually confirmed. Even by visual control can be seen that TC07 and TC12 have the most affinity to α5 containing $GABA_A$Rs. TC11 has little and TC08 no detectable effect on the remaining [^{3}H]Ro15-1788 binding. Images are given as three replicates each, so in Figure 24 all

sections in the same column are treated the same and all sections in the same row were cut from the same brain. The small deviation can even be seen visually

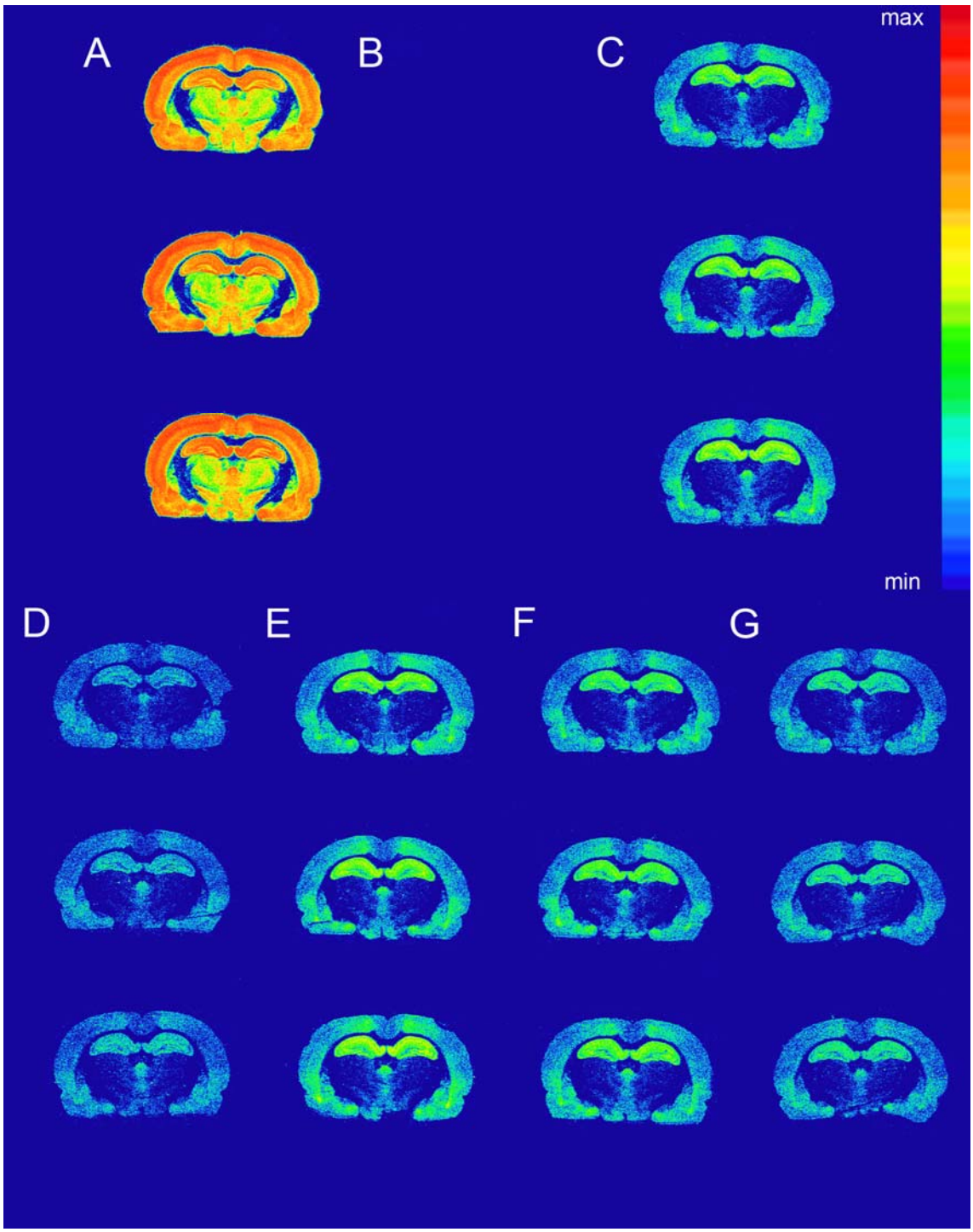

Figure 24: Autoradiographic assay with 1nM [^{3}H]Ro15-1788 on coronal 14µm rat brain sections. **A**, total binding; **B**, non-specific binding; **C**, 1 nM [^{3}H]Ro15-1788 + 10 µM zolpidem; **D**, 512 nM TC07 + 10 µM zolpidem; **E** 512 nM TC08 + 10 µM zolpidem; **F**, TC11 + 10 µM zolpidem; **G** TC12 + 10 µM zolpidem. All sections in the same row are from the same brain. Sections in same column are from three different brains and were treated the same way. In **C**, incubation with 10 µM zolpidem causes major displacement of radiotracer mainly in cortical and thalamus regions. In the hippocampus and small cortical areas displacement is not as effective as in the rest of the brain. The remaining binding of [^{3}H]Ro15-1788 in **C**, is with most effect displaced by

TC07 and TC12. By visual control, there can be seen no displacement caused by incubation with either TC08 or TC11. Nonspecific binding was determined in the presence of an excess concentration of Ro15-4513 and was at background level.

but is even more obvious in **Figure 25**. Here the results from quantifying the above images are given.

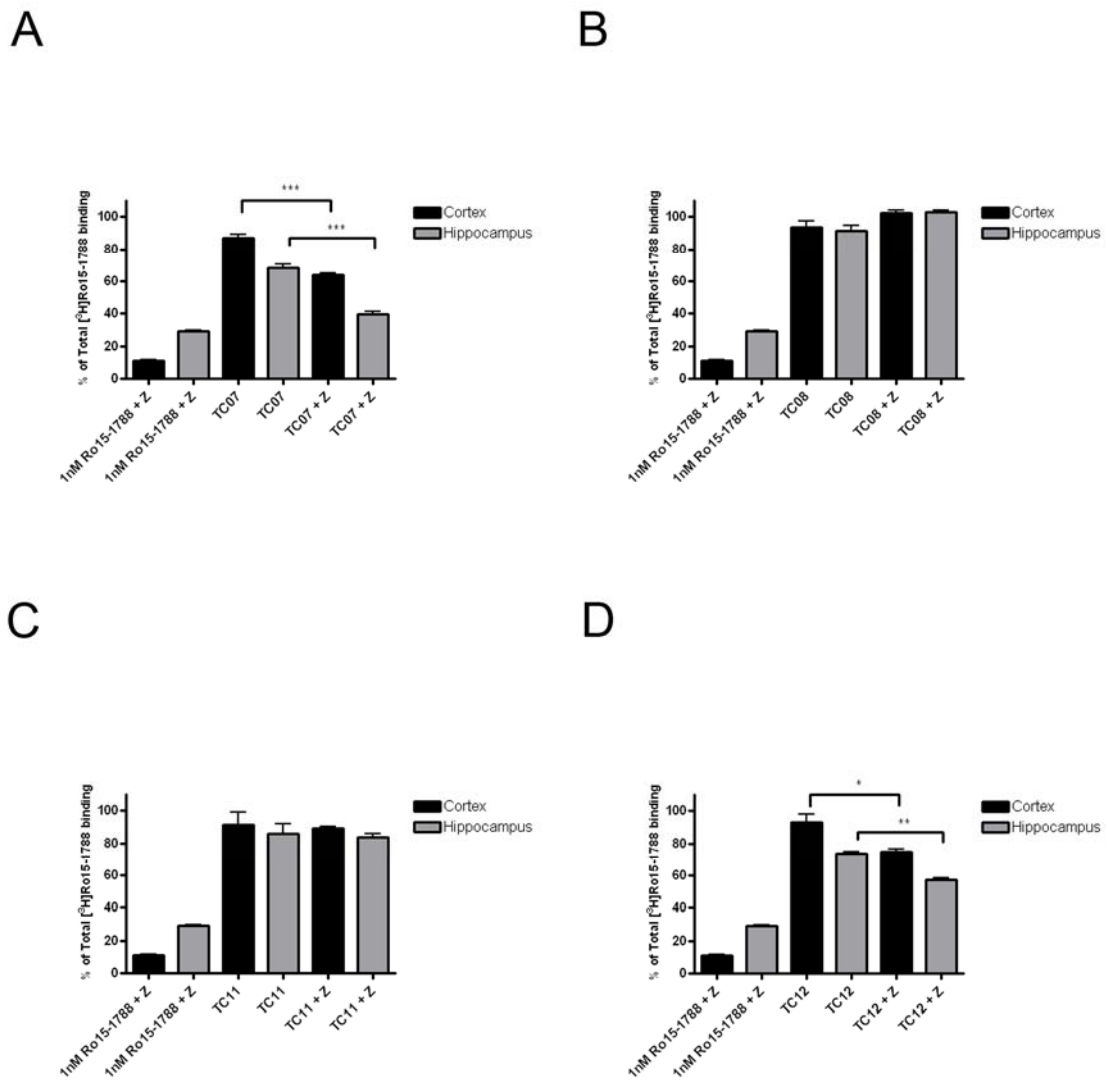

Figure 25: Results of the autoradiography assay displayed in Figure 24 with 1nM [^{3}H]Ro15-1788 binding on 14 µm coronal rat brain sections. Displacement of radiotracer with 10 µM zolpidem (Z) led to a remaining signal of 10 % in the cortex and 30 % in the hippocampus. Displacement of this remaining binding was highest with TC07 (**A**) and TC12 (**D**). No significant further displacement could be measured for TC08 (**B**) or TC11 (**C**). The two central columns are taken from Figure 23 for comparison. After incubation with TC07 and TC12 in the presence of 10 µM zolpidem, a significantly greater displacement could be measured in the cortex as well as

in the hippocampus as compared to experiments without zolpidem. For both compounds displacement is highest in the hippocampus. Shown are means ± SD. (* $p \leq 0,05$; ** $p \leq 0,01$; *** $p \leq 0,001$)

4.6 In Vivo Binding with TC07

In order to check whether the most potent $GABA_AR$ ligand, TC07, was able to cross the blood brain barrier *in vivo* experiments were performed. [^{3}H]Ro15-1788 *in vivo* binding was measured in a terminal study. Data in **Figure 26 A** show that in animals treated with TC07, the binding of [^{3}H]Ro15-1788 is inhibited to a significant extent. In the cerebellum flumazenil binding in treated animals turned out not to be significantly different as compared to total binding (p = 0.1).

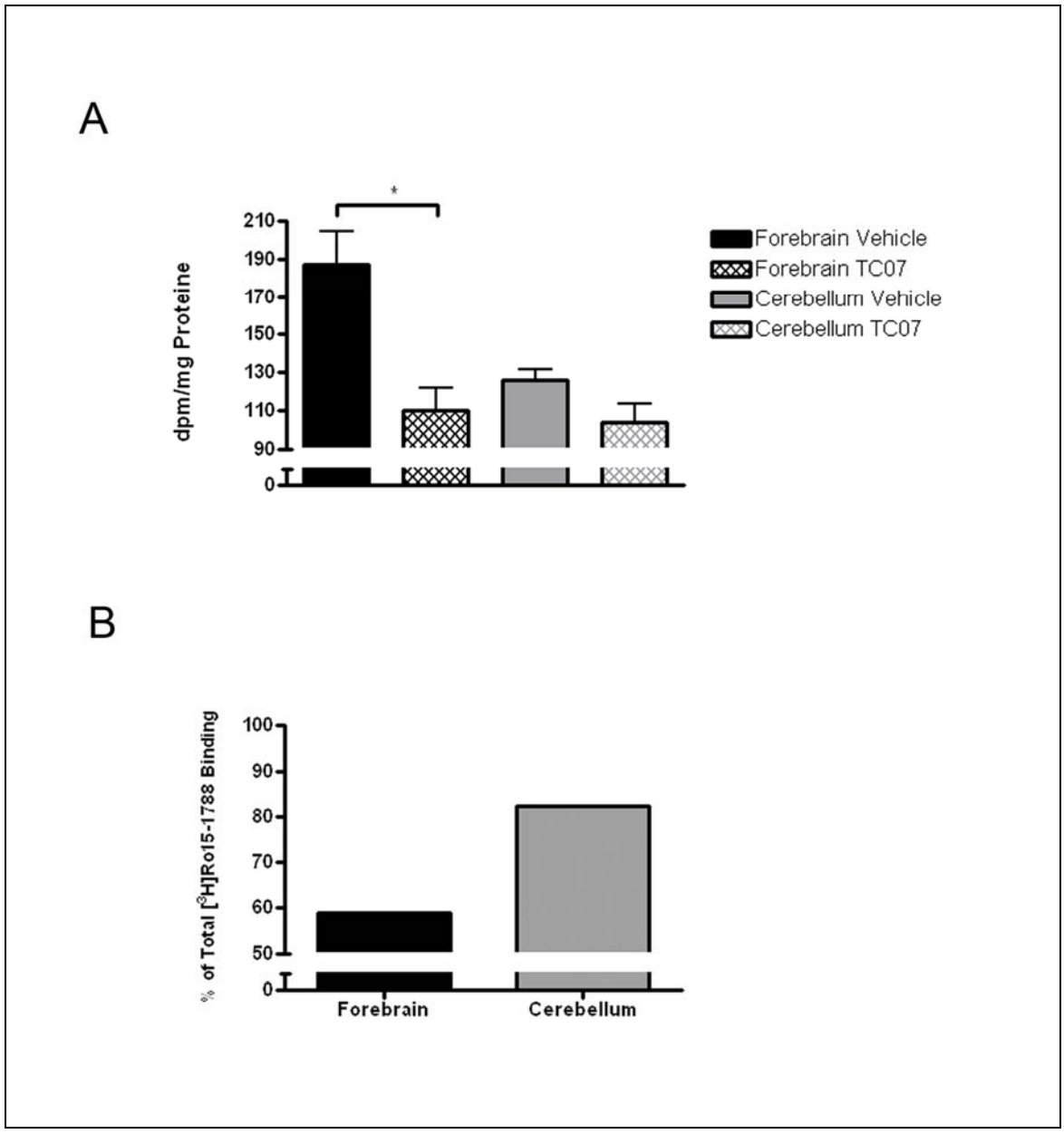

Figure 26: [^{3}H]Ro15-1788 *in vivo* binding measured in a terminal study using eight week old male Sprague-Dawley rats. Animals were treated i.p. 27 min before the injection of the radiotracer with 250 µL vehicle (DMSO), 5 mg/kg TC07 or 5 mg/kg Ro15-4513, for non-specific binding. **A:** Animals treated with TC07; binding of [^{3}H]Ro15-1788 is inhibited statistically significant in the forebrain when compared to vehicle treated animals. In the cerebellum displacement turned out not to be statistically significant (p = 0.1). **B:** Binding in TC07 treated rats in % of the

mean binding in vehicle treated rats. See chapter Methods, page 45, for experimental details. Shown are means ± SD. (* p ≤ 0,05)

4.7 Electrophysiological Evaluation of TC07 and TC12

PET tracers are usually given in such small concentrations that they do not cause a physiological effect. However, TC07 and TC12 were tested for their physiological effect on α5 containing $GABA_A$Rs, not least because the original compounds did not contain fluoride and could therefore have altered pharmacological characteristics, but also because in small rodents concentrations can end up at physiologically relevant concentrations, dependent on the specific activity of the ligand.

For this reason whole cell patch clamp experiments were performed on α5 containing $GABA_A$Rs transiently transfected into HEK293 cells. To determine the EC_{50} and EC_{20} of GABA, a GABA dose-response curve was first obtained. A representative recording is displayed in **Figure 27**, **A**. The experiment was performed on $\alpha5\beta3\gamma2$ Rs with GABA concentrations ranging from 0.1 µM to 1 mM.

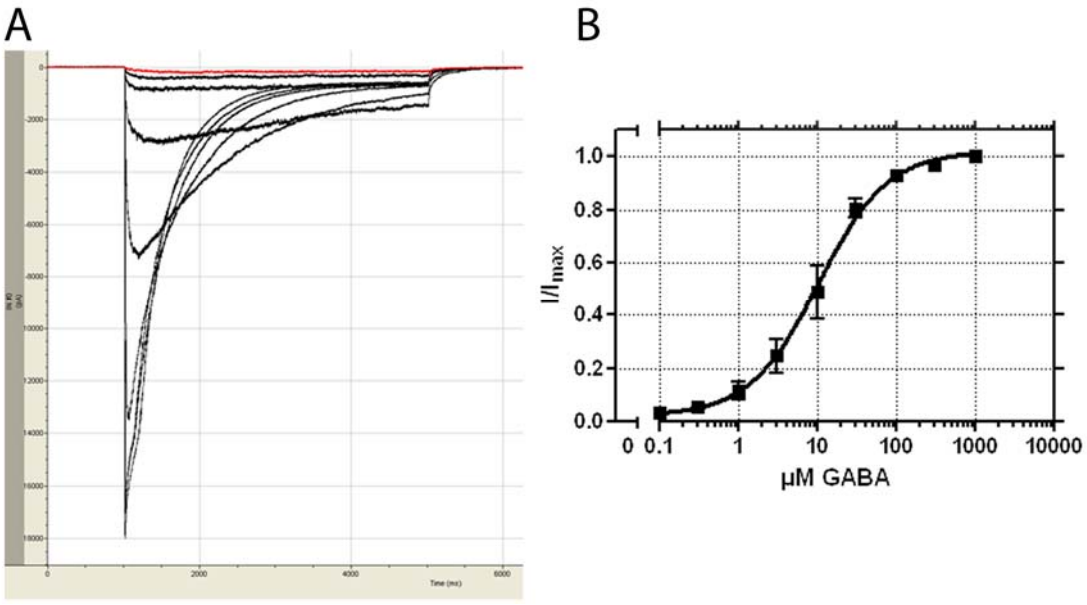

Figure 27: Representative currents (**A**) and dose-response curve (**B**) measured by whole-cell patch clamp recordings in transiently transfected HEK 293 cells. Recombinant $GABA_A$ Rs were expressed containing $\alpha5\beta3\gamma2$ subunits. Cells were exposed to increasing concentrations of GABA starting at 0.1 µM, continuing with 0.3 µM, 1 µM etc. up to 1 mM GABA. Experiments were repeated at least 5 times. Shown are means ± SD.

The results were normalized for the maximum current of each measured cell and fitted with non-linear regression with Graph Pad Prism 4.0. For further recordings the test solutions contained 3 µM GABA (EC_{20}) and rising concentrations of either TC07 or

TC12. According to Street et al. (Street, Sternfeld et al. 2004) the original compounds are inverse agonists for the benzodiazepine binding site. However, TC12 did not show any effect at all (**Figure 28**, **B**). TC07 caused a 40 % reduction of the EC_{20} GABA current (**Figure 28**, **A**).

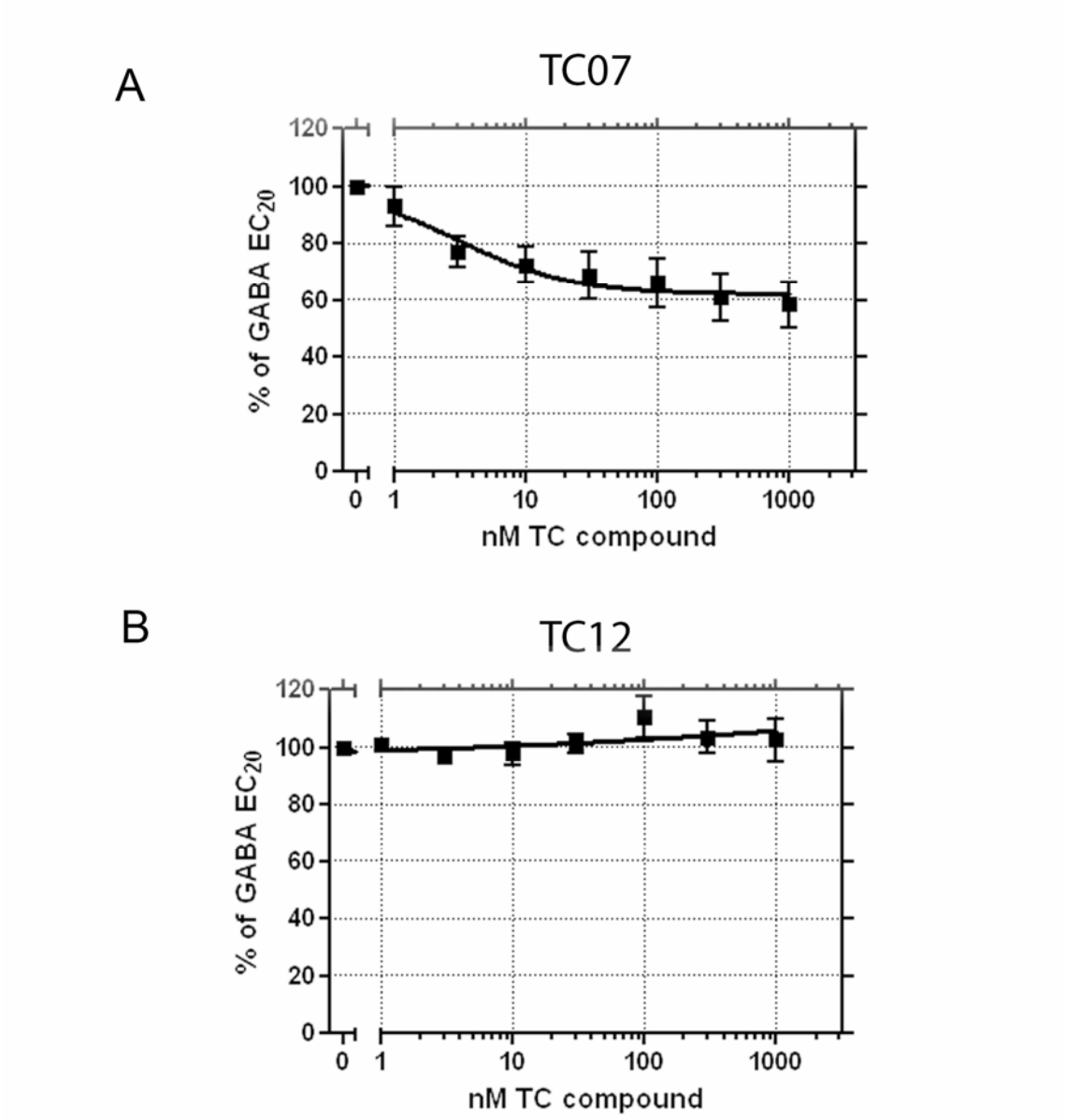

Figure 28: Results of whole-cell patch clamp recordings at HEK 293 cells transiently transfected with recombinant $\alpha5\beta3\gamma2$ $GABA_A$Rs. Recordings were carried out in the presence of 3 µM GABA (EC_{20} at this receptor, cf. **Figure 27**) and increasing concentrations of **A**, TC07 or **B**, TC12. A slight inverse agonistic effect could be detected for TC07 while TC12 displayed no effect. Shown are means ± SD.

4.8 Autoradiographic Analysis of [^{18}F]MHMZ

Autoradiographic images of the 5-HT$_{2A}$ receptor obtained with [^{18}F]MHMZ showed excellent visualization results in rat brain sections (**Figure 29**). Images were in complete agreement with the distribution obtained with [^{3}H]MDL 100907 (Lopez-Gimenez, Mengod et al. 1997) (also **Figure 30**, **B** and **C**). Highest binding was detected in lamina V of the frontal cortex, the caudate-putamen, the motor trigeminal nucleus, the facial nucleus and the pontine nuclei. Minor binding was detected in the olfactory system, the mesencephalon and the hippocampus.

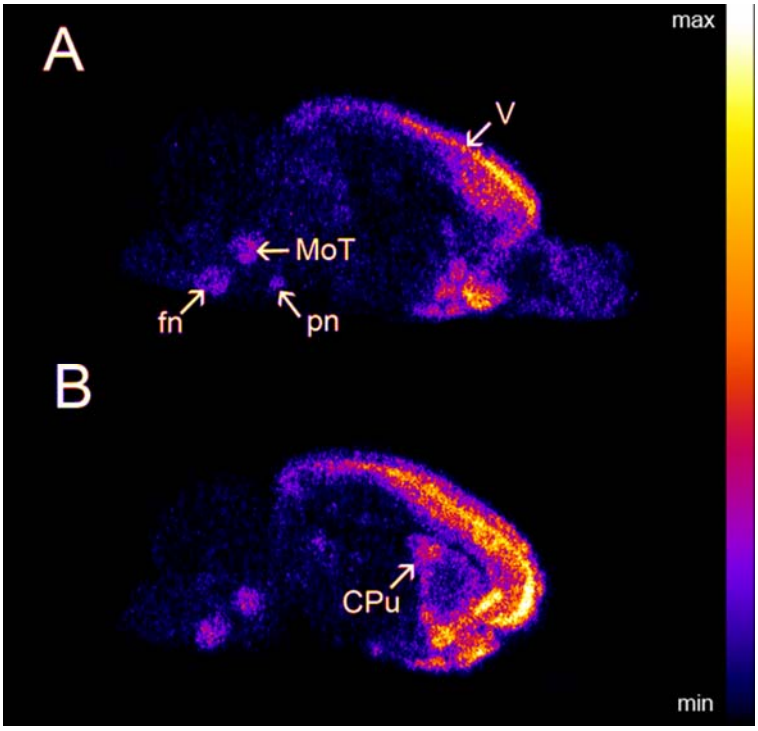

Figure 29: Images of an autoradiography of [^{18}F]MHMZ binding to 14 µm thick rat brain sections; A & B total binding at a concentration of 5 nM with A lateral 0.9 mm and B lateral 2.4 mm from bregma. Major binding was detected in lamina V (V) of the frontal cortex, in the caudate-putamen (CPu) and three regions of the brain stem, the motor trigeminal nucleus (MoT), facial nucleus (fn) and the pontine nuclei (pn). Nonspecific binding was determined in the presence of 10 µM ketanserin which led to total inhibition of [^{18}F]MHMZ binding (c.f. C$^{/}$ **Figure 30**). Specific activity was 1.38 MBq/nmol at the end of the incubation period.

Binding parameters of [^{18}F]MHMZ of different regions of the rat brain obtained with autoradiography assays at sagittal sections are displayed in **Table 8**. Binding in the cerebellum was at the level of non-specific binding so levels of binding in different brain regions are also given relative to that.

Table 8: Binding parameters obtained with [^{18}F]MHMZ from binding experiments at 14 µm sagittal sections of the rat brain (mean ± SEM)

	n	pmol/mm^3	region/cerebellum
Frontal cortex			
Laminae I-IV	4	23.30 ± 1.69	26.9 ± 0.9
Lamina V	4	51.60 ± 5.24	59.5 ± 2.8
Laminae VIa + VIb	4	27.27 ± 2.76	31.4 ± 1.3
Caudate-Putamen	4	16.80 ± 2.33	19.2 ± 1.4

A comparison of the binding of [^{18}F]altanserin and [^{18}F]MHMZ (**Figure 30**) displays that [^{18}F]MHMZ is at least equivalent to [^{18}F]altanserin in terms of specificity for 5-HT$_{2A}$ receptors. **Figure 30** also shows the complete agreement of the binding of [^{3}H]MDL 100907 and [^{18}F]MHMZ.

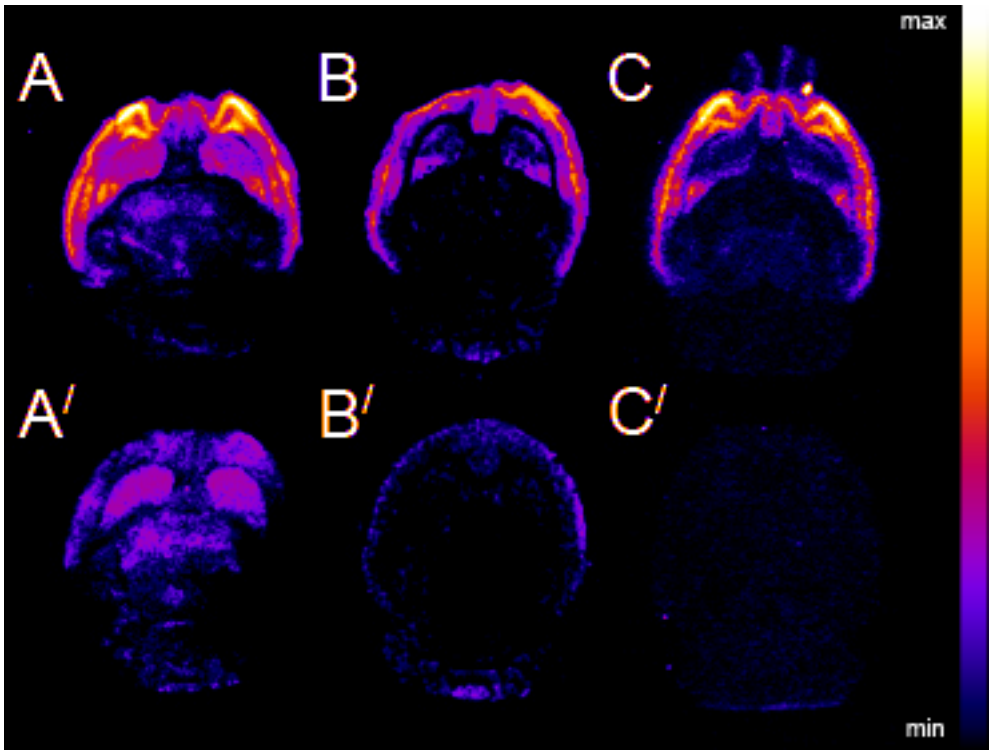

Figure 30: Autoradiographic images of the total binding (**A** - **C**) and non-specific binding (**A$^{/}$** - **C$^{/}$**) respectively of **A**/**A$^{/}$** [^{18}F]altanserin, **B**/**B$^{/}$** [^{3}H]MDL 100907 and **C**/**C$^{/}$** 5 nM [^{18}F]MHMZ at 14 µm rat brain sections. Non-specific binding was determined in the presence of 10 µM ketanserin. Specific activity of [^{18}F]MHMZ and [^{18}F]altanserin was ~160 kBq/nmol (at the end of the incubation period). Washing was for 2 x 10 min for A/A$^{/}$ in ice cold reaction buffer, 2 x 2 min at room temperature with B/B$^{/}$ and 3 x 2 min at room temperature (4 min with buffer containing 0.01 % Triton X-100). Reaction buffer was 50 mM Tris buffer pH 7.4 containing 120 mM $NaCl_2$ and 5 mM KCl.

Competition autoradiographic assays with 5 nM [^{18}F]MHMZ and 10 µM of fallypride (**Figure 31**, C), WAY 100635 (**Figure 31**, D) and prazosin (**Figure 31**, E) showed that

[^{18}F]MHMZ is highly specific for 5-HT$_{2A}$ receptors. Displacement could only be detected with fallypride (**Figure 31**, C). Here, co-incubation led to a displacement of 30 % ± 6 % (n = 4, mean ± SEM) of total binding in the frontal cortex as well as in the caudate-putamen, which does not imply that [^{18}F]MHMZ recognizes D$_2$/D$_3$ receptors but might rather be explained by the known cross affinity of fallypride to 5-HT$_2$ receptors (Stark, Piel et al. 2007).

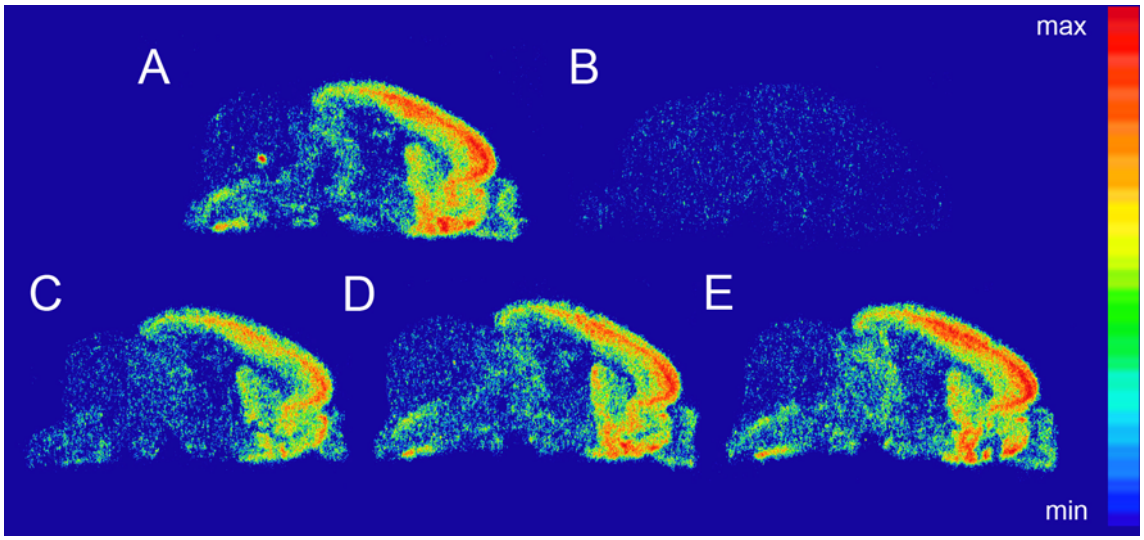

Figure 31: Sagittal autoradiographies on 14 µm rat brain sections with [^{18}F]MHMZ at a concentration of 5 nM (K_i = 9.0 nM for 5-HT$_{2A}$Rs). **A** total binding, **B** non-specific binding measured in the presence of 10 µM ketanserin, **C** co-incubation with 10 µM fallypride, **D** co-incubation with 10 µM WAY 100635, **E** co-incubation with 10 µM prazosin.

4.9 Positron Emission Tomography

First micro PET experiments were performed with [^{18}F]MHMZ. Adult, catheterized Sprague-Dawley rats were anesthetized with isoflurane during the scan. Binding in the cerebellum was at background level as *in vitro*. Also in spite of the much lower resolution of the PET data as compared to autoradiographies the resemblance between the two is striking. Images represent summed images of a period of the last 20 min of the scan time. According to the evaluation of the images (**Figure 33**) this already represents the binding in equilibrium state.

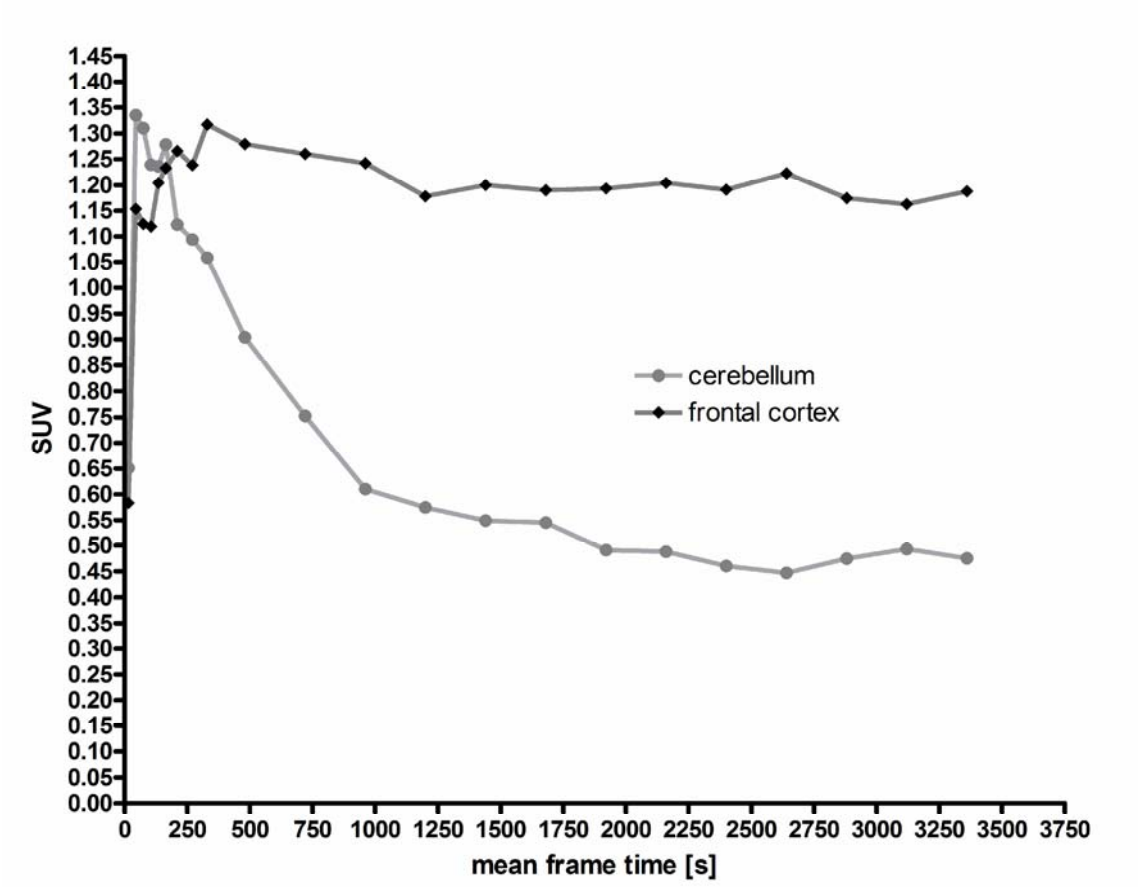

Figure 32: Time-activity curve (TAC) of microPET experiments with [^{18}F]MHMZ in male eight week old Sprague-Dawley rats. The graph shows results of a total binding study in SUV ((% injected dose x bq/ml) x animal weight in g). Uptake of radiotracer in equilibrium state (t > 2000 sec) is more than 50 % higher in cortical regions than in the cerebellum. The binding potential (BP) was determined to be 1.45 for the frontal cortical region using a four parameter reference tissue model supplied with the PMOD software. Cerebellar uptake is employed instead of a plasma input curve in this kind of modeling. Cortex to cerebellum ratio is 2.7.

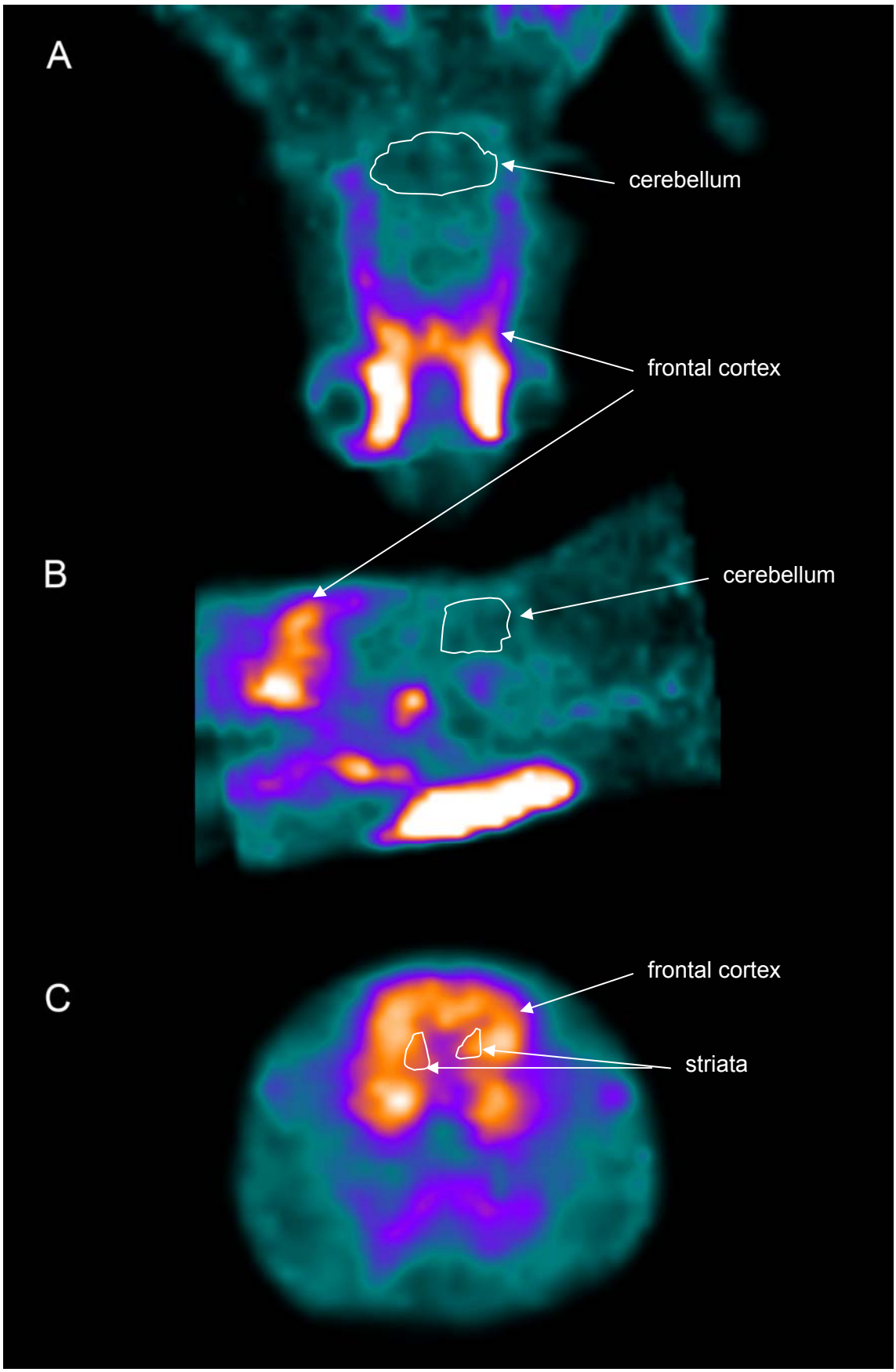

Figure 33: PET images of [^{18}F]MHMZ with **A** transversal, **B** sagittal and **C** coronal orientation

Considering the cerebellum as a reference region and substitute for a plasma input curve, the relative binding of [^{18}F]MHMZ in the frontal cortex was calculated (**Figure 34**) and, using the PMOD software, the BP was determined to be 1.45 for the uptake in the frontal cortical region. The cortex to cerebellum ratio was 2.7. The uptake curve hints on an equilibrium state being reached after around 35 minutes.

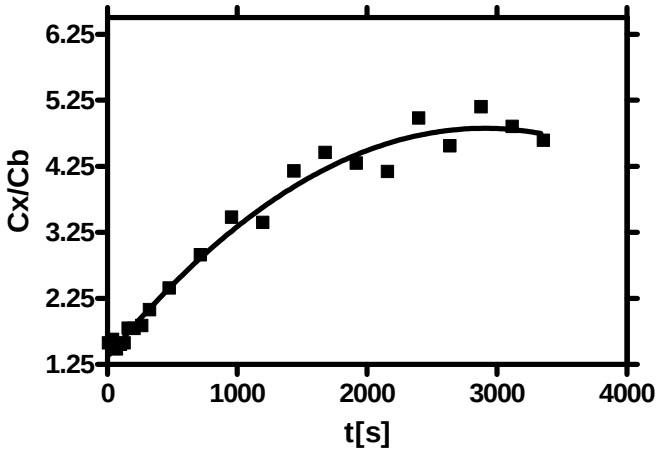

Figure 34: [^{18}F]MHMZ uptake into rat brain. Second order polynomial curve of the mean Bq/mL [^{18}F]MHMZ measured in the cortex divided by the mean Bq/mL measured in the cerebellum in male 8 week SD rats.

4.9.1 [^{18}F]MHMZ Metabolite Study

In order to find out whether or not there are active metabolites produced in vivo

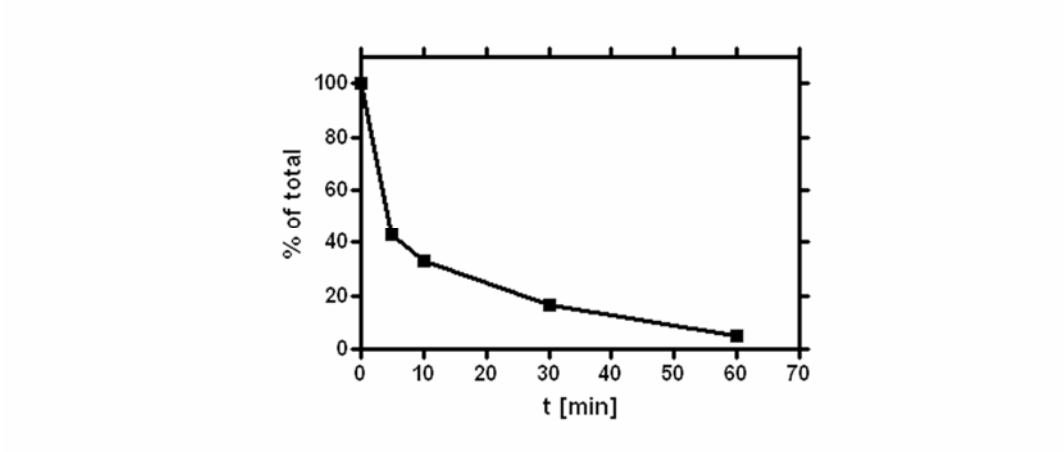

Figure 35: Results of metabolite study in male 8 week old SD rats during microPET scans (n = 3). Displayed are % of [^{18}F]MHMZ of free radioactive compounds in plasma. After 5 min less than 50 % of the free radioactivity are original tracer in blood. Tracer is almost completely metabolised after 60 min. One active metabolite could be detected which is very polar and is not likely to enter the brain. Shown are means ± SD.

along with the uptake of [^{18}F]MHMZ its metabolisation was studied (**Figure 35**). During the scans blood samples were taken at the displayed times and subsequent thin layer chromatography (TLC) revealed that after 5 minutes less than 50 % of the original radio tracer is left in the plasma. At the end of the scans almost no tracer signal could be detected anymore.

5 DISCUSSION

γ-Aminobutyric acid A receptors are widely distributed in the brain. Their subunit composition varies greatly with the receptor isoforms expressed in distinct areas of the brain. The most abundant subunits as determined by immunoprecipitation and *in situ* hybridisation experiments are α1, β2, and γ2, representing 60 % to 90 % of $GABA_A$ receptors in adult rat brain (Benke, Mertens et al. 1991; Quirk, Blurton et al. 1996; Campos, de Cabo et al. 2001; Sieghart and Sperk 2002). The α2, α3, α5, β3, and δ subunits are less abundant and are present in 15 % to 30 % of $GABA_A$ receptors in the rat brain while the remaining subunits (α4, α6, β1, γ1, γ3) are least abundant, each representing <10 % of $GABA_A$ receptors (McKernan, Quirk et al. 1991; Quirk, Gillard et al. 1994; Togel, Mossier et al. 1994; Fritschy and Mohler 1995). The subunit combination α1β2γ2 is the most abundant, while α2β3γ2 and α2βxγ2 (βx = β1, 2, or 3) are the next most prevalent subtypes (**Figure 36**) (Ernst, Brauchart et al. 2003). Receptors containing α5 are prevalent in the hippocampus (Mohler, Knoflach et al. 1995; Quirk, Blurton et al. 1996; Sur, Quirk et al. 1998), while α6-containing receptors are expressed almost exclusively within the cerebellar granule cells, where they coassemble with a β subunit and either γ or δ (Pirker, Schwarzer et al. 2000; Campos, de Cabo et al. 2001; Ernst, Brauchart et al. 2003). Receptors containing α4 constitute more minor receptor subtypes and are expressed primarily in the thalamus and the hippocampus (Dawson, Collinson et al. 2005).

Additional studies show that the majority of native $GABA_A$ receptors are comprised of two α, two β, and one γ subunit (Sieghart, Fuchs et al. 1999) with the actions of 'classical' BZ agonists, such as diazepam, being exerted via receptors containing β, γ2, and either an α1,α2, α3, or α5 subunits (**Figure 36**) (Pritchett, Luddens et al. 1989; Pritchett, Sontheimer et al. 1989; Pritchett and Seeburg 1990). Many drugs of various chemical classes target $GABA_A$ receptors, only one of these being benzodiazepines (Luddens, Seeburg et al. 1994; Luddens and Korpi 1995; Luddens and Korpi 1995; Luddens, Korpi et al. 1995; Luddens and Korpi 2007). Because of its therapeutic relevance the $GABA_A$ receptor and especially the BZ binding site, has been the focus of considerable basic scientific and commercial attention. The elucidation of the molecular structure and of the physiological properties of different $GABA_A$ receptors has formed the basis for strategies to develop drugs which selectively modulate particular subtypes.

Gene targeting approaches, behavioral and physiological experiments demonstrated that the α1 subtype is mainly responsible for the sedative/motor effects of non-selective BZs (McKernan, Rosahl et al. 2000), such as diazepam, while receptors containing the α2/α3 subunits are thought to be responsible for the anxiolytic activity (Bohme, Rabe et al. 2004; Carling, Madin et al. 2005; Atack, Wafford et al. 2006; Fradley, Guscott et al. 2007). A list of $GABA_AR$ subtype selective compounds and the α-subunits involved has been published in a recent review by Rudolph et al. (Rudolph and Mohler 2006).

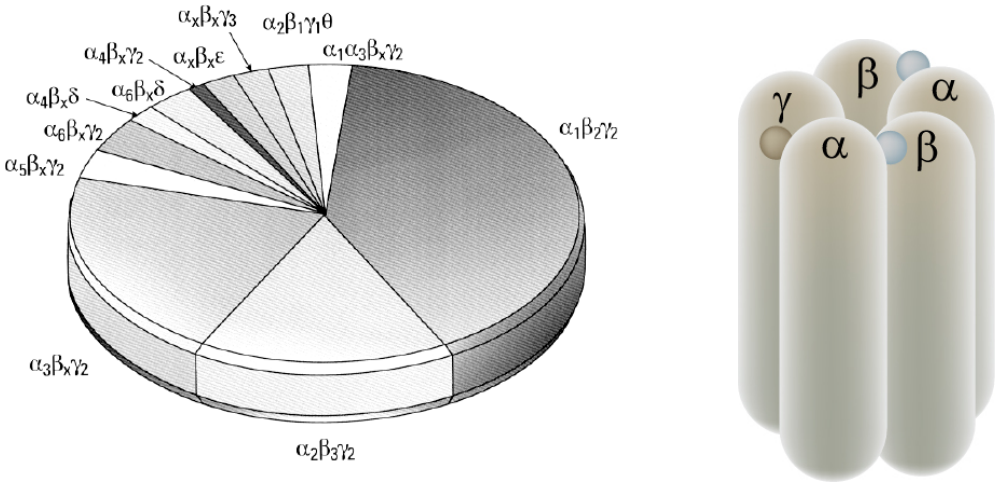

Figure 36: Relative abundance of $GABA_A$ receptor subtypes in the rat brain and binding sites of GABA, between an α and β subunit, as well as benzodiazepines, between an α and a γ subunit (Whiting, Bonnert et al. 1999).

Because of the enrichment in hippocampal CA1 and CA3 regions it has been assumed that the α5 subunit is envolved in learning/memory processes. First evidence supporting this assumption was found in 2002 by Collinson et al. (Collinson, Kuenzi et al. 2002). The authors found that in Morris water maze experiments testing spatial learning, mice lacking the $GABA_AR$ α5 subunit performed better than wildtype mice. Huge interest in α5 subtype selective benzodiazepine binding site inverse agonists was spawned by these results and indeed many promising data was collected ever since, all pointing towards a cognition enhancing effect of these compounds (Chambers, Atack et al. 2002; Chambers, Atack et al. 2003; Chambers, Atack et al. 2004; Sternfeld, Carling et al. 2004; Street, Sternfeld et al. 2004; Szekeres, Atack et al. 2004; van Niel, Wilson et al. 2005; Collinson, Atack et al. 2006; Dawson, Maubach et al. 2006; O'Connor, Jones et al. 2006; Guerrini, Ciciani et al. 2007).

The search for a PET ligand specific for the α5 subunit was the logical next step, given the fact that such ligands might enable the acquisition of *in vivo* data about the involvement of α5 subunit containing $GABA_ARs$ in neurodegenerative diseases causing

cognitive deficits as well as its potential involvement in learning/memory processes. First attempts to lable *in vivo* α5 subunit containing $GABA_A$Rs were made by Maeda et al. as well as by Lingford-Hughes et al. in 2003 and 2002 respectively (Lingford-Hughes, Hume et al. 2002; Maeda, Suhara et al. 2003). Both groups used zolpidem as a way to block α1, α2 and α3 containing receptors (Luddens, Seeburg et al. 1994) and used as radio labeled ligand [^{11}C]Ro15-4513, a ligand which binds with similar affinity to all α-subunits except the α5-subunit, for which it has a 10 - 20 fold higher affinity (Luddens, Seeburg et al. 1994; Sieghart 1995; Gunnersen, Kaufman et al. 1996). Because of the very low concentrations applied *in vivo* using PET tracers the authors hoped to be able to use the tracer's higher affinity for the α5 subunit, together with the blocking by zolpidem, to be able to only lable α5-subunit containing $GABA_A$ Rs. Although both groups conclude with the statement of having found a quantitative method to label α5-subunit containing $GABA_A$Rs in humans and rodents, further studies, especially with pathological questions as their basis, remain yet to be done. However, both groups also repeat the assumption that α5-subunit containing $GABA_A$Rs might be envolved in learning/memory processes.

Hence, starting from published structures (Street, Sternfeld et al. 2004; van Niel, Wilson et al. 2005), six novel, potentially α5-subunit selective, compounds were synthesized for this study by Tanja Capito, currently a PhD student in the lab of Prof. F. Rösch, department of nuclear chemistry at the Johannes Gutenberg-Universität Mainz.

5.1 *TC-Compound In Vitro* Experiments

To get a first idea whether or not these new compounds were α5-subunit selective, classical competition filtration receptor-binding experiments with crude membrane preparations of three different rat brain regions were performed as described on page 40 ff. and as published e.g. in (Luddens, Killisch et al. 1991; Luddens and Korpi 1997). [^{3}H]Ro15-4513 was used as radio labeled tracer. The results for TC07, TC08, TC11 and TC12 point towards an α5-subtype selectivity, as displacement is highest at hippocampal membranes as compared to cortex and cerebellum membranes. The difference between the cerebellum and the hippocampus as well as the difference between the cortex and the hippocampus is highly significant ($p < 0.01$, **) for TC07, TC11 and TC12. TC09 and TC10 caused little or no displacement and were therefore excluded from further experiments. In these experiments the focus has to be on the cerebellum to hippocampus ratio, as the cerebellum contains in a significant amount only α1- and α6-containing $GABA_A$Rs (Pirker, Schwarzer et al. 2000; Campos, de Cabo et al. 2001) and the hippocampus is enriched with α5-containing receptors. The selectivity for α5

over α1 is the most important, as α1-containing $GABA_A$Rs represent ~70 % - 80 % of all the $GABA_A$Rs in the rat brain.

To add proof to the results with 1 nM of [^{3}H]Ro15-4513, an additional set of experiments was done with 6 nM, to have a concentration closer to the K_D values of all α-subunits except α5, which are in the range of 5 to 11 nM. In general the same results as with 1 nM were achieved, the only major difference being that statistical significance for the difference in displacement between cerebellum and hippocampus could only be reached with the 512 nM concentrations of TC07 and TC12. Nonetheless all four compounds were kept for further experiments with [^{3}H]Ro15-1788 (Flumazenil), a tracer that binds with low nanomolar affinity only to the α1, α2, α3 and α5 containing $GABA_A$ receptors. By using this tracer at a concentration of 1 nM, which represents the K_D for these receptor subtypes (Sieghart 1995), α4- and α6-containing receptors could be excluded from the start. The data represent similar results as compared to the 6 nM [^{3}H]Ro15-4513 experiments, with best results, as far as potential α5-selectivity is concerned, given for TC07 and TC12, were statistical significance is reached for the cerebellum to hippocampus ratio at the high concentration.

An additional feature of the [^{3}H]Ro15-1788 experiments was the co-incubation with zolpidem. As mentioned above this ligand recognizes with very high affinity only α1-containing $GABA_A$Rs and with less affinity α2- and α3-containing receptors. Application of an excess of this ligand should therefore inhibit most of the binding to these receptors and leave as residual binding more or less only α5-specific binding. As expected, the total displacement is higher as compared to displacement in the non-zolpidem containing samples. However, the displacement is not at all complete neither with TC07 nor TC12. This might indicate either that the concentration of 512 nM is still too low, that both compounds act only partially on the binding site or that there is still some non-α5 specific binding of [^{3}H]Ro15-1788 binding left which cannot be displaced by TC07 or TC12. Altogether these three different experimental designs delivered promising results and justified a closer look with transiently transfected HEK293 cells.

The use of the same β- and γ-subunit in combination with the six α subunits maximised the comparability of the calculated K_i values. However, in native receptor populations, the α1-subunit predominantly occurs together with the β2 and γ2 subunits while the second most important subunit for this study, the α5-subunit, predominantly occurs with the β3 and γ2 subunits in rats as well as in humans (Sur, Quirk et al. 1998). In previous experiments and projects in our group it was proven that less DNA is needed and total binding is increased when the β3 subunit is used. This made it necessary to proof that

the binding of the TC compounds was not influenced by the type of β subunit employed. Results in **Figure 17** page 54 do not show signs of significant differences in binding depending on the β subunit, no matter whether the α1- or the α5-subunit was combined with either a β2 or β3 subunit. Though curves are representative for almost optimal results of a receptor ligand binding assay, they reflect also one of the biggest challenges when using the TC compounds in aqueous conditions, namely, their poor water solubility. This was true for all compounds but TC07. In preliminary solubility assays it turned out that ~ ≤ 1000 nM was the concentration usable for all compounds. But, as can be seen in the resulting curve fit, total displacement cannot be reached with TC11 and TC12 at this concentration due to poor solubility even at this relatively low concentration. Partial competition might also be a reason for such results as seen with TC11 and TC12 but the solubility problem became obvious very soon and might be the possibility that is more likely here because otherwise the curve would rather look different at lower concentrations. Extrapolation and simulation of perfect solubility decreases the error of the curve and the best-fit parameters reflect a curve with better solubility. Although in vitro experiments are made more difficult by this property, concentrations of a future PET-tracer will be so low that solubility should not be a major issue then.

TC08, TC09 and TC10 do not represent $GABA_AR$ subtype selective benzodiazepine binding site ligands as all K_i values seem to lie beyond 1 µM (**Table 7**). TC07, TC11 and TC12, however, seem to have the desired properties of high α5-subtype and low α1-subtype affinity. In addition the α2/α5 and α3/α5 ratio of all three compounds is acceptable for further research on the compounds. These ratios became the sorting criterion, as it is best for TC11, followed by TC07 and TC12. While TC08, TC09 and TC10 lost their parent compound's subtype selectivity completely, the affinities for α1-, α2-, α3- and α5-subunit containing receptors of TC07 are in almost complete agreement with the data from the parent compound published by Street et al. (2004), showing the same subtype selectivity profile. This is not true for TC11, where the parent compound has a much higher affinity for α3- and a lower affinity for α2-containing receptors. Also TC12 differed from its parent compound as it showed a higher affinity for α2-containing receptors, rendering it less useful as it would have been with the original affinity profile.

5.1.1 Receptor Autoradiography with the TC Compounds

As detailed before, the method of choice for autoradiography signal detection was the storage phosphor technique (see chapter Detection on page 44 and Methodological Evaluation, page 57).

Results in **Figure 20** and **Figure 21** on pages 59 and 60, also **Figure 22** and **Figure 23** on pages 61 and 62. Even visually can be seen that TC07 and TC12 caused a greater displacement in the hippocampus as compared to most other regions of the brain. This observation is further supported by the graphical quantification. In complete agreement with in vitro results, TC08 has no effect while TC11, different from *in vitro* results, appears to have only very little *in situ* affinity to α5-containing receptors. Sur et al., in their autoradiographic experiments comparing [^{3}H]Ro15-1788 binding with [^{3}H]L-655,708 binding, an α5-specific tracer, found that the hippocampal formation was the most abundantly labeled structure.

Table 9: Densities (fmol/mg tissue) of [^{3}H]Ro15-1788 and [^{3}H]L-655,708 binding sites and relative proportion of [^{3}H]L-655,708 sites in selected rat brain regions. Data represent the mean ± S.E.M. of 2 – 12 different sections of a representative animal (Sur, Fresu et al. 1999).

Brain regions	[^{3}H]Ro15-1788	[^{3}H]L-655,708	Ratio (%)
Cerebral cortex			
layers I–III	447 ± 10	7 ± 1	1.6
layer IV	369 ± 9	14 ± 1	3.8
layers V–VI	365 ± 10	17 ± 1	4.6
cingulate cortex	438 ± 9	34 ± 1	7.8
orbital cortex	406 ± 15	30 ± 1	7.4
insular cortex	515 ± 25	25 ± 1	4.8
endopiriform nucleus	362 ± 10	48 ± 8	13
subiculum	370 ± 20	17 ± 1	4.6
Hippocampus			
CA1 stratum oriens	359 ± 21	69 ± 3	19
stratum radiatum and lacunosum moleculare	385 ± 22	87 ± 1	23
CA2 stratum oriens	278 ± 5	68 ± 1	24
stratum radiatum and lacunosum moleculare	315 ± 13	79 ± 1	25
CA3 stratum oriens	328 ± 17	72 ± 1	22
stratum radiatum and lacunosum moleculare	325 ± 24	86 ± 1	26

[^{3}H]L-655,708 binding sites are expressed in CA1 to CA3 fields with a higher density than in the dentate gyrus where in contrast a very high density of [^{3}H]Ro15-1788 sites was noticed. Concomitantly, in their experiments, the contribution of [^{3}H]L-655,708 sites to the total benzodiazepine site population amounts to 19 – 26 % in CA1– CA3 areas and only 10 % in the dentate gyrus. At the cellular level the distribution of [^{3}H]L-655,708 binding sites in both Ammon's horn and dentate gyrus appears to follow a similar pattern. Indeed, they are predominantly observed in dendritic fields of pyramidal neurons and granule cells.

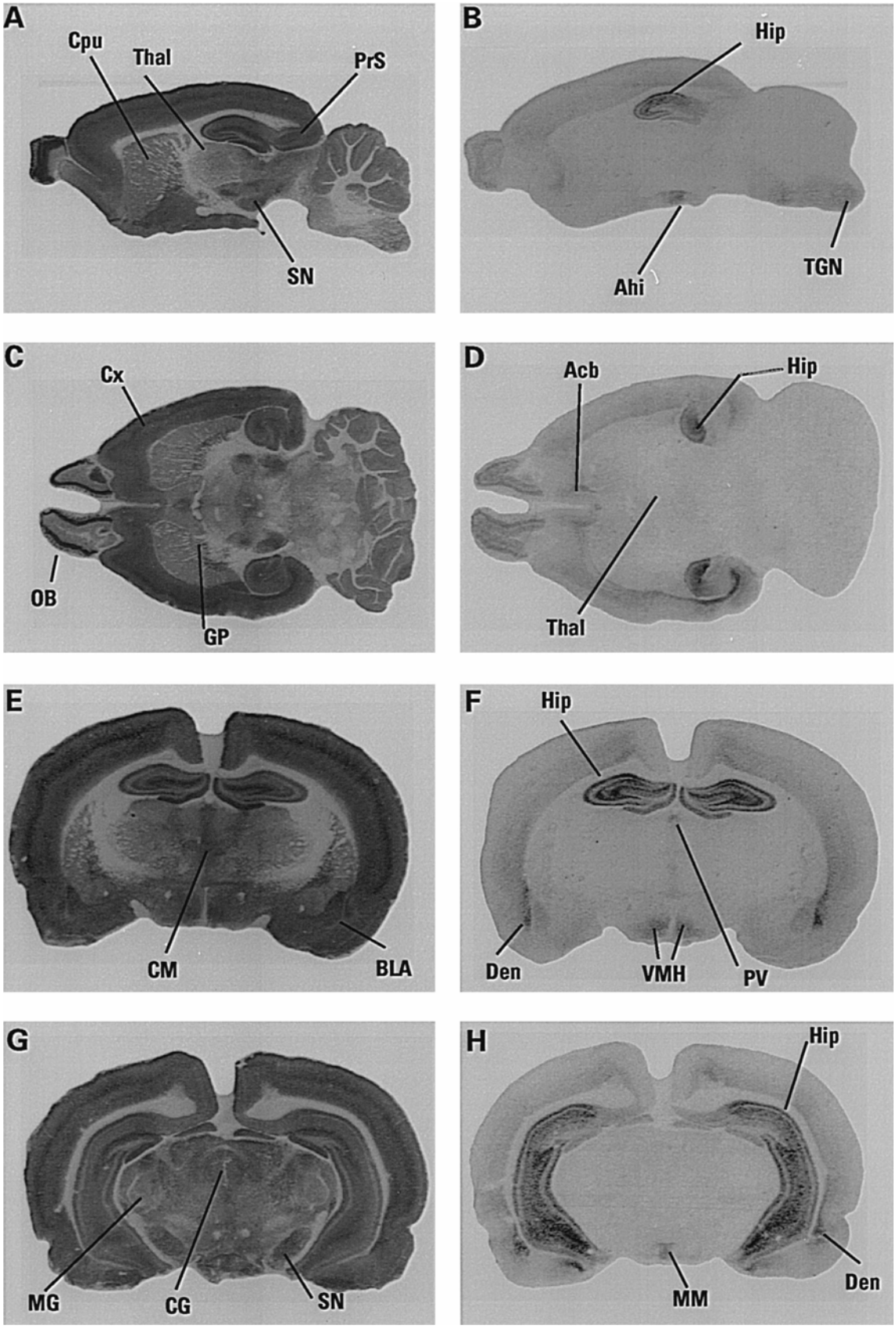

Figure 37: Comparative localization of [^{3}H]Ro15-1788 binding sites (left column) and [^{3}H]L-655,708 binding sites (right column) in rat brain. As illustrated in sagittal (A, B) and horizontal (C, D) sections, [^{3}H]L-655,708 binding sites have a much more restricted localization than [^{3}H]Ro15-1788 sites. Analysis of brain coronal sections (E–H) indicate a preferential localization

of [^{3}H]L-655,708 sites in the hippocampal formation and in a few other nuclei in marked contrast with the presence of [^{3}H]Ro15-1788 sites in most neuronal structures. Abbreviations: Acb, nucleus accumbens; Ahi, amygdalohippocampal area; BLA, basolateral amygdala; CG, central gray; CM, central medial thalamic nucleus; Cpu, caudate putamen; Cx, cortex; Den, dorsal endopiriform nucleus; GP, globus pallidus; Hip, hippocampus; MG, medial geniculate nucleus; MM, medial mammilary nucleus; OB, olfactory bulb; PrS, presubiculum; PV, paraventricular thalamic nucleus; SN, substantia nigra; TGN, trigeminal nuclei; Thal, thalamus; VMH, ventromedial hypothalamic nuclei. Magnification: (3 in A–D and 4.5 in E–H) (Sur, Fresu et al. 1999).

These observations, along with their data of cortical regions are in good agreement with the results of the present work (**Figure 24** and **Figure 25**), where residual [^{3}H]Ro15-1788 binding represents almost exclusively α5-specific binding. Remaining binding in the cortex is ~10 % while remaining binding in the hippocampus is ~20 %. This data is strikingly similar to the results published by Sur et al. This is also true for cortical areas, where Sur et al. found that [^{3}H]L-655,708 sites were present at low levels and accounted for a small proportion of total [^{3}H]Ro15-1788 binding sites, except in cingulated (7.8 %) and orbital (7.4 %) cortex and in the endopiriform nucleus (13 %). Although [^{3}H]L-655,708 sites were slightly more numerous in cortical layers IV – VI than layers I – III, they represented only 4 – 5 % of all [^{3}H]Ro15-1788 binding sites (Sur, Fresu et al. 1999). In the coronal rat brain sections of **Figure 25** displacement of the [^{3}H]Ro15-1788 binding after co-incubation with zopidem was almost complete with TC07 and TC12. Remaining binding can again be explained either by only partial agonism of the TC compounds for the binding site, or by a too small concentration. A third possibility could be that there is still non-α5-specific [^{3}H]Ro15-1788 binding, which would not be displaceable by the TC compounds were they α5-selective *in situ*. TC08 and TC11, for TC11 results in contrast to *in vitro* experiments, did not show significant effects in α5-subtype receptor enriched regions of the rat brain. Altogether, for TC07 and TC12, *in situ* results strongly supported the results obtained in *in vitro* experiments.

5.2 *In vivo* Experiments with TC07

The fact that over all *in situ* experiments worked best with TC07, most likely because of the better solubility in aqueous conditions, led to the decision to single out TC07 for *in vivo* experiments. TC11 and TC12 could have been chosen, too. [^{3}H]Ro15-1788 binding was displaced by TC07 with greater efficacy in the forebrain as compared to the cerebellum (**Figure 26**), in good, but not absolute agreement with the expected results of an α5-selective compound, as a displacement of ~ 40 % is more than seen *in vitro* and *in situ*, where such a degree of inhibition was only obtained in hippocampal areas with their high proportion of α5-containing receptors. However, 5 mg/kg of TC07 might

also displace binding from α2, α3 and maybe even from α1-containing receptors in the hippocampus and cortex. An indication for the latter might be the ~ 20 % displacement in the cerebellum with nearly exclusively α1-containing receptors. However, the significant displacement is a good indication that TC07 crossed the blood brain barrier. To obtain this information was the main purpose of this study.

5.3 Electrophysiological Experiments with TC07 and TC12

In order to see whether or not the two most promising compounds, TC07 and TC12, had a physiological effect similar to their parent compounds, namely inverse agonistic effects, classical whole cell patch clamp experiments were performed on transiently transfected HEK293 cells. After the determination of the GABA dose-response curve and along with that the EC_{50} and EC_{20} (3 µM, curve displayed in **Figure 27** on page 67), increasing concentrations of TC07 and TC12 were applied to the cells and results plotted as percent of the GABA EC_{20} response. Functionally, TC07 has a moderate inverse agonistic effect on α5-containing $GABA_A$ receptors, while TC12, even at a concentrations 1 µM had no detectable effect. TC07 has a maximal efficacy of - 40 %, similar to the most effective parent compound published by Street et al. in 2004. The authors, using Xenopus laevis oocytes and human $GABA_A$Rs found a maximal effect of - 45 % for the parent compound.

5.4 [^{18}F]MHMZ, a 5-HT_{2A} Receptor Specific PET-Ligand

Serotonergic 5-HT_{2A} receptors are of central interest in the pathophysiology of schizophrenia, Alzheimer's disease, personality disorders and other psychiatric disorders (Kristiansen, Elfving et al. 2005). The serotonergic system has also been implicated in sleep, aging and pain (Lemaire, Cantineau et al. 1991). Thus, *in vivo* studies of 5-HT_{2A} receptor occupancy would provide a significant advance in the understanding of the mentioned disorders and conditions. A number of neurotransmitter analogs labeled with β^+ - emitter containing radioligands were synthesized as radiopharmaceuticals for the imaging of 5-HT_{2A} receptors, such as [^{11}C]MDL 100907 (Yiyun Huang 1999), [^{18}F]altanserin (Hamacher and Coenen 2006) and [^{11}C]SR 46349B (Alexoff, Shea et al. 1995). The first two represent the radioligands of choice for *in vivo* 5-HT_{2A} PET imaging because of their high affinity and selectivity for the 5-HT_{2A} receptor (altanserin: K_i = 0.13 nM (Hamacher and Coenen 2006); (R) - MDL 100907: K_i = 0.57 nM (Heinrich, Bottcher et al. 2006)). Affinities are more than 100-fold lower for 5-HT_{2C}-, α_1-, D_1- and D_2-receptors. It was proposed that the selectivity of [^{11}C]MDL 100907 for 5-HT_{2A} receptor is slightly higher than the selectivity for this receptor of [^{18}F]altanserin (Meltzer,

Smith et al. 1998). Both tracers show in *in vitro* and in *in vivo* experiments, high affinity, selectivity and a good ratio of specific to non-specific binding for 5-HT_{2A} receptors (Ping-Zhong Tan 1999). The advantage of [^{18}F]altanserin over [^{11}C]MDL 100907 is the possibility to perform equilibrium scans lasting several hours and to transport the tracer to other facilities based on the 110 minute half-life of [^{18}F]fluorine. A drawback of [^{18}F]altanserin is its rapid and extensive metabolism. Four metabolites are formed in humans that cross the blood brain barrier (Ping-Zhong Tan 1999), whereas metabolites of [^{11}C]MDL 100907 do not enter the brain to any larger extent (Scott and Heath 1998).

Part of the aim of this study was to develop an ^{18}F-analog of MDL 100907 (**Figure 6**, page 31) combining advantages of both ligands, the better selectivity of MDL 100907 and the superior isotopic properties of [^{18}F]fluorine.

A radioligand competition binding assay was carried out by Mikael Palner, group of Prof. Gitte Knudsen, Rigshospitalet, Copenhagen, with GF-62 cells, a clonal cell line expressing high amounts (5 - 7 pmol/mg) of the 5-HT_{2A} receptor. MHMZ showed a 4.5 times lower affinity as compared to the parent compound MDL 100907 but it still was in the nanomolar range.

5.4.1 Results from Autoradiography Experiments

Autoradiographic images of the 5-HT_{2A} receptor obtained with [^{18}F]MHMZ showed excellent visualization results in rat brain sections (**Figure 29**, page 69). Images are in complete agreement with the distribution obtained with [^{3}H]MDL 100907 (Lopez-Gimenez, Mengod et al. 1997) (**Figure 30**, page 70, **B** and **C**). Highest binding was detected in lamina V of the frontal cortex, the caudate-putamen, the motor trigeminal nucleus, the facial nucleus and the pontine nuclei. Minor binding was detected in the olfactory system, the mesencephalon and the hippocampus. Competition autoradiographic assays of 5 nM [^{18}F]MHMZ with 10 µM of fallypride, WAY 100635 and prazosin showed that [^{18}F]MHMZ is highly specific for 5-HT_{2A} receptors (**Figure 31**, page 71), as displacement could only be detected with fallypride. Here, co-incubation led to a displacement of 30 % (n = 4, ± 6 % SEM) of total binding in the frontal cortex as well as in the caudate-putamen, which might be due to the known cross affinity of fallypride to 5-HT_2 receptors (Stark, Piel et al. 2007).

A comparison of the binding of [^{18}F]altanserin and [^{18}F]MHMZ (**Figure 30**, page 70) displays that [^{18}F]MHMZ is at least equivalent to [^{18}F]altanserin in terms of specificity for 5-HT_{2A} receptors. Moreover, the binding of [^{3}H]MDL 100907 and [^{18}F]MHMZ agree completely (Herth, Debus et al. 2008).

5.4.2 MicroPET Experiments

To date, the parent compound for PET imaging of [^{18}F]MHMZ, [^{11}C]MDL 100907, is the most specific ligand for the 5-HT$_{2A}$Rs with the best signal to noise ratio. First imaging studies in monkeys, published in the mid nineties by Lundkvist et al., found that the distribution *in vivo* was in concordance with the then already known location of high densities of 5-HT$_{2A}$Rs. They determined a cortex to cerebellum ratio of 3.5 to 4.5 after 60 - 80 min and equilibrium to be reached after ~40 min (Lundkvist, Halldin et al. 1996). Two years later Lars Farde's group published the first study with [^{11}C]MDL 100907 in man. The authors state that the highest radioactivity concentration was observed in the neocortex, whereas radio activity was lower in the cerebellum, pons, thalamus, striatum and white matter. Also that the BP in the neocortical regions was 4 - 6 times higher, whereas BP in the striatum was slightly higher than that in the cerebellum, also demonstrating a regional distribution in good agreement with 5-HT$_{2A}$ receptor densities measured *in vitro*. The BP in the cerebellum in man was small but not negligible. Their preliminary study suggests that [^{11}C]MDL 100,907 is a suitable PET radioligand for studies on 5-HT$_{2A}$ receptors in man. According to their data the high selectivity of MDL 100,907 represents a major advantage as compared to other available radioligands with poor selectivity. Thus, [^{11}C]MDL 100,907 is recommended in the future for PET studies in healthy subjects and schizophrenic patients, including the determination of drug-induced 5-HT$_{2A}$ receptor occupancy (Ito, Nyberg et al. 1998).

In 2000 Kakiuchi et al. found an age-related reduction of [^{11}C]MDL 100907 binding to central 5-HT$_{2A}$Rs in the monkey (Kakiuchi, Nishiyama et al. 2000). Watabe et al. did an extensive characterisation of the kinetics of the tracer in the rhesus monkey in the same year (Watabe, Channing et al. 2000) while Hirani et al. found out three years later that fenfluramine has an effect on 5-HT$_{2A}$Rs but does not displace [^{11}C]MDL 100907 in the rat (Hirani, Sharp et al. 2003). This data representing one of the very few small animal PET studies published in the field. Only in 2005 the then two most specific and potential PET ligands for clinical routine for the imaging of the 5-HT$_{2A}$R were compared by Kristiansen et al. with remarkably better results for MDL 100907 (Kristiansen, Elfving et al. 2005). Recently in 2006 and 2007 Bhagwagar et al found an increased [^{11}C]MDL 100907 binding in patients having recovered from depression (Bhagwagar, Hinz et al. 2006) and Hinz et al. a revised tracer kinetic model (Hinz, Bhagwagar et al. 2007). Also in 2007 Hurlemann et al. published a study where they report of having found decreases in 5-HT$_{2A}$ receptor density in the at risk mental state of schizophrenic patients using [18F]altanserin as a radio tracer (Hurlemann, Matusch et al. 2007). This very successful and promising study underlines the importance of having a highly specific imaging tool for the 5-HT$_{2A}$ receptor.

Results from small animal PET measurements performed for the present work show that the *in vivo* distribution is in very good agreement with the distribution seen in the autoradiographic images of **Figure 30**, page 70 and **Figure 31**, page 71. In addition the high uptake can be seen in the same brain regions as described by Lundkvist et al. According to the 4-parameter reference model, which assumes that the distribution volume of the non-displaceable compartment is the same for the tissue of interest and the reference tissue (also see **chapter 2.1.3** on page 14 and **chapter 3.10**, page 46), the BP (BP = k_3/k_4) for uptake in the rat frontal cortex is 1.45 (Lammertsma, Bench et al. 1991). The cortex to cerebellum ratio was determined to be 2.7 after ~30 min. Equilibrium was reached between 28 to 35 minutes post injection. The Equilibrium state was reached earlier than observed by Lundkvist et al. This is not too surprising given the faster metabolism of rodents as compared to primates. Once the equilibrium state was reached specific binding was constant for the rest of the scan time (60 min, see TAC, **Figure 32**), which may allow even scans up to 120 min.

Although the cortex to cerebellum ratio along with the rest of the data is quite similar to previously published data in the literature, obtained with the parent compound, it has yet to be proven with, e.g. ketanserin displacement experiments, that the detected high uptake in the frontal cortex actually represents specific binding.

During the data aquisition arterial blood samples were taken and analysed with thin layer chromatography (TLC) to gain some insights into the metabolisation of the tracer and potential radio active metabolites which might interfere with specific binding or decrease the signal to noise ratio. This plasma analyses showed that [^{18}F]MHMZ underwent fast metabolism. One polar metabolite was found in rat plasma which is not likely to cross the blood brain barrier. The percentage of unmetabolized fractions were 43 %, 32 %, 16 %, 7 % at 5, 10, 30 and 60 min, respectively.

6 OUTLOOK

All experiments performed with the TC compounds employed the non-labeled reference compounds. After successful and reproducible [^{18}F], or even better [^{3}H], labelling, TC07, TC12 and maybe TC11 need to undergo a dedicated and detailed characterisation, ranging from *in vitro* determination of K_D, on and off-time and, especially important, non-specific binding, to *in situ* binding properties in rat brain section autoradiographies. In addition to that *in vivo* testing needs to be done like *in vivo* organ distribution and brain region distribution measured *ex vivo* in rats or mice, then preferably with the [^{18}F]-labelled compounds. Metabolism studies to determine potential active metabolites and the biological half-life of the compounds need to be measured before small animal PET experiments can be conducted.

Here the first step would be a total binding scan over 120 minutes. The next step could be a blocking and challenge experiments, e.g. using flumazenil or Ro15-4513 as competitors.

The major demanding task for the validation of PET experiments with $GABA_AR$ selective tracers will be to find an appropriate volatile or other anesthetic. Most anesthetics exert their action through $GABA_A$ receptor subtypes. Should at least one of the potential PET-ligands prove to be useful appropriate animal models would be the next step to elucidate their diagnostic value in degenerative diseases like Alzheimer's disease or in the mechanisms of learning and memory. These data should eventually pave the way for the use of these ligands as tools for the diagnosis of these physiological or pathophysiological processes in man.

Many of the experiments mentioned above have already been performed with [^{18}F]MHMZ. However, more detailed PET studies, including challenge and blocking studies, are still missing. The biodistribution studies have to be deepened along with the brain region distribution of the tracer measured *ex vivo*. Toxicology studies are already planned and provided that it will result in a non-toxicity of the tracer first human PET studies in healthy volunteers would be possible. Should the tracer prove to be useful in patients it might develop into a tool for research on and the diagnosis of schizophrenia. In addition to that it could be used for drug occupancy studies with drugs acting on the $5\text{-}HT_{2A}$ receptors and of course for task dependent studies of e.g. depressive patients. Last, but not least, it might be a useful tool for the early diagnosis of Alzheimer's disease.

7 SUMMARY

Initially, six new benzodiazepine derivatives, TC07, TC08, TC09, TC10, TC11 and TC12, produced as non-labeled standards on the basic structure of benzodiazepines, were tested with competitive radioligand binding assays for their binding properties to membranes of rat cerebellum, hippocampus and cortex, as well as membranes of HEK293 cells, transiently expressing recombinant $GABA_A$Rs. *In situ* competition receptor autoradiographic assays on rat brain sections were performed with [^{3}H]Ro15-4513 and [^{3}H]Ro15-1788 as radiolabeled tracers. Results from TC07, TC11 and TC12 hinted towards a binding selectivity for α5-subunit containing $GABA_A$Rs with nanomolar affinities for those receptors.

In vivo binding experiments in the rat, with [^{3}H]Ro15-1788 as tracer and TC07 as competitor, showed that TC07 displaces more tracer in the forebrain than in the cerebellum. The regional distribution of α5-subunit containing $GABA_A$ receptors in the rat brain – extremely small amount in the cerebellum, about 20 % in the hippocampus – added strength to the possibility of TC07 being α5-receptor selective and that TC07 crosses the blood brain barrier.

Electrophysiological recordings in transiently transfected HEK293 cells expressing $\alpha5\beta3\gamma2$ $GABA_A$Rs indicate that TC12 is a pure benzodiazepine antagonist while TC07 seems to act as a weak inverse agonist (negative modulator) on the benzodiazepine binding site. This inverse agonistic action, at least theoretically, might enable the use of TC07 as a so-called cognitive enhancer in future experiments, even apart from its potential use as a PET ligand.

Taken together the results of this study justify the ^{18}F radio-chemical labeling of three of the six tested compounds with a suggested sequence of TC07, TC12 and TC11.

Precursors and reference compounds of [^{18}F]MHMZ were synthesized in high yields as published (Herth, Debus et al. 2008).

Autoradiographic studies showed excellent *in situ* binding with high specificity of [^{18}F]MHMZ for 5-HT_{2A} receptors and very low non-specific binding. [^{18}F]MHMZ undergoes fast metabolism resulting in one polar active metabolite which is not likely to cross the blood brain barrier.

Transversal, sagittal and coronal microPET images of the rat brain showed high uptake in the frontal cortex and striatum and low uptake in the cerebellum, which reflects the typical 5-HT_{2A} receptor distribution. The *in vivo* distribution is in good agreement with

the distribution seen in the autoradiographic images. According to the 4-parameter reference tissue model, the binding potential for uptake in the rat frontal cortex is 1.45. The cortex to cerebellum ratio was determined to be 2.7 after ~ 30 min, which is strikingly close to the data published for [^{11}C]MDL 100907 (Lundkvist, Halldin et al. 1996). Equilibrium was reached after ~ 35 minutes post injection.

Except from the slightly decreased affinity the reported *in vitro* data are comparable to those of [^{3}H]MDL 100907. The presented data suggest that the aim of developing a novel ^{18}F-analog of MDL 100907 (**1**) combining the better selectivity of MDL 100907 as compared to altanserin and the superior isotopic properties for the clinical routine of [^{18}F]fluorine as compared to [^{11}C]carbon could be achieved.

All together, the auspicious results of [^{18}F]MHMZ justify further experiments like *ex vivo* brain regional distribution and detailed *in vivo* small animal PET as well as human PET studies to verify the potential of this new 5-HT_{2A} imaging ligand.

8 ZUSAMMENFASSUNG

Für diese Arbeit wurden sechs neue Benzodiazepinderivate, TC07, TC08, TC09, TC10, TC11 und TC12, hergestellt. Diese wurden mittels Radioligandenbindungsassay sowohl auf ihre Bindungseigenschaften für Membranen des Cerebellum, des Hippocampus und des Cortex der Ratte hin untersucht, als auch für Membranen von HEK293 Zellen, die transient rekombinante $GABA_A$ Rezeptoren exprimierten. Zusätzlich wurden kompetitive *in situ* Rezeptorautoradiographien an Rattenhirnschnitten mit den Liganden [^{3}H]Ro15-4513 und [^{3}H]R015-1788 durchgeführt. Zusammen ergaben sich aus diesen Experimenten deutliche Hinweise auf eine Selektivität der Verbindungen TC07, TC11 und TC12 für α5-Untereinheiten enthaltende $GABA_A$ Rezeptoren mit α5-Affinitäten im niedrigen nanomolaren Bereich.

In vivo Bindungsexperimente in Ratten, mit [^{3}H]Ro15-1788 als Tracer und TC07 als Kompetitor, ergaben, dass TC07 mehr [^{3}H]Ro15-1788 im Vorderhirn als im Cerebellum verdrängt. Bezog man die regionale Verteilung der α5-Untereinheit des $GABA_A$ Rezeptors im Rattenhirn mit ein – sehr wenige α5-Untereinheiten im Cerebellum, etwa 20 % der $GABA_A$ Rezeptor-Untereinheiten im Hippocampus – untermauerten diese Ergebnisse die Vermutung, TC07 könne α5-selektiv sein. Diese Daten bestätigten darüberhinaus, dass TC07 die Blut-Hirn-Schranke passieren kann.

Für elektrophysiologische Messungen mit TC07 und TC12 wurden die oben erwähnten transient transfizierten HEK293 Zellen verwendet, welche die $GABA_A$ Rezeptor Untereinheitenkombination $\alpha5\beta3\gamma2$ exprimierten. Das Dosis-Antwort Verhalten ergab keinen signifikanten Effekt für TC12. Die Daten von TC07 dagegen lassen auf einen schwach negativ modulatorischen Effekt schließen, was, zumindest theoretisch, die Möglichkeit eröffnet, TC07 auch als sogenannten cognitive enhancer einzusetzen. Der errechnete K_i-Wert lag in derselben Größenordnung wie der K_i-Wert, der anhand der Bindungsassaydaten errechnet wurde.

Insgesamt rechtfertigen die bisherigen Ergebnisse die radiochemische Markierung mit ^{18}F von drei der sechs getesteten Verbindungen in der Reihenfolge TC07, TC12 und TC11.

Des Weiteren wurde [^{18}F]MHMZ, ein potentiell 5-HT_{2A} selektiver Ligand und PET-Tracer einschließlich Vorläufer und Referenzverbindungen, mit hohen Ausbeuten synthetisiert (Herth, Debus et al. 2008). Autoradiographieexperimente mit Rattenhirnschnitten zeigten hervorragende *in situ* Bindungseigenschaften der neuen Verbindung.

Die Daten wiesen eine hohe Selektivität für 5-HT_{2A} Rezeptoren in Verbindung mit einer niedrigen unspezifischen Bindung auf. [^{18}F]MHMZ erfährt *in vivo* eine schnelle Metabolisierung, wobei ein polarer aktiver Metabolit entsteht, welcher vermutlich nicht die Blut-Hirn-Schranke passieren kann.

Transversale, sagittale und coronale Kleintier-PET-Bilder des Rattenhirns zeigten eine hohe Anreicherung im frontalen Cortex und im Striatum, während im Cerebellum so gut wie keine Anreicherung festzustellen war. Diese Verteilung deckt sich mit der bekannten Verteilung der 5-HT_{2A} Rezeptoren. Die *in vivo* Anreicherung scheint sich ebenfalls gut mit der Verteilung der in den Autoradiographieexperimenten gemessenen Bindung zu decken. Nach Berechnungen mit dem 4-Parameter Referenzgewebe Modell beträgt das Bindungspotential (BP) für den frontalen Cortex 1,45. Das Cortex zu Cerebellum Verhältnis wurde auf 4,4 nach 30 Minuten Messzeit bestimmt, was bemerkenswert nah an den von Lundkvist et al. für [^{11}C]MDL 100907 publizierten Daten liegt.

Abgesehen von der etwas niedrigeren Affinität waren die gemessenen *in vitro*, *in situ* und *in vivo* Daten denen von [^{3}H]MDL 100907 und [^{11}C]MDL 100907 sehr ähnlich, so dass wir ein [^{18}F]Analogon in der Hand haben, das die bessere Selektivität von MDL 100907 verglichen mit Altanserin mit der längeren Halbwertszeit und den besseren Eigenschaften für die klinische Routine von ^{18}F verglichen mit ^{11}C verbindet.

Die Ergebnisse von [^{18}F]MHMZ rechtfertigenden weitere Experimente, um diesen Liganden für die klinische Routine am Menschen nutzbar zu machen.

9 REFERENCES

Adams, K. H., L. H. Pinborg, et al. (2004). "A database of [(18)F]-altanserin binding to 5-HT(2A) receptors in normal volunteers: normative data and relationship to physiological and demographic variables." Neuroimage **21**(3): 1105-13.

Alexoff, D. L., C. Shea, et al. (1995). "Plasma input function determination for PET using a commercial laboratory robot." Nucl Med Biol **22**(7): 893-904.

Alhaider, A. A., A. M. Ageel, et al. (1993). "The quipazine- and TFMPP-increased conditioned avoidance response in rats: role of 5HT1C/5-HT2 receptors." Neuropharmacology **32**(12): 1427-32.

Atack, J. R., P. Scott-Stevens, et al. (2007). "Comparison of Lorazepam [7-Chloro-5-(2-chlorophenyl)-1,3-dihydro-3-hydroxy-2H-1,4-benzodiazepin-2- one] Occupancy of Rat Brain {gamma}-Aminobutyric AcidA Receptors Measured Using in Vivo [3H]Flumazenil (8-Fluoro 5,6-dihydro-5-methyl-6-oxo-4H-imidazo[1,5-a][1,4]benzodiazepine-3-carboxyl ic Acid Ethyl Ester) Binding and [11C]Flumazenil Micro-Positron Emission Tomography." J Pharmacol Exp Ther **320**(3): 1030-7.

Atack, J. R., K. A. Wafford, et al. (2006). "TPA023 [7-(1,1-dimethylethyl)-6-(2-ethyl-2H-1,2,4-triazol-3-ylmethoxy)-3-(2-fluor ophenyl)-1,2,4-triazolo[4,3-b]pyridazine], an agonist selective for alpha2- and alpha3-containing GABAA receptors, is a nonsedating anxiolytic in rodents and primates." J Pharmacol Exp Ther **316**(1): 410-22.

Bantick, R. A., J. F. Deakin, et al. (2001). "The 5-HT1A receptor in schizophrenia: a promising target for novel atypical neuroleptics?" J Psychopharmacol **15**(1): 37-46.

Barnard, E. A., P. Skolnick, et al. (1998). "International Union of Pharmacology. XV. Subtypes of gamma-aminobutyric acidA receptors: classification on the basis of subunit structure and receptor function." Pharmacol Rev **50**(2): 291-313.

Barnes, N. M. and T. Sharp (1999). "A review of central 5-HT receptors and their function." Neuropharmacology **38**(8): 1083-152.

Benke, D., S. Mertens, et al. (1991). "GABAA receptors display association of gamma 2-subunit with alpha 1- and beta 2/3-subunits." J Biol Chem **266**(7): 4478-83.

Berezhnoy, D., Y. Nyfeler, et al. (2004). "On the benzodiazepine binding pocket in GABAA receptors." J Biol Chem **279**(5): 3160-8.

Bhagwagar, Z., R. Hinz, et al. (2006). "Increased 5-HT(2A) receptor binding in euthymic, medication-free patients recovered from depression: a positron emission study with [(11)C]MDL 100,907." Am J Psychiatry **163**(9): 1580-7.

Biver, F., F. Lotstra, et al. (1997). "In vivo binding of [18F]altanserin to rat brain 5HT2 receptors: a film and electronic autoradiographic study." Nucl Med Biol **24**(4): 357-60.

Biver, F., D. Wikler, et al. (1997). "Serotonin 5-HT2 receptor imaging in major depression: focal changes in orbito-insular cortex." Br J Psychiatry **171**: 444-8.

Bloomfield, P. M., S. Rajeswaran, et al. (1995). "The design and physical characteristics of a small animal positron emission tomograph." Phys Med Biol **40**(6): 1105-26.

Bohme, I., H. Rabe, et al. (2004). "Four amino acids in the alpha subunits determine the gamma-aminobutyric acid sensitivities of GABAA receptor subtypes." J Biol Chem **279**(34): 35193-200.

Bradford, M. (1976). Anal. Biochem.(248): 72.

Campos, M. L., C. de Cabo, et al. (2001). "Expression of GABA(A) receptor subunits in rat brainstem auditory pathways: cochlear nuclei, superior olivary complex and nucleus of the lateral lemniscus." Neuroscience **102**(3): 625-38.

Carling, R. W., A. Madin, et al. (2005). "7-(1,1-Dimethylethyl)-6-(2-ethyl-2H-1,2,4-triazol-3-ylmethoxy)-3-(2-fluoro phenyl)-1,2,4-triazolo[4,3-b]pyridazine: a functionally selective gamma-aminobutyric acid(A) (GABA(A)) alpha2/alpha3-subtype selective agonist that exhibits potent anxiolytic activity but is not sedating in animal models." J Med Chem **48**(23): 7089-92.

Carter, D. B., D. R. Thomsen, et al. (1992). "Functional expression of GABAA chloride channels and benzodiazepine binding sites in baculovirus infected insect cells." Biotechnology (N Y) **10**(6): 679-81.

Chambers, M. S., J. R. Atack, et al. (2002). "6,7-Dihydro-2-benzothiophen-4(5H)-ones: a novel class of GABA-A alpha5 receptor inverse agonists." J Med Chem **45**(6): 1176-9.

Chambers, M. S., J. R. Atack, et al. (2003). "Identification of a novel, selective GABA(A) alpha5 receptor inverse agonist which enhances cognition." J Med Chem **46**(11): 2227-40.

Chambers, M. S., J. R. Atack, et al. (2004). "An orally bioavailable, functionally selective inverse agonist at the benzodiazepine site of GABAA alpha5 receptors with cognition enhancing properties." J Med Chem **47**(24): 5829-32.

Cheng, Y. and W. H. Prusoff (1973). "Relationship between the inhibition constant (K1) and the concentration of inhibitor which causes 50 per cent inhibition (I50) of an enzymatic reaction." Biochem Pharmacol **22**(23): 3099-108.

Cohen, R. M. (2007). "The application of positron-emitting molecular imaging tracers in Alzheimer's disease." Mol Imaging Biol **9**(4): 204-16.

Collinson, N., J. R. Atack, et al. (2006). "An inverse agonist selective for alpha5 subunit-containing GABA(A) receptors improves encoding and recall but not consolidation in the Morris water maze." Psychopharmacology (Berl) **188**(4): 619-28.

Collinson, N., F. M. Kuenzi, et al. (2002). "Enhanced learning and memory and altered GABAergic synaptic transmission in mice lacking the alpha 5 subunit of the GABAA receptor." J Neurosci **22**(13): 5572-80.

Compton, S. J. and C. G. Jones (1985). Anal. Biochem.(369): 151.

Cook, J. B., K. L. Foster, et al. (2005). "Selective GABAA alpha5 benzodiazepine inverse agonist antagonizes the neurobehavioral actions of alcohol." Alcohol Clin Exp Res **29**(8): 1390-401.

Dawson, G. R., N. Collinson, et al. (2005). "Development of subtype selective GABAA modulators." CNS Spectr **10**(1): 21-7.

Dawson, G. R., K. A. Maubach, et al. (2006). "An inverse agonist selective for alpha5 subunit-containing GABAA receptors enhances cognition." J Pharmacol Exp Ther **316**(3): 1335-45.

Delong, R. (2007). "GABA(A) receptor alpha5 subunit as a candidate gene for autism and bipolar disorder: a proposed endophenotype with parent-of-origin and gain-

of-function features,with or without oculocutaneous albinism." Autism **11**(2): 135-47.

Ernst, M., D. Brauchart, et al. (2003). "Comparative modeling of GABA(A) receptors: limits, insights, future developments." Neuroscience **119**(4): 933-43.

Erspamer, V. and B. Asero (1952). "Identification of enteramine, the specific hormone of the enterochromaffin cell system, as 5-hydroxytryptamine." Nature **169**(4306): 800-1.

Fazakes de St. Groth, S. e. a. (1963). Biochim. Biophys. Acta(377): 71.

Fradley, R., M. Guscott, et al. (2007). "Differential contribution of GABAA receptor subtypes to the anticonvulsant efficacy of benzodiazepine site ligands." J Psychopharmacol.

Fritschy, J. M. and H. Mohler (1995). "GABAA-receptor heterogeneity in the adult rat brain: differential regional and cellular distribution of seven major subunits." J Comp Neurol **359**(1): 154-94.

Gaddum, J. H. and K. A. Hameed (1954). "Drugs which antagonize 5-hydroxytryptamine." Br J Pharmacol Chemother **9**(2): 240-8.

Gartside, S. E., E. Hajos-Korcsok, et al. (2000). "Neurochemical and electrophysiological studies on the functional significance of burst firing in serotonergic neurons." Neuroscience **98**(2): 295-300.

Gray, J. A. and B. Roth (2007). Serotonin Systems. Handbook of Contemporary Neuropharmacology. D. R. Sibley, I. Hanin, M. Kuhar and P. Skolnick, John Wiley & Sons, Inc.**:** 257-297.

Grunder, G., T. Siessmeier, et al. (2001). "[18F]Fluoroethylflumazenil: a novel tracer for PET imaging of human benzodiazepine receptors." Eur J Nucl Med **28**(10): 1463-70.

Guerrini, G., G. Ciciani, et al. (2007). "Novel 3-iodo-8-ethoxypyrazolo[5,1-c][1,2,4]benzotriazine 5-oxide as promising lead for design of alpha5-inverse agonist useful tools for therapy of mnemonic damage." Bioorg Med Chem **15**(7): 2573-86.

Gunn, R. N., S. R. Gunn, et al. (2001). "Positron emission tomography compartmental models." J Cereb Blood Flow Metab **21**(6): 635-52.

Gunn, R. N., A. A. Lammertsma, et al. (1997). "Parametric imaging of ligand-receptor binding in PET using a simplified reference region model." Neuroimage **6**(4): 279-87.

Gunnersen, D., C. M. Kaufman, et al. (1996). "Pharmacological properties of recombinant "diazepam-insensitive" GABAA receptors." Neuropharmacology **35**(9-10): 1307-14.

Hadingham, K. L., P. B. Wingrove, et al. (1993). "Role of the beta subunit in determining the pharmacology of human gamma-aminobutyric acid type A receptors." Mol Pharmacol **44**(6): 1211-8.

Hamacher, K. and H. H. Coenen (2006). "No-carrier-added nucleophilic 18F-labelling in an electrochemical cell exemplified by the routine production of [18F]altanserin." Appl Radiat Isot **64**(9): 989-94.

Harvey, J. A. (2003). "Role of the serotonin 5-HT(2A) receptor in learning." Learn Mem **10**(5): 355-62.

Haugbol, S., L. H. Pinborg, et al. (2007). "Reproducibility of 5-HT(2A) receptor measurements and sample size estimations with [(18)F]altanserin PET using a bolus/infusion approach." Eur J Nucl Med Mol Imaging **34**(6): 910-915.

Heinrich, T., H. Bottcher, et al. (2006). "1-(1-phenethylpiperidin-4-yl)-1-phenylethanols as potent and highly selective 5-HT2A antagonists." ChemMedChem **1**(2): 245-55.

Hensman, R., F. S. Guimaraes, et al. (1991). "Effects of ritanserin on aversive classical conditioning in humans." Psychopharmacology (Berl) **104**(2): 220-4.

Herth, M. M., F. Debus, et al. (2008). "Total synthesis and evaluation of [18F]MHMZ." Bioorg Med Chem Lett **18**(4): 1515-9.

Hevers, W. and H. Luddens (1998). "The diversity of GABAA receptors. Pharmacological and electrophysiological properties of GABAA channel subtypes." Mol Neurobiol **18**(1): 35-86.

Hinz, R., Z. Bhagwagar, et al. (2007). "Validation of a tracer kinetic model for the quantification of 5-HT(2A) receptors in human brain with [(11)C]MDL 100,907." J Cereb Blood Flow Metab **27**(1): 161-72.

Hirani, E., T. Sharp, et al. (2003). "Fenfluramine evokes 5-HT2A receptor-mediated responses but does not displace [11C]MDL 100907: small animal PET and gene expression studies." Synapse **50**(3): 251-60.

Hjorth, S., H. J. Bengtsson, et al. (2000). "Serotonin autoreceptor function and antidepressant drug action." J Psychopharmacol **14**(2): 177-85.

Houser, C. R. and M. Esclapez (2003). "Downregulation of the alpha5 subunit of the GABA(A) receptor in the pilocarpine model of temporal lobe epilepsy." Hippocampus **13**(5): 633-45.

Howell, O., J. R. Atack, et al. (2000). "Density and pharmacology of alpha5 subunit-containing GABA(A) receptors are preserved in hippocampus of Alzheimer's disease patients." Neuroscience **98**(4): 669-75.

Hurlemann, R., A. Matusch, et al. (2007). "5-HT(2A) receptor density is decreased in the at-risk mental state." Psychopharmacology (Berl).

Inoue, H., H. Nojima, et al. (1990). "High efficiency transformation of Escherichia coli with plasmids." Gene **96**(1): 23-8.

Ito, H., S. Nyberg, et al. (1998). "PET imaging of central 5-HT2A receptors with carbon-11-MDL 100,907." J Nucl Med **39**(1): 208-14.

Jacobs, B. L. and E. C. Azmitia (1992). "Structure and function of the brain serotonin system." Physiol Rev **72**(1): 165-229.

Kakiuchi, T., S. Nishiyama, et al. (2000). "Age-related reduction of [11C]MDL100,907 binding to central 5-HT(2A) receptors: PET study in the conscious monkey brain." Brain Res **883**(1): 135-42.

Kobayashi, M., M. Ohno, et al. (1995). "Concurrent blockade of beta-adrenergic and muscarinic receptors disrupts working memory but not reference memory in rats." Physiol Behav **58**(2): 307-14.

Kristiansen, H., B. Elfving, et al. (2005). "Binding characteristics of the 5-HT2A receptor antagonists altanserin and MDL 100907." Synapse **58**(4): 249-57.

Lammertsma, A. A., C. J. Bench, et al. (1996). "Comparison of methods for analysis of clinical [11C]raclopride studies." J Cereb Blood Flow Metab **16**(1): 42-52.

Lammertsma, A. A., C. J. Bench, et al. (1991). "Measurement of cerebral monoamine oxidase B activity using L-[11C]deprenyl and dynamic positron emission tomography." J Cereb Blood Flow Metab **11**(4): 545-56.

Lammertsma, A. A. and S. P. Hume (1996). "Simplified reference tissue model for PET receptor studies." Neuroimage **4**(3 Pt 1): 153-8.

Laurie, D. J., P. H. Seeburg, et al. (1992). "The distribution of 13 GABAA receptor subunit mRNAs in the rat brain. II. Olfactory bulb and cerebellum." J Neurosci **12**(3): 1063-76.

Lemaire, C., R. Cantineau, et al. (1991). "Fluorine-18-altanserin: a radioligand for the study of serotonin receptors with PET: radiolabeling and in vivo biologic behavior in rats." J Nucl Med **32**(12): 2266-72.

Lingford-Hughes, A., S. P. Hume, et al. (2002). "Imaging the GABA-benzodiazepine receptor subtype containing the alpha5-subunit in vivo with [11C]Ro15 4513 positron emission tomography." J Cereb Blood Flow Metab **22**(7): 878-89.

Logan, J., J. S. Fowler, et al. (1996). "Distribution volume ratios without blood sampling from graphical analysis of PET data." J Cereb Blood Flow Metab **16**(5): 834-40.

Lopez-Gimenez, J. F., G. Mengod, et al. (1997). "Selective visualization of rat brain 5-HT2A receptors by autoradiography with [3H]MDL 100,907." Naunyn Schmiedebergs Arch Pharmacol **356**(4): 446-54.

Luddens, H., I. Killisch, et al. (1991). "More than one alpha variant may exist in a GABAA/benzodiazepine receptor complex." J Recept Res **11**(1-4): 535-51.

Luddens, H. and E. Korpi (2007). Benzodiazepines. Handbook of Contemporary Neuropharmacology. D. R. Sibley, I. Hanin, M. Kuhar and P. Skolnick, John Wiley & Sons, Inc. **2:** 93-131.

Luddens, H. and E. R. Korpi (1995). "Biological function of GABAA/benzodiazepine receptor heterogeneity." J Psychiatr Res **29**(2): 77-94.

Luddens, H. and E. R. Korpi (1995). "GABA antagonists differentiate between recombinant GABAA/benzodiazepine receptor subtypes." J Neurosci **15**(10): 6957-62.

Luddens, H. and E. R. Korpi (1997). "Methods for transient expression of hetero-oligomeric ligand-gated ion channels." Methods Mol Biol **83**: 55-63.

Luddens, H., E. R. Korpi, et al. (1995). "GABAA/benzodiazepine receptor heterogeneity: neurophysiological implications." Neuropharmacology **34**(3): 245-54.

Luddens, H., P. H. Seeburg, et al. (1994). "Impact of beta and gamma variants on ligand-binding properties of gamma-aminobutyric acid type A receptors." Mol Pharmacol **45**(5): 810-4.

Lundkvist, C., C. Halldin, et al. (1996). "[11C]MDL 100907, a radioligland for selective imaging of 5-HT(2A) receptors with positron emission tomography." Life Sci **58**(10): PL 187-92.

Ma, T. C. and Q. H. Yu (1993). "Effect of 20(S)-ginsenoside-Rg2 and cyproheptadine on two-way active avoidance learning and memory in rats." Arzneimittelforschung **43**(10): 1049-52.

Maeda, J., T. Suhara, et al. (2003). "Visualization of alpha5 subunit of GABAA/benzodiazepine receptor by 11C Ro15-4513 using positron emission tomography." Synapse **47**(3): 200-8.

Massou, J. M., C. Trichard, et al. (1997). "Frontal 5-HT2A receptors studied in depressive patients during chronic treatment by selective serotonin reuptake inhibitors." Psychopharmacology (Berl) **133**(1): 99-101.

Maubach, K. (2003). "GABA(A) receptor subtype selective cognition enhancers." Curr Drug Targets CNS Neurol Disord **2**(4): 233-9.

McKay, P. F., K. L. Foster, et al. (2004). "A high affinity ligand for GABAA-receptor containing alpha5 subunit antagonizes ethanol's neurobehavioral effects in Long-Evans rats." Psychopharmacology (Berl) **172**(4): 455-62.

McKernan, R. M., K. Quirk, et al. (1991). "GABAA receptor subtypes immunopurified from rat brain with alpha subunit-specific antibodies have unique pharmacological properties." Neuron **7**(4): 667-76.

McKernan, R. M., T. W. Rosahl, et al. (2000). "Sedative but not anxiolytic properties of benzodiazepines are mediated by the GABA(A) receptor alpha1 subtype." Nat Neurosci **3**(6): 587-92.

Meltzer, C. C., J. C. Price, et al. (1999). "PET imaging of serotonin type 2A receptors in late-life neuropsychiatric disorders." Am J Psychiatry **156**(12): 1871-8.

Meltzer, C. C., G. Smith, et al. (1998). "Serotonin in aging, late-life depression, and Alzheimer's disease: the emerging role of functional imaging." Neuropsychopharmacology **18**(6): 407-30.

Meltzer, C. C., G. Smith, et al. (1998). "Reduced binding of [18F]altanserin to serotonin type 2A receptors in aging: persistence of effect after partial volume correction." Brain Res **813**(1): 167-71.

Meltzer, H. Y., S. Matsubara, et al. (1989). "Classification of typical and atypical antipsychotic drugs on the basis of dopamine D-1, D-2 and serotonin2 pKi values." J Pharmacol Exp Ther **251**(1): 238-46.

Messa, C., C. Colombo, et al. (2003). "5-HT(2A) receptor binding is reduced in drug-naive and unchanged in SSRI-responder depressed patients compared to healthy controls: a PET study." Psychopharmacology (Berl) **167**(1): 72-8.

Meyer, J. H. and M. Ichise (2001). "Modeling of receptor ligand data in PET and SPECT imaging: a review of major approaches." J Neuroimaging **11**(1): 30-9.

Meyer, J. H., S. Kapur, et al. (2001). "The effect of paroxetine on 5-HT(2A) receptors in depression: an [(18)F]setoperone PET imaging study." Am J Psychiatry **158**(1): 78-85.

Mitterhauser, M., W. Wadsak, et al. (2004). "Biological evaluation of 2'-[18F]fluoroflumazenil ([18F]FFMZ), a potential GABA receptor ligand for PET." Nucl Med Biol **31**(2): 291-5.

Mohler, H., F. Knoflach, et al. (1995). "Heterogeneity of GABAA-receptors: cell-specific expression, pharmacology, and regulation." Neurochem Res **20**(5): 631-6.

Myers, R. (2001). "The biological application of small animal PET imaging." Nucl Med Biol **28**(5): 585-93.

Nanni, C., D. Rubello, et al. (2007). "Role of small animal PET for molecular imaging in pre-clinical studies." Eur J Nucl Med Mol Imaging **34**(11): 1819-22.

Neher, E., B. Sakmann, et al. (1978). "The extracellular patch clamp: a method for resolving currents through individual open channels in biological membranes." Pflugers Arch **375**(2): 219-28.

O'Connor, D., P. Jones, et al. (2006). "Aldehyde oxidase and its contribution to the metabolism of a structurally novel, functionally selective GABAA alpha5-subtype inverse agonist." Xenobiotica **36**(4): 315-30.

Opacka-Juffry, J., E. Hirani, et al. (1999). "Evaluation of [methyl-3H]L655,708 and [ethyl-3H]RY80 as putative PET ligands for central GABA(A) receptors containing alpha5 subunit." Nucl Med Biol **26**(7): 743-8.

Otani, K., H. Ujike, et al. (2005). "The GABA type A receptor alpha5 subunit gene is associated with bipolar I disorder." Neurosci Lett **381**(1-2): 108-13.

Papadimitriou, G. N., D. G. Dikeos, et al. (2001). "GABA-A receptor beta3 and alpha5 subunit gene cluster on chromosome 15q11-q13 and bipolar disorder: a genetic association study." Am J Med Genet **105**(4): 317-20.

Papadimitriou, G. N., D. G. Dikeos, et al. (1998). "Association between the GABA(A) receptor alpha5 subunit gene locus (GABRA5) and bipolar affective disorder." Am J Med Genet **81**(1): 73-80.

Pazos, A., R. Cortes, et al. (1985). "Quantitative autoradiographic mapping of serotonin receptors in the rat brain. II. Serotonin-2 receptors." Brain Res **346**(2): 231-49.

Pazos, A. and J. M. Palacios (1985). "Quantitative autoradiographic mapping of serotonin receptors in the rat brain. I. Serotonin-1 receptors." Brain Res **346**(2): 205-30.

Pazos, A., A. Probst, et al. (1987). "Serotonin receptors in the human brain--IV. Autoradiographic mapping of serotonin-2 receptors." Neuroscience **21**(1): 123-39.

Persson, A., E. Ehrin, et al. (1985). "Imaging of [11C]-labelled Ro 15-1788 binding to benzodiazepine receptors in the human brain by positron emission tomography." J Psychiatr Res **19**(4): 609-22.

Phelps, M. E. e. (2004). PET: molecular imaging and its biological applications. New York, Springer-Verlag, Inc.

Pinborg, L. H., K. H. Adams, et al. (2003). "Quantification of 5-HT2A receptors in the human brain using [18F]altanserin-PET and the bolus/infusion approach." J Cereb Blood Flow Metab **23**(8): 985-96.

Pinborg, L. H., K. H. Adams, et al. (2004). "[18F]altanserin binding to human 5HT2A receptors is unaltered after citalopram and pindolol challenge." J Cereb Blood Flow Metab **24**(9): 1037-45.

Pineyro, G. and P. Blier (1999). "Autoregulation of serotonin neurons: role in antidepressant drug action." Pharmacol Rev **51**(3): 533-91.

Ping-Zhong Tan, R. M. B. T. F. D. S. C. R. B. I. (1999). "Rapid synthesis of F-18 and H-2 dual-labeled altanserin, a metabolically resistant PET ligand for 5-HT_{<FONT SIZE='-1'>2a</FONT>} receptors." Journal of Labelled Compounds and Radiopharmaceuticals **42**(5): 457-467.

Pirker, S., C. Schwarzer, et al. (2000). "GABA(A) receptors: immunocytochemical distribution of 13 subunits in the adult rat brain." Neuroscience **101**(4): 815-50.

Poulter, M. O., L. A. Brown, et al. (1999). "Differential expression of alpha1, alpha2, alpha3, and alpha5 GABAA receptor subunits in seizure-prone and seizure-resistant rat models of temporal lobe epilepsy." J Neurosci **19**(11): 4654-61.

Pritchett, D. B., H. Luddens, et al. (1989). "Type I and type II GABAA-benzodiazepine receptors produced in transfected cells." Science **245**(4924): 1389-92.

Pritchett, D. B. and P. H. Seeburg (1990). "Gamma-aminobutyric acidA receptor alpha 5-subunit creates novel type II benzodiazepine receptor pharmacology." J Neurochem **54**(5): 1802-4.

Pritchett, D. B., H. Sontheimer, et al. (1989). "Importance of a novel GABAA receptor subunit for benzodiazepine pharmacology." Nature **338**(6216): 582-5.

Quirk, K., P. Blurton, et al. (1996). "[3H]L-655,708, a novel ligand selective for the benzodiazepine site of GABAA receptors which contain the alpha 5 subunit." Neuropharmacology **35**(9-10): 1331-5.

Quirk, K., N. P. Gillard, et al. (1994). "gamma-Aminobutyric acid type A receptors in the rat brain can contain both gamma 2 and gamma 3 subunits, but gamma 1 does

not exist in combination with another gamma subunit." Mol Pharmacol **45**(6): 1061-70.

Rapport, M. M. (1949). "Serum vasoconstrictor (serotonin) the presence of creatinine in the complex; a proposed structure of the vasoconstrictor principle." J Biol Chem **180**(3): 961-9.

Reisner, A. H., P. Nemes, et al. (1975). Anal. Biochem.(509): 64.

Rudolph, U., F. Crestani, et al. (1999). "Benzodiazepine actions mediated by specific gamma-aminobutyric acid(A) receptor subtypes." Nature **401**(6755): 796-800.

Rudolph, U. and H. Mohler (2006). "GABA-based therapeutic approaches: GABAA receptor subtype functions." Curr Opin Pharmacol **6**(1): 18-23.

Sander, T., R. Kretz, et al. (1997). "Linkage analysis between idiopathic generalized epilepsies and the GABA(A) receptor alpha5, beta3 and gamma3 subunit gene cluster on chromosome 15." Acta Neurol Scand **96**(1): 1-7.

Saxena, P. R., P. De Vries, et al. (1998). "5-HT1-like receptors: a time to bid goodbye." Trends Pharmacol Sci **19**(8): 311-6.

Schaefer-Prokop, C. M. and M. Prokop (1997). "Storage phosphor radiography." Eur Radiol **7 Suppl 3**: S58-65.

Schmidt, K. C. and F. E. Turkheimer (2002). "Kinetic modeling in positron emission tomography." Q J Nucl Med **46**(1): 70-85.

Scott, D. O. and T. G. Heath (1998). "Investigation of the CNS penetration of a potent 5-HT2a receptor antagonist (MDL 100,907) and an active metabolite (MDL 105,725) using in vivo microdialysis sampling in the rat." J Pharm Biomed Anal **17**(1): 17-25.

Sedmack, J. J. and S. E. Grossberg (1977). Anal. Biochem.(544): 79.

Seeburg, P. H., W. Wisden, et al. (1990). "The GABAA receptor family: molecular and functional diversity." Cold Spring Harb Symp Quant Biol **55**: 29-40.

Sheline, Y. I., M. A. Mintun, et al. (2004). "Decreased hippocampal 5-HT(2A) receptor binding in older depressed patients using [18F]altanserin positron emission tomography." Neuropsychopharmacology **29**(12): 2235-41.

Sheline, Y. I., M. A. Mintun, et al. (2002). "Greater loss of 5-HT(2A) receptors in midlife than in late life." Am J Psychiatry **159**(3): 430-5.

Shih, J. C., K. Chen, et al. (1999). "Monoamine oxidase: from genes to behavior." Annu Rev Neurosci **22**: 197-217.

Sieghart, W. (1995). "Structure and pharmacology of gamma-aminobutyric acidA receptor subtypes." Pharmacol Rev **47**(2): 181-234.

Sieghart, W., K. Fuchs, et al. (1999). "Structure and subunit composition of GABA(A) receptors." Neurochem Int **34**(5): 379-85.

Sieghart, W. and G. Sperk (2002). "Subunit composition, distribution and function of GABA(A) receptor subtypes." Curr Top Med Chem **2**(8): 795-816.

Smith, G. S., J. C. Price, et al. (1998). "Test-retest variability of serotonin 5-HT2A receptor binding measured with positron emission tomography and [18F]altanserin in the human brain." Synapse **30**(4): 380-92.

Spector, T. (1978). Anal. Biochem.(142): 86.

Sperk, G., C. Schwarzer, et al. (1997). "GABA(A) receptor subunits in the rat hippocampus I: immunocytochemical distribution of 13 subunits." Neuroscience **80**(4): 987-1000.

Staley, J. K., C. H. Van Dyck, et al. (2001). "Comparison of [(18)F]altanserin and [(18)F]deuteroaltanserin for PET imaging of serotonin(2A) receptors in baboon brain: pharmacological studies." Nucl Med Biol **28**(3): 271-9.

Stark, D., M. Piel, et al. (2007). "In vitro affinities of various halogenated benzamide derivatives as potential radioligands for non-invasive quantification of D(2)-like dopamine receptors." Bioorg Med Chem **15**(21): 6819-29.

Stephens, D. N., J. Pistovcakova, et al. (2005). "Role of GABA(A) alpha5-containing receptors in ethanol reward: The effects of targeted gene deletion, and a selective inverse agonist." Eur J Pharmacol **526**(1-3): 240-50.

Sternfeld, F., R. W. Carling, et al. (2004). "Selective, orally active gamma-aminobutyric acidA alpha5 receptor inverse agonists as cognition enhancers." J Med Chem **47**(9): 2176-9.

Street, L. J., F. Sternfeld, et al. (2004). "Synthesis and biological evaluation of 3-heterocyclyl-7,8,9,10-tetrahydro-(7,10-ethano)-1,2,4-triazolo[3,4-a]phth alazines and analogues as subtype-selective inverse agonists for the GABA(A)alpha5 benzodiazepine binding site." J Med Chem **47**(14): 3642-57.

Suhara, T., Y. Okubo, et al. (2002). "Decreased dopamine D2 receptor binding in the anterior cingulate cortex in schizophrenia." Arch Gen Psychiatry **59**(1): 25-30.

Suhara, T., F. Yasuno, et al. (2001). "Dopamine D2 receptors in the insular cortex and the personality trait of novelty seeking." Neuroimage **13**(5): 891-5.

Sur, C., L. Fresu, et al. (1999). "Autoradiographic localization of alpha5 subunit-containing GABAA receptors in rat brain." Brain Res **822**(1-2): 265-70.

Sur, C., K. Quirk, et al. (1998). "Rat and human hippocampal alpha5 subunit-containing gamma-aminobutyric AcidA receptors have alpha5 beta3 gamma2 pharmacological characteristics." Mol Pharmacol **54**(5): 928-33.

Szekeres, H. J., J. R. Atack, et al. (2004). "3,4-Dihydronaphthalen-1(2H)-ones: novel ligands for the benzodiazepine site of alpha5-containing GABAA receptors." Bioorg Med Chem Lett **14**(11): 2871-5.

Tai, Y. C., A. Ruangma, et al. (2005). "Performance evaluation of the microPET focus: a third-generation microPET scanner dedicated to animal imaging." J Nucl Med **46**(3): 455-63.

Titov, S. A., I. Shamakina, et al. (1983). "[Effect of lysyl vasopressin and vasotocin on a disorder of the conditioned avoidance reaction by a serotonin receptor blockader]." Biull Eksp Biol Med **95**(2): 31-3.

Togel, M., B. Mossier, et al. (1994). "gamma-Aminobutyric acidA receptors displaying association of gamma 3-subunits with beta 2/3 and different alpha-subunits exhibit unique pharmacological properties." J Biol Chem **269**(17): 12993-8.

Udo de Haes, J. I. (2005). In vivo imaging of dopamin and serotonin release: response to psychopharmacological challenges. Department of Psychiatry. Groningen, University of Groningen**:** 204.

van Dyck, C. H., J. C. Soares, et al. (2000). "Equilibrium modeling of 5-HT(2A) receptors with [18F]deuteroaltanserin and PET: feasibility of a constant infusion paradigm." Nucl Med Biol **27**(8): 715-22.

van Niel, M. B., K. Wilson, et al. (2005). "A new pyridazine series of GABAA alpha5 ligands." J Med Chem **48**(19): 6004-11.

Vitiello, B., A. Martin, et al. (1997). "Cognitive and behavioral effects of cholinergic, dopaminergic, and serotonergic blockade in humans." Neuropsychopharmacology **16**(1): 15-24.

Wainwright, A., D. J. Sirinathsinghji, et al. (2000). "Expression of GABA(A) receptor alpha5 subunit-like immunoreactivity in human hippocampus." Brain Res Mol Brain Res **80**(2): 228-32.

Watabe, H., M. A. Channing, et al. (2000). "Kinetic analysis of the 5-HT2A ligand [11C]MDL 100,907." J Cereb Blood Flow Metab **20**(6): 899-909.

Weible, A. P., M. D. McEchron, et al. (2000). "Cortical involvement in acquisition and extinction of trace eyeblink conditioning." Behav Neurosci **114**(6): 1058-67.

Whiting, P. J., T. P. Bonnert, et al. (1999). "Molecular and functional diversity of the expanding GABA-A receptor gene family." Ann N Y Acad Sci **868**: 645-53.

Williams, G. V., S. G. Rao, et al. (2002). "The physiological role of 5-HT2A receptors in working memory." J Neurosci **22**(7): 2843-54.

Willins, D. L., A. Y. Deutch, et al. (1997). "Serotonin 5-HT2A receptors are expressed on pyramidal cells and interneurons in the rat cortex." Synapse **27**(1): 79-82.

Wurtman, R. J., F. Hefti, et al. (1980). "Precursor control of neurotransmitter synthesis." Pharmacol Rev **32**(4): 315-35.

Yatham, L. N., P. F. Liddle, et al. (2001). "Effects of rapid tryptophan depletion on brain 5-HT(2) receptors: a PET study." Br J Psychiatry **178**: 448-53.

Yiyun Huang, K. M. C. A. M. (1999). "An efficient synthesis of the precursors of [11C]MDL 100907 labeled in two specific positions." Journal of Labelled Compounds and Radiopharmaceuticals **42**(10): 949-957.

Zhou, F. C., J. H. Tao-Cheng, et al. (1998). "Serotonin transporters are located on the axons beyond the synaptic junctions: anatomical and functional evidence." Brain Res **805**(1-2): 241-54.

10 Appendix

10.1 Materials, Buffers, Media, Software and Hardware

Table 10: Buffers and Media

Buffer	Experiment	Contents
DPBS (Cambrex Bio Science, Verviers, Belgium)	HEK cell culture maintenance	
Medium (MEM, Gibco, Invitrogen, Auckland, New Zealand)	HEK cell culture maintenance	MEM - medium + 10 % heat deactivated fetal calf serum (FCS, Gibco) 2 mM Penicillin/Streptomycin (Gibco) 2 mM Glutamin (Gibco) store at 4 °C
Cell Culture Salt Solution	HEK cell culture maintenance, cell dislodgement	40 mM Tris/HCl (dilute from 1 M stock solution), 1 mM EDTA, 250 mM NaCl, pH 7,4 NaOH
2,5 M $CaCl_2$*$2H_2O$	HEK cell transfection	2,5 M $CaCl_2$*$2H_2O$
2 x BBS	HEK cell transfection	50 mM BES, 280 mM NaCl, 1,5 mM Na_2HPO_4* $2H_2O$, pH 6,95-6,97 NaOH
10 mM TRIS/HCl pH 7,5	Binding assay	10 L, by dilution from 1 M stock solution
50 mM Tris/HCl pH 7,5 autoradiography buffer (1 L)	Autoradiography	50 ml 1M Tris/HCl buffer, 120 mM NaCl, fill to 1 L with deionized water
50 mM Tris/HCl pH 7,5 autoradiography buffer for [^{18}F]MHMZ experiments (1 L)	Autoradiography	50 ml 1 M Tris/HCl buffer, 120 mM NaCl, 5 mM KCl, fill to 1 L with deionized water
1 M TRIS/HCl pH 7,5	Binding assay, autoradiography	1 M TRIS base, concentrated hydrochloric acid, dionized water
1 M TRIS/Citrate pH 7,4	Binding assay, rat brain preparation, in vivo binding, receptor autoradiography	1 M TRIS base, citrate, pH 7,4
50 mM TRIS/Citrate pH 7,4	Binding assay, rat brain preparation, in vivo binding, receptor autoradiography	50 mM TRIS/Citrate pH 7,4, by dilution from 1 M stock solution
1,4 mg BSA solution	BSA standard curve, Bradford assay, BIORAD	1,4 mg bovine serum albumin (BSA)
100 x TE buffer	Molecular biology, DNA (plasmid) maxi preparation	1 M Tris/HCl, 0,1 M Na_2-EDTA, pH 7,5 with concentrated hydro-

		chloric acid
1 x TE buffer	Molecular biology, DNA (plasmid) maxi preparation	By dilution from 1 M stock solution
Terrific broth **a)**, **b)**	E.coli bacteria culture	**a)** 12 g Bacto-Trypton, 24 g Bacto-Yeast Extract, 4 ml glycerol, fill up to 900 mL with destilled water, **b)** 0,17 M KH_2PO_4, 0.72 M K_2HPO_4, shortly before using mix a) + b) and add antibiotic in desired concentration
TFB I	Competent bacteria	10 mM $CaCl_2$, 15 % (v/v) glycerin, 30 mM potassium acetate pH 5.8, 100 mM rubidium chloride, 50 mM mangan chloride
TFB II	competent bacteria	10 mM MOPS pH 7.0, 10 mM $RbCl_2$, 75 mM $CaCl_2$, 15 % (v/v) glycerin
LB medium	E.coli bacteria culture	dissolve in 1 L deionized water 10 g bacto-tryptone, 5 g bacto-yeast, 10 g NaCl, adjust pH to 7.0 with NaOH, sterilize by autoclaving
SOC medium	Bacteria culture	for 1 L dissolve 20 g Bacto-tryptone, 5 g Bacto-yeast, 0.5 g NaCl, 2.5 mL 1 M KCl, pH 7.0 with NaOH, sterilize and add 20 mL 1 M glucose before use
Solution I (glucose)	Plasmid maxi preparation	50 mM glucose (1 % w/v) in 25 mM Tris-HCl, pH 8.0, 1 mM EDTA (from 0.5 M EDTA, pH 8.0, stock solution)
Solution II (NaOH/SDS) (prepare fresh every time)	Plasmid maxi preparation	1 % SDS (Sodium-Dodecyl-Sulfate) (from 10 % SDS stock solution) in 0.2 M NaOH
Solution III (potassium acetate solution)	Plasmid maxi preparation	600 mL 5 M potassium solution with 115 mL pure acetic acid with 285 mL H_2O
CsCl-solution	Plasmid maxi preparation	90 g CsCl dissolve in 90 mL 1 x TE Puffer
Saltwater saturated Isopropanol	Plasmid maxi preparation	in a 500 mL bottle with screw top ~ 1 00 mL H_2O saturate with NaCl (until crystallization starts) ~ 300 mL add isopropanol and mix thoroughly, there should be visible three phases after ~ 30 min. fresh isopropanol can be added repeatedly

0,5M EDTA	Plasmid maxi preparation	84.06 g Na_2-EDTA dissolve in ~ 400 mL H_2O, adjust pH with 1 M NaOH to 8.0 and volume to 500 mL with deionized water, autoclave
Buffer P1 (resuspension buffer)	Plasmid maxi preparation, Qiagen Kit	50 mM Tris•Cl, pH 8.0, 10 mM EDTA, 100 µg/ml RNase A
Buffer P2 (lysis buffer)	Plasmid maxi preparation, Qiagen Kit	200 mM NaOH, 1 % (w/v) SDS
Buffer P3 (neutralization buffer)	Plasmid maxi preparation, Qiagen Kit	3 M potassium acetate, pH 5.5
Buffer FWB2 (QIAfilter wash buffer)	Plasmid maxi preparation, Qiagen Kit	1 M potassium acetate, pH 5.5
Buffer QBT (equilibration buffer)	Plasmid maxi preparation, Qiagen Kit	750 mM NaCl, 50 mM MOPS, pH 7.0, 15 % (v/v) isopropanol, 0.15 % (v/v) Triton® X-100
Buffer QC (wash buffer)	Plasmid maxi preparation, Qiagen Kit	1 M NaCl 50 mM, MOPS, pH 7,0, 15 % (v/v) isopropanol
Buffer QF (elution buffer)	Plasmid maxi preparation, Qiagen Kit	1.25 M NaCl, 50 mM Tris•Cl, pH 8.5, 15 % (v/v) isopropanol
Buffer QN (elution buffer)	Plasmid maxi preparation, Qiagen Kit	1.6 M NaCl, 50 mM MOPS, pH 7.0, 15% (v/v) isopropanol
STE buffer	Plasmid maxi preparation, Qiagen Kit	100 mM NaCl, 10 mM Tris•Cl, pH 8.0, 1 mM EDTA
Cell Resuspension Solution	Promega PureYield™ Plasmid Maxiprep System	50 mM Tris-HCl, pH 7.5, 10 mM EDTA, pH 8.0, 100 µg/mL RNase A
Cell Lysis Solution	Promega PureYield™ Plasmid Maxiprep System	0.2 M NaOH, 1% (w/v) SDS
Neutralization Solution	Promega PureYield™ Plasmid Maxiprep System	4.1 M guanidine hydrochloride, pH 4.8, 760 mM potassium acetate, 2.1 M glacial acetic acid
Column Wash	Promega PureYield™ Plasmid Maxiprep System	163 mM potassium acetate, 22.6 mM Tris-HCl, pH 7.5, 0.11 mM EDTA, pH 8.0
Bath Solution	Electrophysiology	135 mM NaCl, 5.3 mM KCl, 2 mM $MgSO_4$, 2 mM $CaCl_2$, 10 mM HEPES, pH 7.35 – 7.38
Intracellular Solution	Electrophysiology	10 mM NaCl, 80 mM KCl, 2 mM $MgCl_2$, 2 mM $CaCl_2$, 50 mM KOH, 10 mM EGTA, 10 mM HEPES, 3.1 mM ATP, 0.4 mM GTP

Table 11: Software

Word 2003, Microsoft Office XP, Microsoft Corporation
Excel 2003, Microsoft Office XP, Microsoft Corporation
CorelDraw Graphics Suite 12, Corel Corporation
Illustrator CS3, Adobe
Acrobat 8.0 Professional, Adobe
Photoshop CS3, Adobe
Origin 7.5, OriginLab, Inc.
HEKA PULSE, Version 8.77
Clampfit 8.1, Axon Instruments, Inc.
Prism 4, GraphPad Software, Inc.
ABF Utility 2.1.68, Justin Lee, Synaptosoft
Endnote 9.0, Thomson
ImageJ 1.33u, NIH, USA
ImageQuant 5.2, Molecular Dynamics, GE Healthcare
Activity
IDL Virtual Machine 6.0
ASIPro VM
Multigauge FujiFilm
Micro PET manager
MicroQ
MicroView
PMOD

Table 12: Hardware

hardware	type	Manufacturer
laminar airflow cabinet	SterilGard	The Baker Company, Sanford, Maine, USA
incubator	Stericult 200	Labotect Labortechnik, Göttin-gen, Germany

bacteria incubator	INP-500	Memmert GmbH + Co. KG, Schwabach, Germany
incubator shaker	Innova 4300	New Brunswick Scientific, Edison, USA
ultra turrax	T25	Jahnke & Kunkel, IKA Labortechnik, Staufen, Germany
microscope cell culture	IX 50	Olympus, Hamburg, Germany
microscope fluorescence	AX 70	Olympus, Hamburg, Germany
gel-documentation camera	Documentation System	Intas Science Imaging Instruments GmbH, Göttingen, Germany
ultraviolet lamp table	N90	Konrad Benda, Wiesloch, Germany
video printer	Mitsubishi P91	Mitsubishi Europe, Hatfield, UK
electrophoresis chamber	standard agarose gel electrophoresis chamber	Bio-Rad Laboratories GmbH, München, Germany
voltage generator	Power Pac 300	Bio-Rad Laboratories GmbH, München, Germany
vacuum concentrator	Bachofer Mini 30	Bachofer, Reutlingen, Germany
ultra centrifuge	Optima L70-K	Beckman, USA
centrifuge	Megafuge 1O-R	Heraeus, über Kendro, Langenselbold, Germany
centrifuge	RC 5B plus	Sorvall, über Kendro, Langenselbold, Germany
centrifuge	Biofuge 13	Heraeus, über Kendro, Langenselbold, Germany
ultraviolet lamp	254nm und 366nm lamp	Konrad Benda, Wiesloch, Germany
counter	LS 6000 SC	Beckman, USA
micro photometer	GeneQuant II	Pharmacia Biotech, Freiburg, Germany
nano drop photometer		
photometer	Lambda Bio UV/VIS Spectrometer	Perkin Elmer, Norwalk, USA
cooling cabinet (0°C)	Queue	Nunc, Wiesbaden, Germany
freezer (-20°C)	economic froster	Bosch, Stuttgart, Germany

freezer (-80°C)	Advantage	Nunc, Wiesbaden, Germany
microtome	Jung CM 3000	Leica, Nussloch, Germany
amplifier	EPC-9 PatchClamp	HEKA elektronik, Lambrecht, Germany
inverse microscope electro-physiol.	IX 70	Olympus, Hamburg, Germany
oscilloscope	SSI-2522, digital storage	Sampo, Taiwan
rotating valve	valco cheminert multiposition valve	Valco Instruments, Houston, Texas, USA
pipette puller	Model P-97, Flaming/Brown micro pipette puller	Sutter Instruments Co., USA
air cushioned table	IsoStationTM Vibration Isolated Workstation	Newport, Darmstadt, Germany
manipulator	Narishige MHW-3 & MX-2	Narishige Scientific Instrument Lab, Japan
applicator	SF77B	Warner Instruments, USA
silver wire	AG-5T	Science Products, Hofheim, Germany
microPET	microPET Focus 120	Siemens Medical Solutions USA, Inc., Malvern, USA
micro imager	µ IMAGER	Biospace, Paris, France
phosphor imager	Storm Scanner	Molecular Dynamics, now GE Healthcare, USA
phosphor imager	FLA-7000	FUJIFILM Europe GmbH, Düs-seldorf, Germany
cell harvester	M24 harvester	Brandel, Gaithersburg, USA
vacuum pump	standard membrane pump	z.B. KNF, Freiburg, Germany

Table 13: Other Materials

commercially available radioiso-topes	binding Assays, autoradio-graphies	[^{3}H]Ro15-4513, PerkinElmer, NEN, Boston, USA. Kat.nr. NET925250UC
commercially available radioiso-topes	binding Assays, autoradio-graphies	[^{3}H]Ro15-1788, PerkinElmer, NEN, Boston, USA. Kat.nr. NET757025UC

glass fiber filter paper	filtration binding assays	Schleicher & Schüll
Amersham Hyperfilm-^{3}H	receptor autoradiography	Amersham Biosciences, UK Limited, Buckinghamshire, England
liquid scintillator Aquasafe 300 Plus	binding assays	Zinsser Analytic, Frankfurt, Germany/Berks, UK
restriction Enzymes	restriction digest	New England Biolabs, USA
HEK 293 cells	binding Assay, electrophysiology	
raw borosilicate glass tubes	GB150F-10, 0.86 x 1.5 x 100 mm	Science Products, Hofheim, Germany
pap pen	autoradiography	Kisker Bioscience
imaging plate/phosphor screen	autoradiography	Fujifilm, Europe

10.2 $GABA_A$ Receptor Subunit Vectors

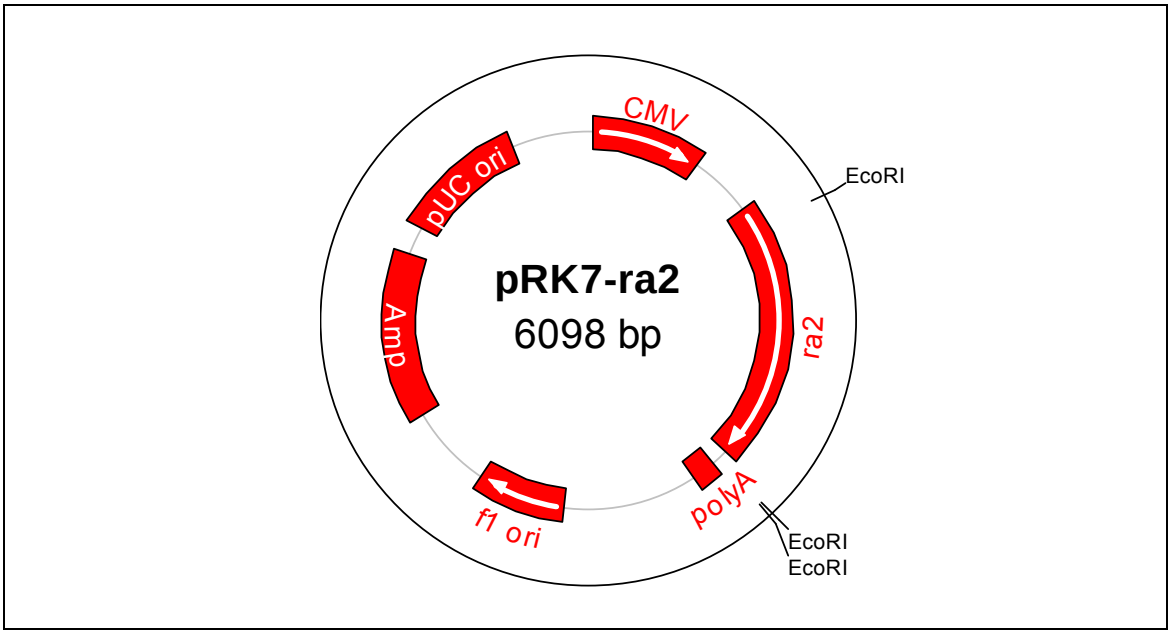

Figure 38: α2 vector

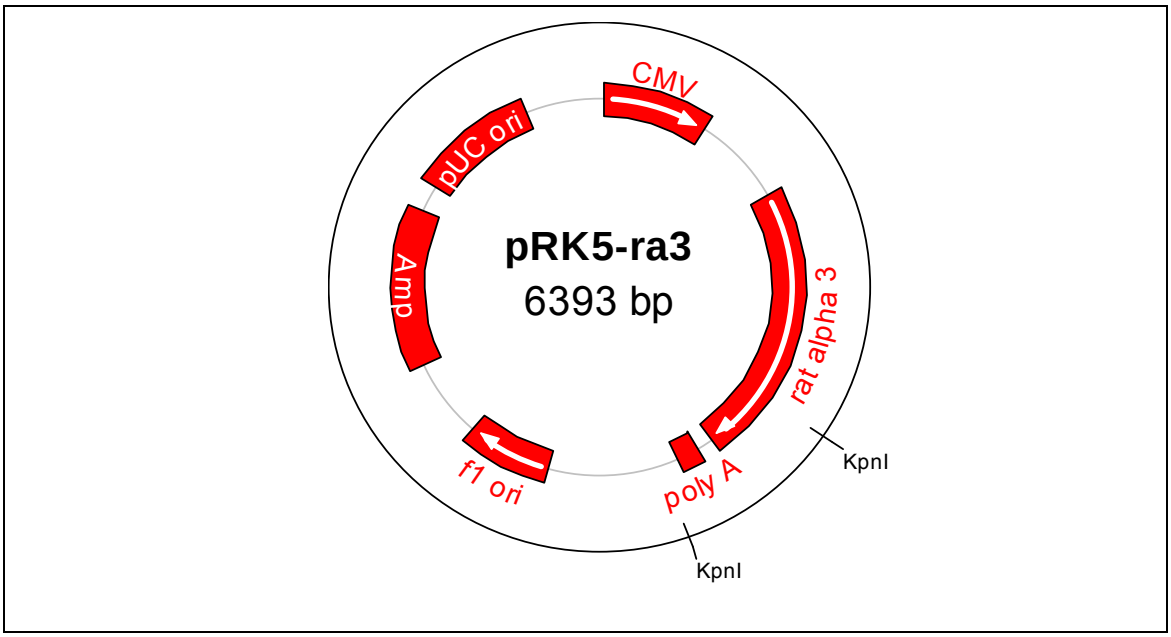

Figure 39: α3 vector

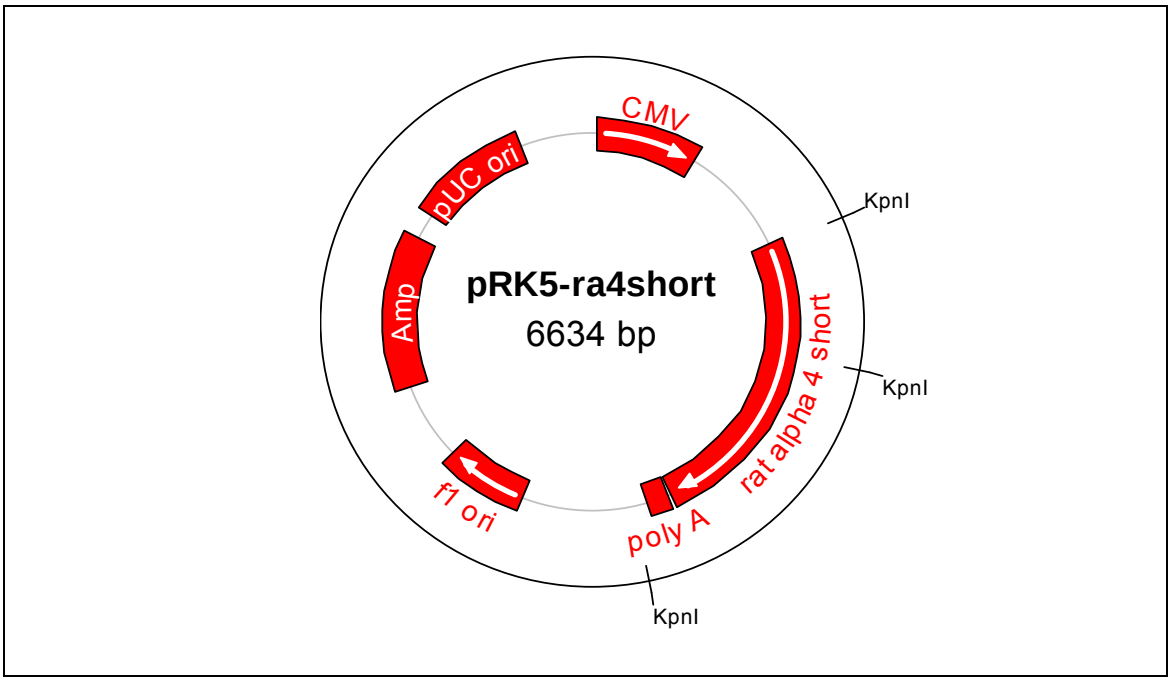

Figure 40: α4 vector

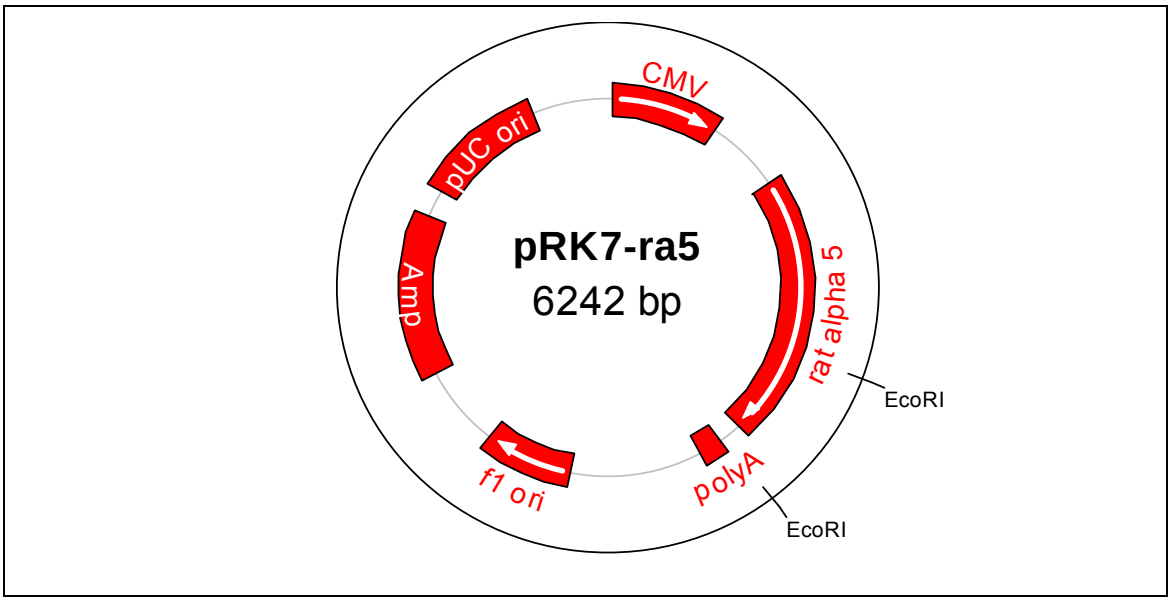

Figure 41: α5 vector

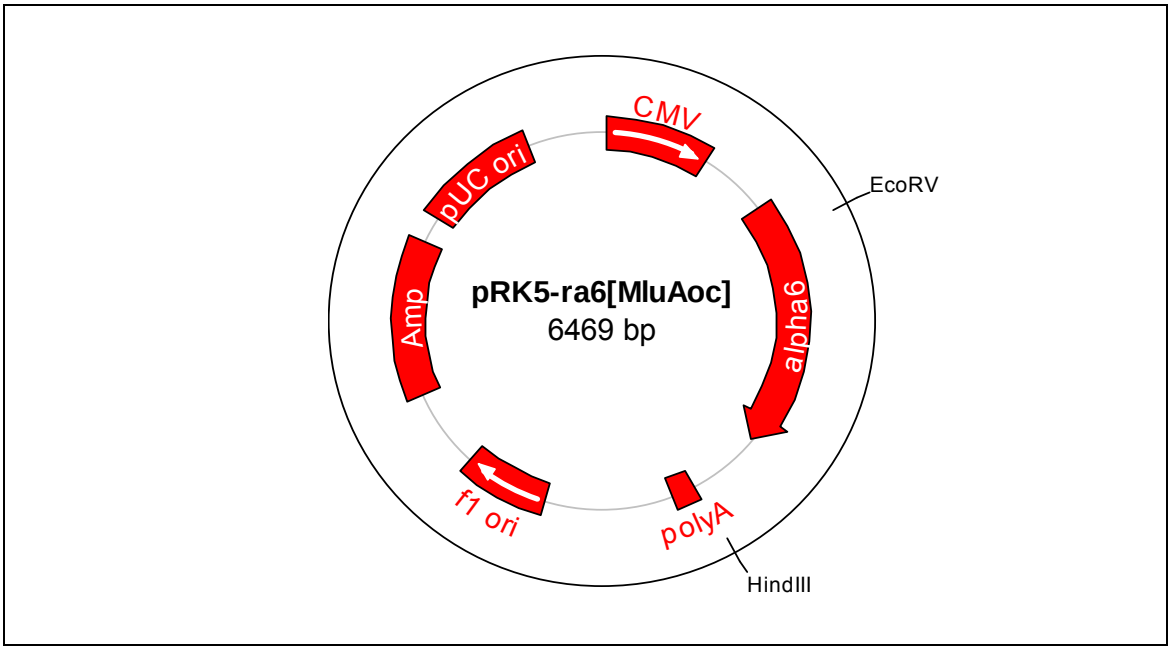

Figure 42: α6 vector

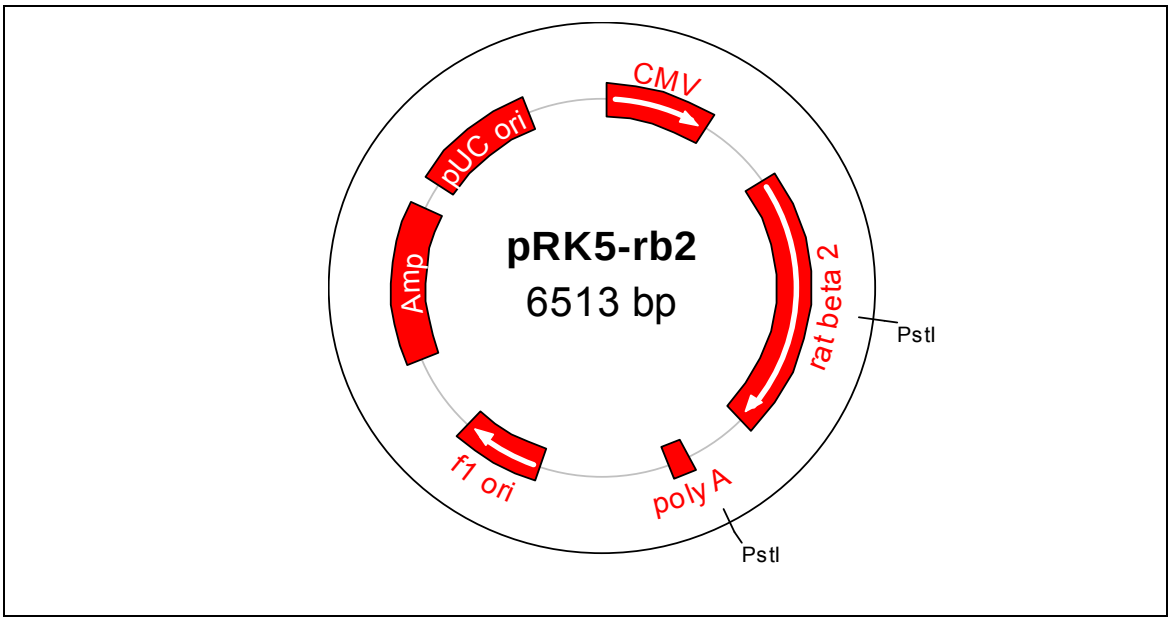

Figure 43: β2 vector

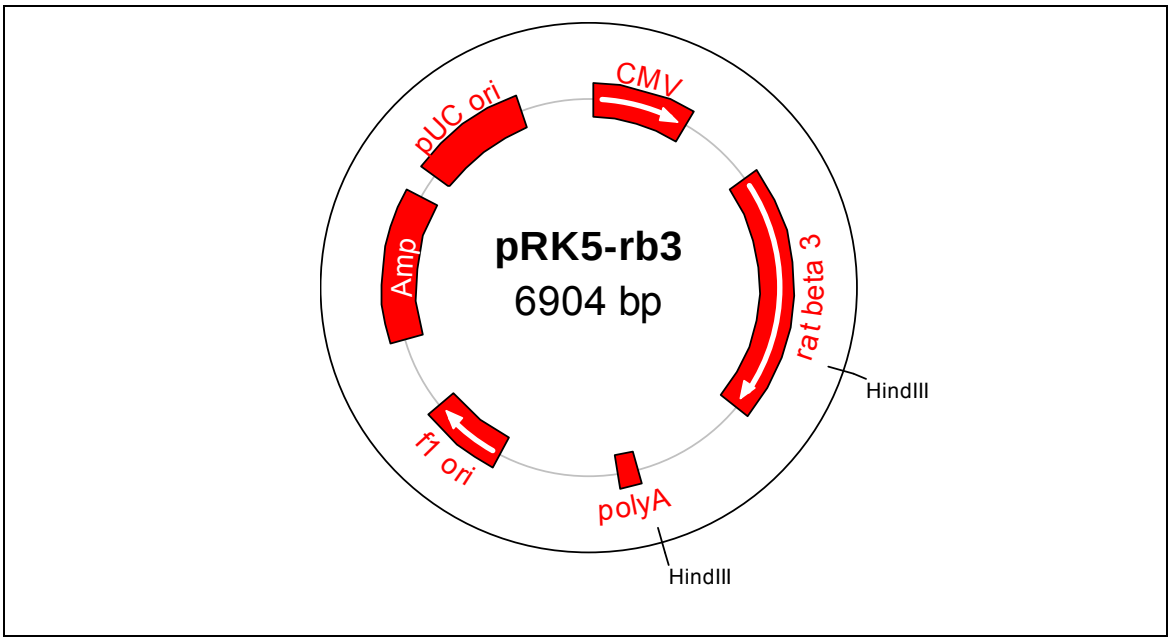

Figure 44: β3 vector

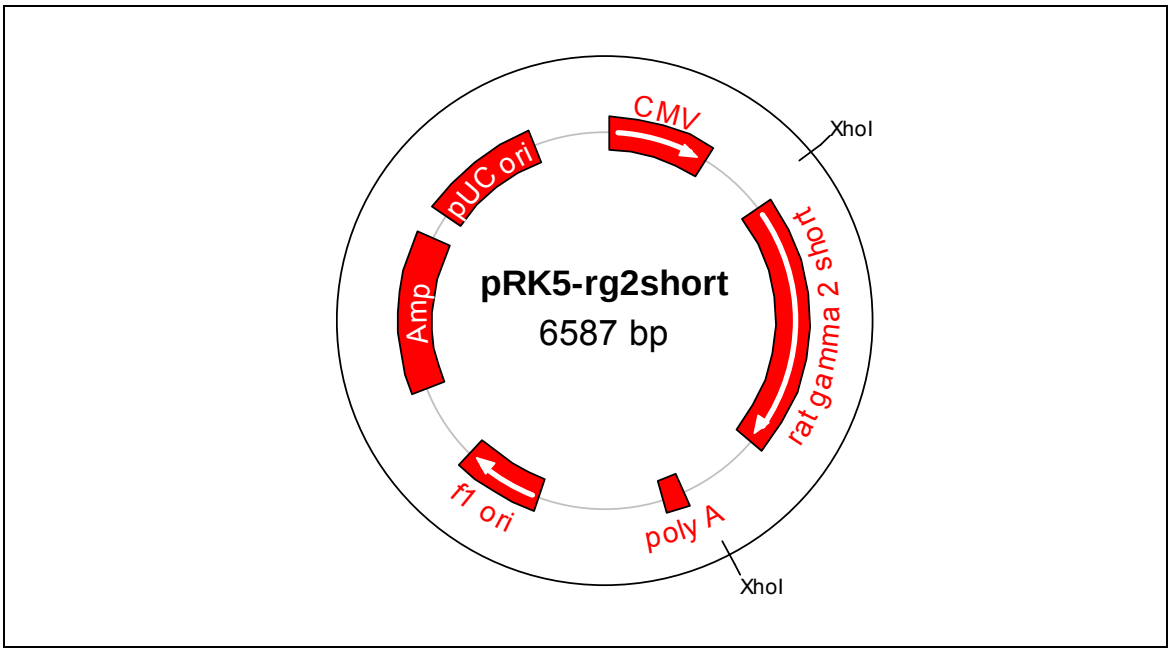

Figure 45: γ2 vector

11 Index

Veröffentlichungen:

Herth MM, Debus F, Piel M, Palner M, Knudsen GM, Lüddens H, Rösch F. *Total synthesis and evaluation of [(18)F]MHMZ*. Bioorg Med Chem Lett. 2008 Feb; 18 (4): 1515 - 1519

Korpi ER, Debus F, Linden AM, Malécot C, Leppä E, Vekovischeva O, Rabe H, Böhme I, Aller MI, Wisden W, Lüddens H. *Does ethanol act preferentially via selected brain GABAA receptor subtypes? The current evidence is ambiguous.* Alcohol. 2007 May; 41(3): 163 - 76.